ISSN 1454-8518

ANNALS OF THE UNIVERSITY OF PETROŞANI

ELECTRICAL ENGINEERING

VOL. 11 (XXXVIII)

UNIVERSITAS PUBLISHING HOUSE
PETROŞANI - ROMANIA 2009

ISSN 1454-8518

EDITOR OF PUBLICATION
Prof.dr.eng. Ioan-Lucian BOLUNDUȚ: Email: ibol@upet.ro

ADVISORY BOARD

Prof. Dr. Eng. Pop Emil - University of Petroşani, *Romania*; **Acad. Prof. Dr. Pivnyak Ghenadi** – National mining uninersity of Ukraine; **Prof. Dr. Eng. Munteanu Radu** - Tehnichal University of Cluj-Napoca, *Romania*; **Acad. Prof. Dr. Eng. Dasic Predrag** – High Technological Technical School, Krusevac, *Serbia and Montenegro*, **Prof. Dr. Eng. Cierpisz Stanisław –** Silesian University of Technology, Poland; **Prof. Dr. Eng. Bitoleanu Alexandru** - University of Craiova, *Romania*; **Prof. Dr. Eng. Păsculescu Mihai** - University of Petroşani, *Romania*; **Prof. Dr. Eng. Coloşi Tiberiu** - Tehnichal University of Cluj-Napoca, *Romania*; **Prof. Dr.Eng. Szabo Willibald** – "Transilvania" University of Braşov, *Romania;* **Prof. Dr. Eng. Poanta Aron** - University of Petroşani, *Romania*; **Prof. Dr. Eng. Manolea Gheorghe** - University of Craiova, *Romania*; **Prof. Dr. Eng. Vasilievici Alexandru** - Politechnical University of Timişoara, *Romania*; **Assoc. Prof. Dr. Dubois Daniel** - University of Liège, *Belgium*; **Assoc**. **Prof. Dr.Eng. Kovács Ernö** - University of Moskolc, *Hungary*; **Prof. Dr. Eng. Klepikov Vladimir Borisovich –** National Technical University of Kharkov, Ukraine; **Prof. Dr. Eng. Truşcă Vasile** - University "Politechnica" of Bucharest, *Romania*; **Prof. Dr. Eng. Fotău Ion** - University of Petroşani, *Romania,* **Dr. Eng. Nicoale Dan** – Dessault Systems Simulia Corp, Providence, *USA*, **Assist. Prof. Dr. Eng Negrut Dan** – University of Wisconsin-Madison, *USA*

EDITORIAL BOARD

Editor-in-chief:

Prof. Dr. Eng. Fotău Ion	University of Petroşani
Assoc.Prof. Dr.Eng Marcu Marius	University of Petroşani

Associate Editors:

Prof. Dr. Eng. Poanta Aron	University of Petroşani
Assoc.Prof. Dr.Eng Uțu Ilie	University of Petroşani
Assoc.Prof. Dr.Eng. Pătrăşcoiu Nicolae	University of Petroşani

Editor Secretary:

Assistant Eng. PhD Student Sochirca Bogdan	University of Petroşani

Editorial office address:
University of Petroşani, 20 University Street, 332006 Petroşani, Romania,
Phone: (40) 254/54.29.94; 54.25.80; 54.25.81; 54.33.82;
Fax: (40) 254/54.34.91; 54.62.38, Telex: 72524 univp, E-mail: marcu@upet.ro

This publication is with international distribution. It is sending in 28th countries.

CONTENTS

PĂTRĂŞCOIU NICOLAE, TOMUŞ ADRIAN MARIUS, GAIȚĂ – LUKACS IOANA, *USING VIRTUAL INSTRUMENTATION TO ACHIEVE A DATA LOGGER BASED ON A DMM*.....5

POANTA ARON, SOCHIRCA BOGDAN, *AUTOMATIC COMMAND OF A CONVEYOR BELT USING P.L.C*.....10

PĂTRĂŞCOIU NICOLAE, GAIȚĂ – LUKACS IOANA, TOMUŞ ADRIAN MARIUS, *VIRTUAL INSTRUMENT TO CONTROL DC MOTOR OPERATION*.....16

POPESCU FLORIN GABRIEL, MARCU MARIUS DANIEL, ORBAN MARIA DANIELA, *SIMULATION SOFTWARE FOR STATIC RECTIFIERS AND STATIC SWITCH CONTROLLERS*.....22

EGRI ANGELA , SIRB VALI-CHIVUȚA , STOICUȚA OLIMPIU, *VECTORIAL POSITION CONTROL SYSTEM OF THE GMF360 INDUSTRIAL ROBOT*.....32

ROMANESCU ANDREI, PĂSCULESCU DRAGOŞ, *THE EXPLOITATION OF HIGH ELECTRICAL POWER TRANSFORMERS AND AUTOTRANSFORMERS*.....42

MANDRESCU CORNELIU, STOICUȚA OLIMPIU, STOICUȚA NADIA *COMPARATIVE STUDY FROM THE KALMAN FILTER'S STABILITY POINT OF VIEW AND THE LUENBERGER ESTIMATOR WITHIN A VECTORIAL CONTROL SYSTEM IN WHICH THE LUENBERGER ESTIMATOR IS PROJECTED ON SELF VALUE ROTARY BASED METHOD*.....50

ŞTEFAN CONSTANTIN, PĂSCULESCU DRAGOŞ, *POSSIBILITIES TO MODERNIZE THE DISPATCH SYSTEMS, COMMAND AND CONTROL OF THE NEUTRALIZATION INSTALLATIONS OF INDUSTRIAL WATERS*.....60

SIRB VALI-CHIVUȚA, EGRI ANGELA, STOICUȚA OLIMPIU, *CIM CONTROL WITH EXTENDED KANBANS SYSTEM*.....66

UȚU ILIE, *MONITORING QUALITY OF ELECTRICITY FROM A LINE LIGNITE EXTRACTION TECHNOLOGICAL*.....72

BADEA FLORIN, *A VOICE COMMANDED WPF DATABASE MANAGEMENT APPLICATION*.....78

TĂBĂCARU TEODOR, *FUZZY CONTROL OF DC DRIVE.....88*
ROMANESCU ANDREI, PĂSCULESCU DRAGOȘ, *INFLUENCE OF THE LOAD DISTRIBUTION ALONG LINE ON THE LOCATION OF SERIES CAPACITOR IN MEDIUM VOLTAGE NETWORKS.....93*

Annals of the University of Petroşani, Electrical Engineering, 11 (2009) pages 5-9

USING VIRTUAL INSTRUMENTATION TO ACHIEVE A DATA LOGGER BASED ON A DMM

NICOLAE PĂTRĂŞCOIU[1], ADRIAN MARIUS TOMUŞ[2]
IOANA GAIȚĂ – LUKACS[3]

ABSTRACT: *The paper describes the procedure and how to use a program created in LabVIEW called virtual instrument and the digital multimeter (DMM) MAS 345 with RS – 232 interface to achieve a data logger.*

KEYWORDS: *LabVIEW, digital multimeter, MAS 345, RS-232, VISTA*

1. INTRODUCTION

A multimeter is a general purpose instrument which is used to make various electrical measurements, such as AC and DC voltage and current, and resistance. Multimeters may also have other functions, such as diode and continuity tests.

The multimeter MAS 345 is an autoranging professional measuring instrument. Digit reading is 3999 counts and the bar graph, capable of performing functions:

	Range		Range
DC voltage measuring	**0 … 1000 V**	**Capacitance measuring**	**0 … 400 nF**
AC voltage measuring	**0 … 750 V**	**Temperature measuring**	**0 … 750 ^{o}C**
DC current measuring	**0 … 10 A**	**Diode testing**	**-**
AC current measuring	**0 … 10 A**	**Transistor testing**	**1 … 1000**
Resistance measuring	**0 … 40 MΩ**	**Audible continuity testing**	**-**

In addition to these features the multimeter MAS 345 ensure the transfer of data, for all of measurement quantities, via serial bus RS – 232. Multimeter provides

[1] *PhD Assoc. Prof. Eng. at University of Petrosani*
[2] *PhD Student Assit. Eng. at University of Petrosani*
[3] *PhD Student Eng. at University of Petrosani*

digitization of all measured quantities and also realise the serial data transmission protocol such that the MAS 345 can be considered a data acquisition unit

Retrieving data from it, an operation known as data acquisition and their processing involves the creation of appropriate software that is a virtual instrument. Acquisition is the means by which physical signals are converted into digital formats and brought into the computer. Popular methods for acquiring data include plug-in DAQ and instrument devices, GPIB instruments, VXI instruments, and RS-232 instruments.

2. VIRTUAL INSTRUMENT REALIZATION

To create the virtual instrument was used LabVIEW programming environment because ensure predefined functions in its libraries. **VISA** is a standard I/O API for instrumentation programming and **VISA** functions can control GPIB, serial, USB, Ethernet, PXI, or VXI instruments, making the appropriate driver calls depending on the type of instrument which is used so it do not have to learn instrument-specific communication protocol. Before begin using **VISA**, is necessary to choose the appropriate method of instrument control.

To do this is necessary to know how data transmission by multimeter and its documentation follows:

Mode: *baud rate = 600, parity = none, data bit s= 7, stop bits = 2*
Format: *ASCII Code*
BYTE 1-2: *MEASURING MODE (ex; DC, AC, OH, CA, TE ...)*
BYTE 4: *SIGN(-)*
BYTE 5-9: *Decimal point and value of current measurement (ex;10.00, 3.999)*
BYTE 10-13: *Unit (ex; mV,A,KOHM, nF...)*
BYTE 14: *Carriage Return*

2.1. Diagram bloc of the virtual instrument

Block diagram of the virtual instrument used to realize data logger with data acquisition from multimeter MAS 345 is shown in figure 1.

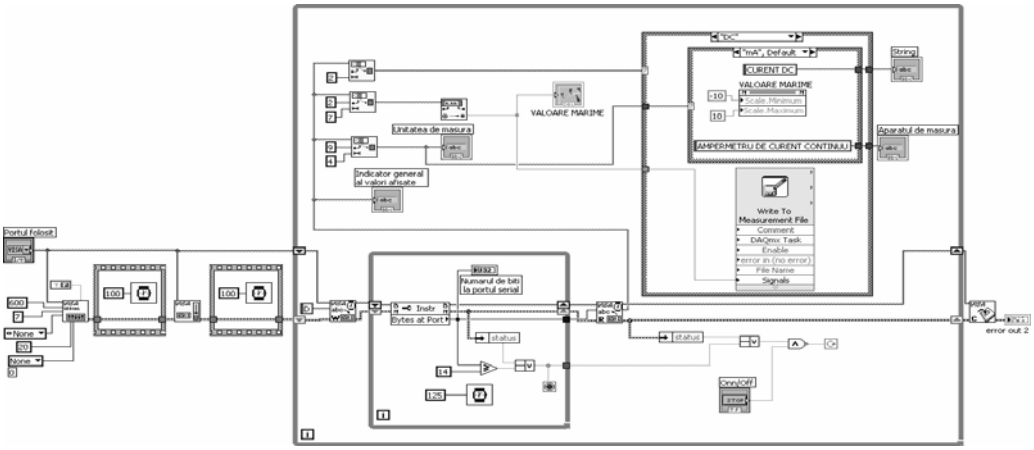

Figure 1. Diagram bloc of the virtual instrument

Initialization of the program acquisition is accomplished through **VISA Configure Serial Port VI** function which initializes the serial port specified by VISA resource name to the specified settings. Specific settings are taken from the operation of RS-232 protocol, specified above, and connecting them to the **VISA Configure Serial Port VI** is shown in Figure 2

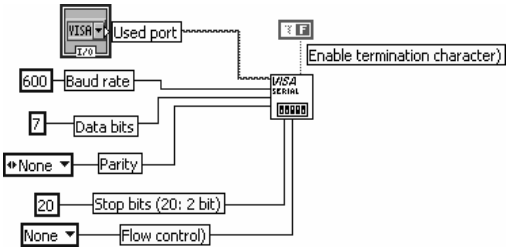

Figure 2. VISA Configure Serial Port VI

Since data acquisition is done with a low acquisition rate in the block diagram are introduced two sequences for delay execution of the program then reads the serial port COM1 through a **WHILE** loop. To read the information is necessary to send to the serial port, wherein the multimeter is connected, the command expressed by the letter "D" (from data) via **VISA Write** function.

Information is taken in ASCII code format, using the VISA Read function, and each reading is expressed with a code length of 14 bytes. Information is as string so that its decoding is done by extracting the bytes and to do this is used **String Subset** function which returns the substring of the input string beginning at offset and containing length number of characters.

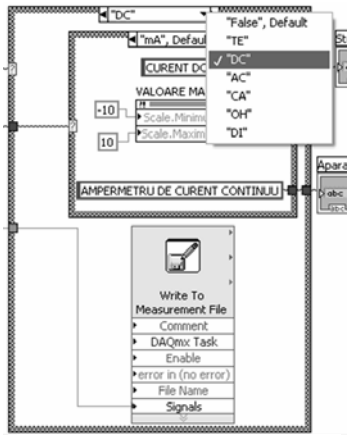

Figure 3. Type instrument selection

String represented by the first 2 bytes, coding type of the instrument, is used as a selection tool for a CASE structure. The structure CASE has 7 possible cases, as shown in figure 3, corresponding to 7 operating modes of multimeter MAS 345 and their selection is done for the string content of bytes 1-2

Each of these cases contains the following information to be displayed on the front panel of the virtual instrument: the type of instrument selected, the unit of measured value and scale limits for analog indicator on the front panel. Since the limits for the indicator analog scales differ depending on the quantity measured, as shown above, these limits are reached through **Property Node**. By its use is possible to set the maximum value and minimum value allowed in the range.

Since the size of the measured value is represented together with the decimal point everything as a string by Byte 5 – 9 so after extracting the substring of characters of information via the **String Subset** functions is converted to digital format through **Fract/Exp String to Number** function.

Numerical value obtained by measuring the quantity applied to the multimeter input is shown both as analog and digital form. To attach the unit, to the measured quantity, of the string acquired via serial port are extracted bytes 10-13 which encodes this unit. If the measured quantities are voltage or current since these quantities can be

DC or AC must display appropriate type and this is achieved through a different structure CASE intercalated in the CASE structure used to select the type instrument.

In each of the 7 cases is used function **Write to Measurement File Express VI**, which writes the date to text-based measurement files *(. lvm*) or binary measurement files (. *tdm* or . *tdms*) so that they can be stored and later retrieved in Excel. Using this function the measured dates are store into proper text file that can be readable from MS Excel. Here it can quickly create a chart that can be an option for acquired data representation.

2.2. Front panel of the virtual instrument

Some captures of the front panel of the virtual instrument for measuring AC and DC voltage, resistance, capacity or temperature are shown in Figure 4

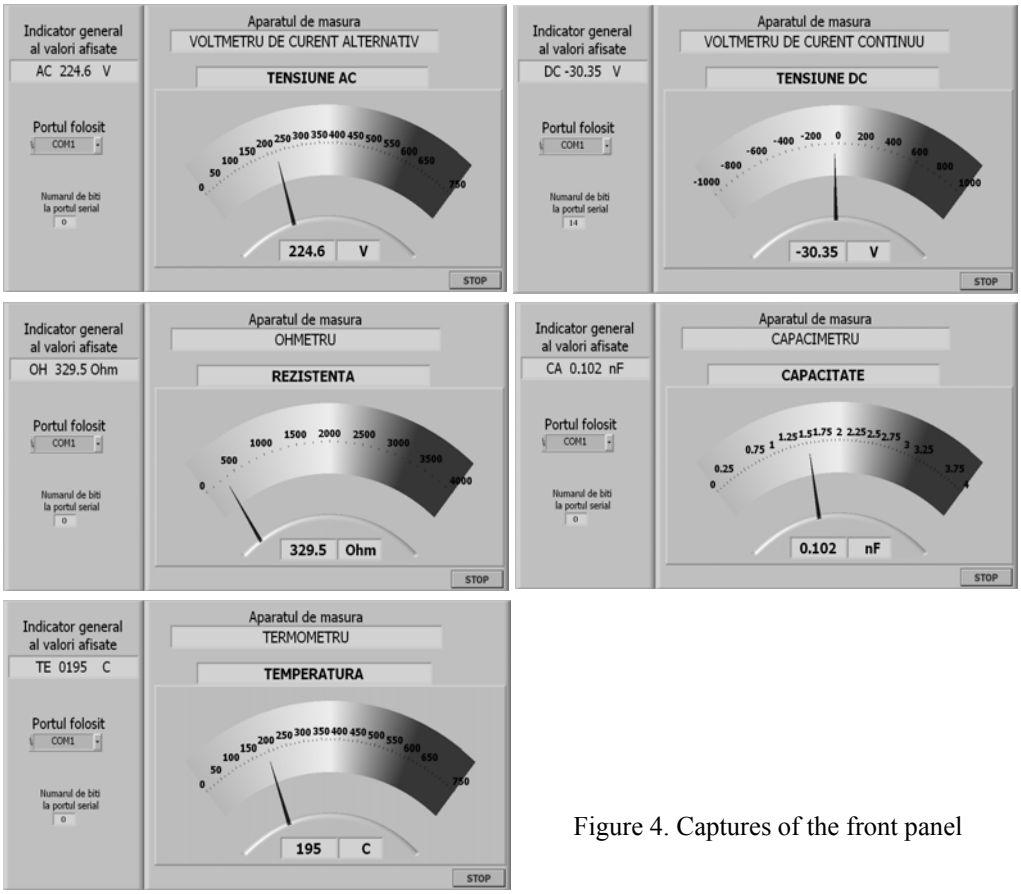

Figure 4. Captures of the front panel

Here we can see that for each measured quantity on the front panel are displayed: the type of instrument used, the size, the unit. Also according to the multimeter using the appropriate limits for the analogue scale indicator are established. On the front panel is used a single control, to select serial port number and all orders are taken through the serial port of the MAS 345 meter connected to it

3. CONCLUSIONS

Virtual instrumentation provides the ability to connect measuring devices to a computer so as to provide a record of the measurements.

The user can set the number of records made or the period on which those records are made.

REFERENCES

[1]. Pătrăşcoiu N., *Sisteme de achizitie si prelucrare a datelor. Instrumentatie virtuala* Ed. Didactica si Pedagogica, Bucuresti, 2004

[3]. * * * *LabVIEW for Measurement and Data Analysis,* National Instruments, Ian..2003

[4]. * * * *MAS345. Operator's Instruction Manual*. http://www.p-mastech.com/products/04_dm/mas345_hys004695.pdf

Annals of the University of Petroşani, Electrical Engineering, 11 (2009) pages 10-15

AUTOMATIC COMMAND OF A CONVEYOR BELT USING P.L.C

POANTA ARON[1], SOCHIRCA BOGDAN[2]

ABSTRACT: *In this paper it is described an automatic system with programmable logic controller for the command of a belt conveyer. By the technical and functioning specification, from which result the opportunity of using a programmable logic controller, it will be realized the design of the system, the algorithm for the command of a belt conveyer, and the implementation of the system.*

KEYWORDS*: automatic command, plc, conveyer belt, timing diagram*

1. TECHNICAL SPECIFICATION

The design of the system presumes to formulate the technical and functional specification. To set up these specifications we have to take in consideration the requirement of the nature condition.

-technological condition

-safety and protection condition

-command, signaling and dispatch condition

The technological conditions assume:

-the start of the system to be done by an external button

-in the case of multi motor drive need to be done by a delay between each motor

-the stop of the system need to be done by an external button or by a fault condition

-the possibility to integrate the system in a complex automatic system

The safety and protection conditions assume:

-the possibility to stop the conveyer belt from any point of the system

-the automatic stop of the conveyer belt in the case of any fault that appear in the functioning of the system

The command, signaling and dispatch conditions assume:

[1] *Ph.D Prof Eng. at University of Petrosani*

[2] *Ph.D Student Assistant Eng. at University of Petrosani*

-emit acoustic signal before starting each motor

-the possibility to send information regarding the conveyer belt to a dispatch point

-the existing of an emergency button which will stop the entire process.

2. THE ALGORITHM

The general functioning algorithm was realized regarding with the technical specification and it is described in figure 1.

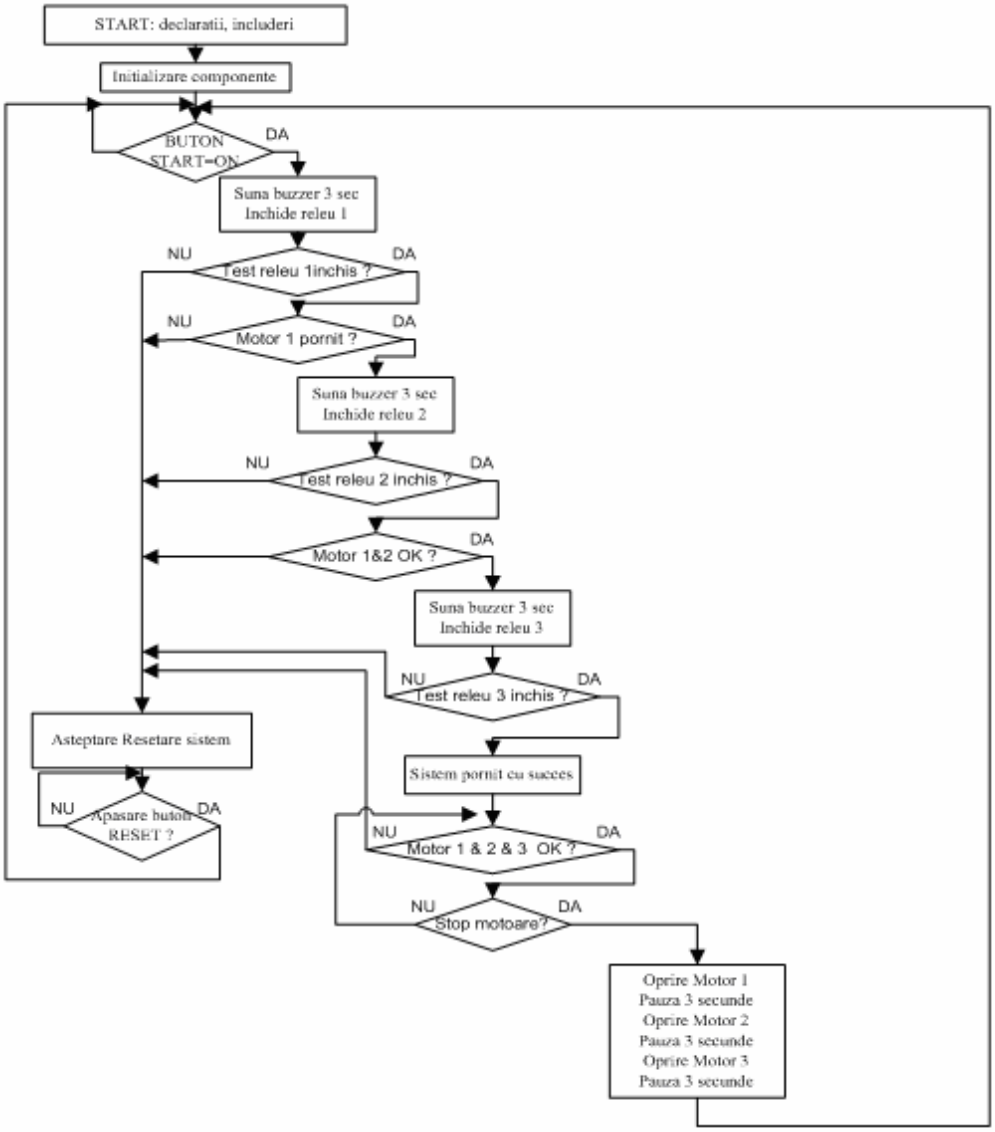

Figure 1. The system algorithm

3. THE SYSTEM

The algorithm was implemented in Klockner Moeller EASY 512. The system structure can be observed in figure 2.

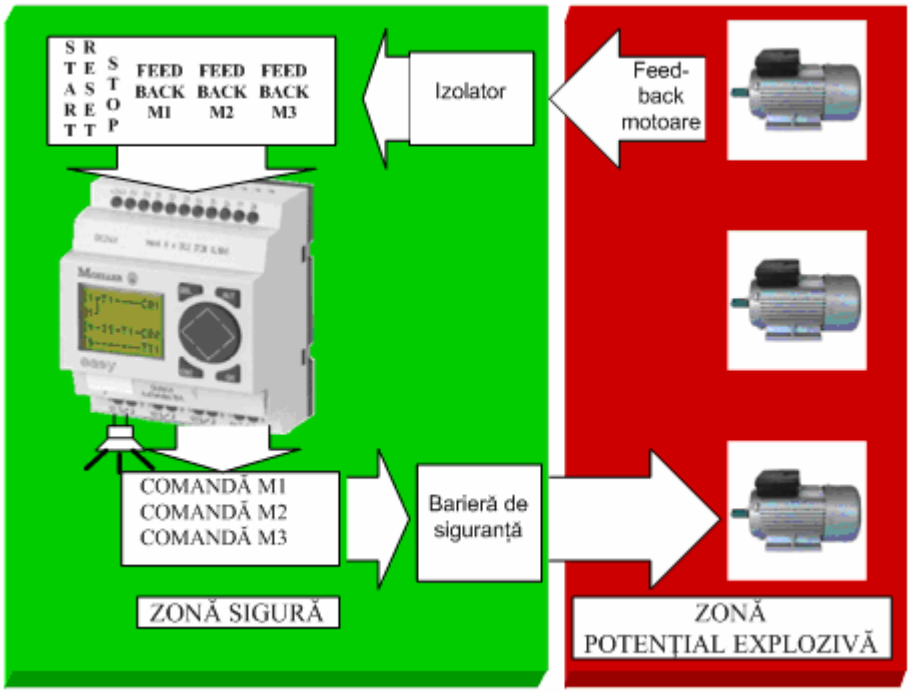

Figure 2. The system description

The input output of the PLC will be:
I_1-start button
I_2-general fault
I_3-stop button
I_4-M_1 fault
I_5-M_2 fault
I_6-M_3 fault
Q_1-acuoustic signaling
Q_2-command M_1
Q_3-command M_2
Q_4-command M_3

The combination between I_2 and I_3 will reset the system and will restart the system after a fault occurs.

In figure 3 is described the start of the system. After the start button is pressed (I_1) the acoustic signal will be herd for about 3 seconds, after that the command to start the motor 1 will be given, another acoustic signal and the motor 2 will start and after another 3 seconds of acoustic signal the motor 3 will start. This can be observed in the start timing diagram form the figure 3.

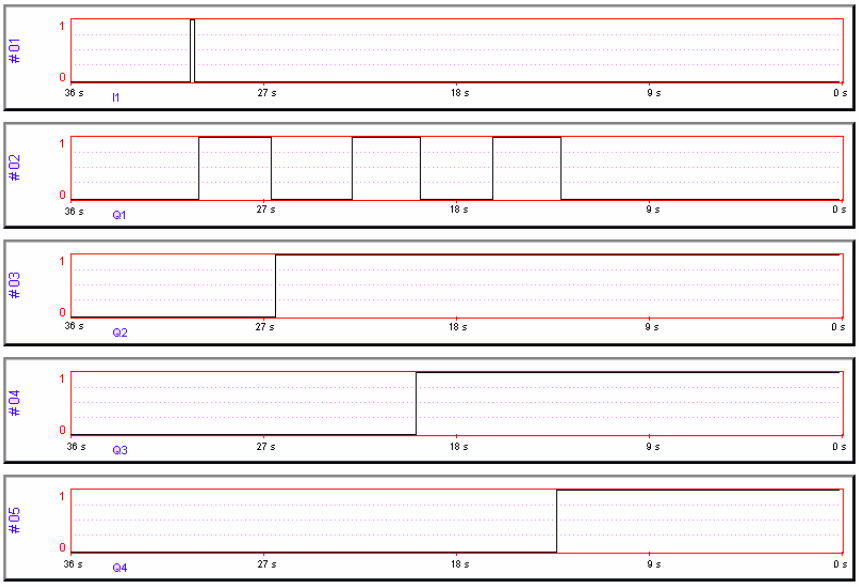

Figure 3. Timing diagram for starting the system

In case a general fault will occurs the system will give the command to stops all the motors. (figure 4)

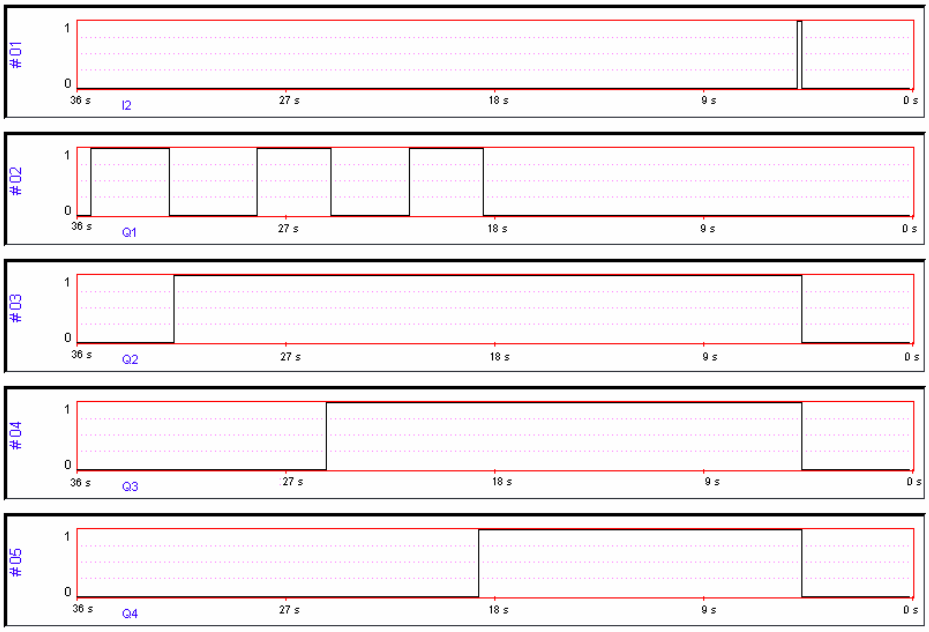

Figure 4. General fault occurs

In figure 5 it can be observed that when a fault for the motor 1 appear the system will stop automatically and to restart the system will be necessary the

combination between I_1 and I_2, for security reasons. After a fault occurred if the start button is pressed, this action will have no effect. After a fault, is necessary to activate the reset button, and only after that the start button will be active.

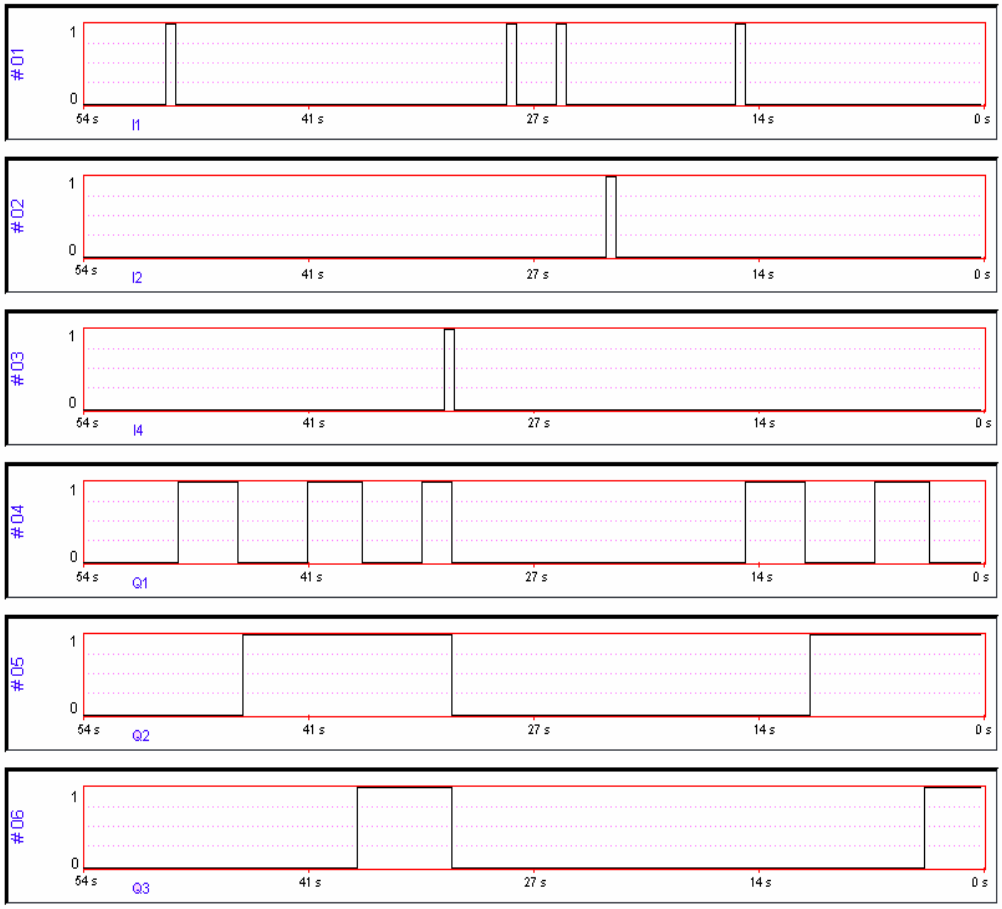

Figure 5 Motor 1 fault

The stop button will be link to I_3 input of the plc. A signal on this input will initialize the stop procedure. After 3 second when the stop button was pressed, it will be send the command for the motor 1 to stop, after another 3 second will send the command to stop the motor 2, and after another 3 second will sent the command for motor 3 to stop. After all the motor was stopped, the whole system can be started by pressing the start button. If not all the motor was started the push of the stop button will not be take in consideration by the system. (figure 6)

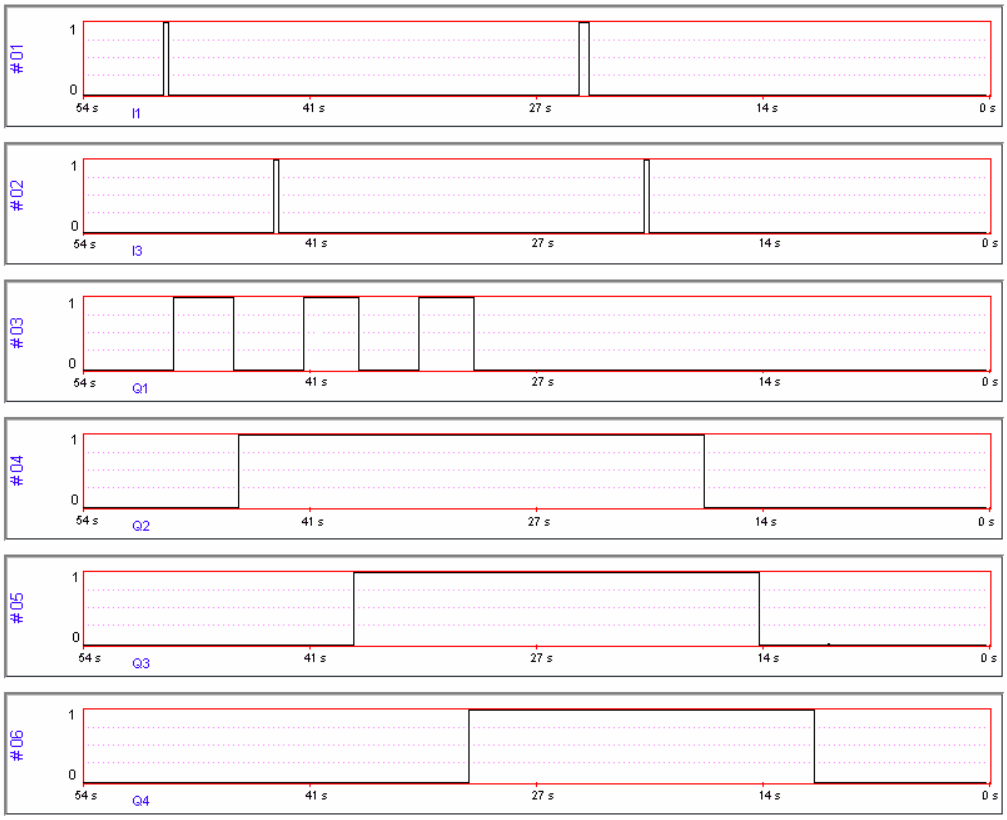

Figure 6. The stop procedure

4. CONCLUSION

The use of the PLC and easy software facilitation make possible elimination of some equipments such as time relay, the BACAIT command bloc, amplifiers from the speed sensors, and other. All this will lead to a lower cost of a conveyer belt system.

The possibility to interconnect many PLC will lead to a better dispatcherisation of the entire process.

REFERENCES

[1]. **Pop E., Leba M.,** - *Microcontrollere şi automate programabile*, Editura Didactică şi Pedagogică, Bucureşti 2003.

[2]. Poanta A., Patrascoiu N., - *Circuite si echipamente electronice in industria miniera* , Editura Didactică şi Pedagogică, Bucureşti 1997

[3]. * * *, *EASY PLC Data Sheet*

Annals of the University of Petroşani, Electrical Engineering, 11 (2009) pages 16-21

VIRTUAL INSTRUMENT TO CONTROL DC MOTOR OPERATION

NICOLAE PĂTRĂŞCOIU[1], IOANA GAIȚĂ – LUKACS[2] ADRIAN MARIUS TOMUŞ[3],

Abstract: *The paper describes the procedure how to use a program created in LabVIEW called virtual instrument and data acquisition card PCI-6024E to control a direct current (DC) motor operation.*

Keywords: *LabVIEW, virtual instrument, Matlab script, PCI-6024E*

1. INTRODUCTION

The traditional DC motor needs two current supplies, one through the stator windings (armature) to provide the magnetic field and the other through the rotor windings to interact with the magnetic field to generate the motive force. The speed of a DC motor can be varied by controlling the field flux, the armature resistance or the terminal voltage applied to the armature circuit. The three most common speed control methods are field resistance control, armature voltage control, and armature resistance control. To control the operation of a DC motor is necessary to know the parameters in the normal functioning of this. The values of these parameters may be provided by the motor's manufacturer or can be determined a priori by the simulation of motor's operation. LabVIEW program called virtual instrument, which we propose in this paper has three components namely: the simulation of the DC motor, start of the DC motor and measure parameters during DC motor operation through a data acquisition system. All three components are integrated into the same virtual instrument so that the user can select one of these through a TAB control type connected to a CASE type structure.

[1] *PhD Assoc. Prof. Eng. at University of Petrosani*
[2] *PhD Student Eng. at University of Petrosani*
[3] *PhD Student Assit. Eng. at University of Petrosani*

2. FRONT PANEL OF THE VIRTUAL INSTRUMENT

Front panels of the virtual instrument are shown in Figure 1.

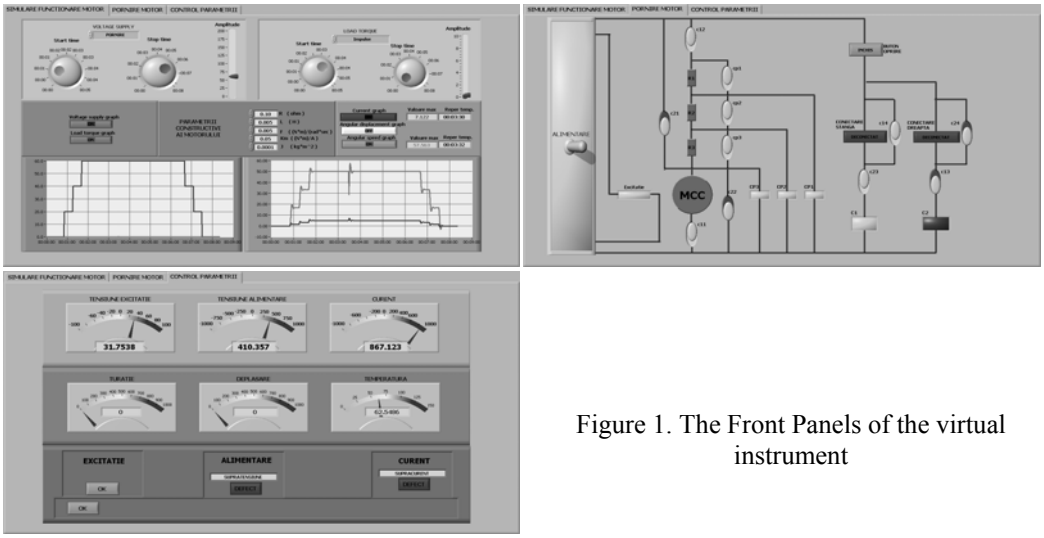

Figure 1. The Front Panels of the virtual instrument

The first front panel is used to simulate DC motor and through it the user can see the motor operation under various operating conditions. Here the user can select the by corresponding controls forms (impulse, step, ramp or custom) and values of the voltage applied to the armature circuit as well forms and values of the DC motor load. The used controls are POWER SUPPLY and LOAD TORQUE. With these input values, to which are added and the construction parameters of DC motor, by simulation can make observations on the evolution over time of the armature current, rotational speed and angular displacement. For each of these quantity are recorded and displayed their maximum values with time of occurs their.

The second front panel is used to command and visualize sequences of starting of the DC motor when start-up of motor is made either by steps of voltage or steps of current. It can be observed starting operation scheme by closing contactors and circuits, achieving closing retention contacts and interlock contacts to prevent reverse connection. Here are used as control buttons for connecting the power supply, starting the motor in one direction and in the other and stopping the motor also. Other elements are type indicator and their activation is done through the digital inputs of the data acquisition board PCI-6024. Auxiliary contacts of contactors from the DC motor control scheme are connected to the digital inputs of the data acquisition board, so that it is possible to be observed proper function of control scheme. It is also possible to measure either the times or the currents connecting the speed steps to start the DC motor.

The third front panel is used both for displaying the values of measurements taken from the engine such as: excitation voltage, supply voltage, current, speed and angular displacement and control values are exceeded prescribed for them. Measurements taken from DC motor values are shown as analog and digital form and

are recording in a database with a frequency set by the user and the recording frequency can be changed depending on the needs imposed by the operation at a time.

3. DIAGRAM BLOC OF THE VIRTUAL INSTRUMENT

Block diagram represent the program of operation for virtual instrument and is composed of mathematical and logical functions and programming structures. For each of the three components of the virtual instrument, represented by the three front panels, is built one block diagram. Selection of each block diagram is achieved by the TAB control with which is possible to select one of the cases from CASE structure. To maintain the running each block diagram is used Property Node function by which are get references to pages contained by the TAB control.

Block diagram corresponding of the DC motor simulation is shown in Figure 2

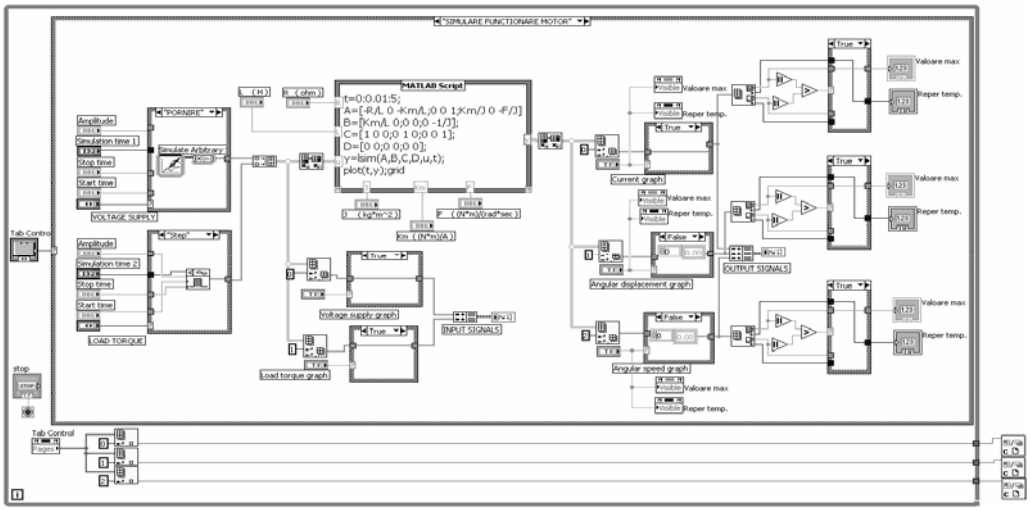

Figure 2. Block diagram of the DC motor simulation

The base element of this diagram bloc that is used to simulation DC motor working is the Matlab script node. Through this, is inserting into LabVIEW program the matrix A, B, C, D of the motor state-space model and the simulation function also.

To obtain matrices A, B, C, D of the mathematical model in state-space form is considered analytical model of the DC motor with constant flow defined by the equations:

$$\begin{aligned} \frac{di_S(t)}{dt} &= \frac{1}{L}\cdot v_S(t) - \frac{R}{L}\cdot i_S(t) - \frac{K_m}{L}\cdot \omega(t) \\ \frac{d\omega(t)}{dt} &= -\frac{F}{J}\cdot \omega(t) + \frac{K_m}{J}\cdot i_a(t) - \frac{1}{J}\cdot m_L(t) \\ \omega(t) &= \frac{d\alpha(t)}{dt} \end{aligned} \qquad (1)$$

where: $v_S(t)$, $i_S(t)$ – supply voltage and current; $m_L(t)$ load torque;$\omega(t)$ – angular speed; $\alpha(t)$ – angular displacement; R, L – winding electric resistance and inductance; K_m – DC motor constant; F – coefficient of friction; J – moment of inertia reduced to motor axis.

To build the state-space model brings in this mathematical model the input, state and output vectors i.e.:

- state vector x(t) whose components is represented by $i_S(t)$, $\alpha(t)$ and $\omega(t)$
- input vector u(t) whose components is represented by $v_S(t)$ and $m_L(t)$:
- output vector y(t) whose components we consider that is the same with state vector components so that is possible to simulate these three physical quantities.

With these vectors is possible to write equation (1) as a matrix form from which are extracted matrices A, B, C and D:

$$\underbrace{\begin{vmatrix} \dot{i}_S(t) \\ \dot{\alpha}(t) \\ \dot{\omega}(t) \end{vmatrix}}_{\dot{x}} = \underbrace{\begin{vmatrix} -\frac{R}{L} & 0 & -\frac{K_m}{L} \\ 0 & 0 & 1 \\ \frac{K_m}{J} & 0 & -\frac{F}{J} \end{vmatrix}}_{A} \cdot \underbrace{\begin{vmatrix} i_S(t) \\ \alpha(t) \\ \omega(t) \end{vmatrix}}_{x} + \underbrace{\begin{vmatrix} \frac{1}{L} & 0 \\ 0 & 0 \\ 0 & -\frac{1}{J} \end{vmatrix}}_{B} \cdot \underbrace{\begin{vmatrix} v_S(t) \\ m_L(t) \end{vmatrix}}_{u}$$

$$y(t) = \underbrace{\begin{vmatrix} 1 & 0 & 0 \\ 0 & 1 & 0 \\ 0 & 0 & 1 \end{vmatrix}}_{C} \cdot \begin{vmatrix} i_S(t) \\ \alpha(t) \\ \omega(t) \end{vmatrix} + \underbrace{\begin{vmatrix} 0 & 0 \\ 0 & 0 \\ 0 & 0 \end{vmatrix}}_{D} \cdot \underbrace{\begin{vmatrix} v_S(t) \\ m_L(t) \end{vmatrix}}_{u} \tag{2}$$

Given matrices A, B, C and D can use the Matlab function ***lsim***:

$$y = lsim\ (A\ ,\ B,\ C,\ D,\ v,\ t) \tag{3}$$

where vector *t* specifies the time samples for the simulation and consists of regularly spaced time samples *t* to simulate the D.C. motor like an LTI system.

The motor constructive parameters R, L, K_m, F and J represent the model parameters and these are sets by controls placed on front panel named with the same letters like mentioned parameters. For the respectively controls are chosen the steps of values corresponding to the real values of these parameters. The values set by these controls represent the inputs for script node with real data type.

The bloc diagram that assures command and visualization of the sequences of starting of the DC motor is shown in Figure 3.

The basic element of this block diagram is the CASE structure with the choice of two possible cases: true or false. Selection of either state is guided by state motor control buttons for the selected option is "*Switch until released*". In this way after each command the scheme will be prepared to receive always a new command. The algorithm operation and selection of cases through the command buttons is shown in

Figure 4. Achievement of each stages of the command is made by using the structure SEQUENCE so that each sequence contains specific commands and delays needed.

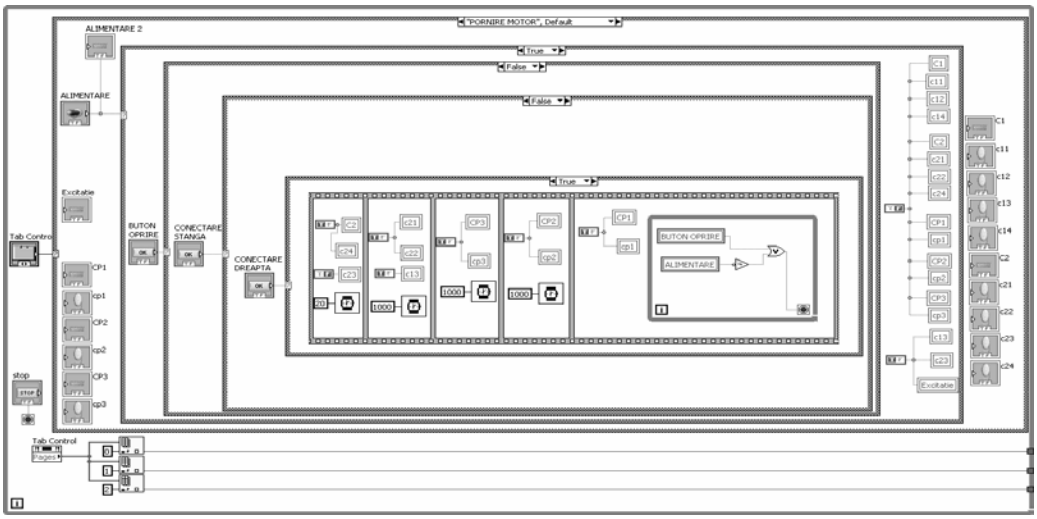

Figure 3. Block diagram of the DC motor command

Block diagram of the virtual instrument that assures real time monitoring of the DC motor parameters is shown in figure 5. The basic element of this block diagram is the DAQ Assistant Express VI that creates, edits, and runs tasks using NI-DAQmx toolkit.

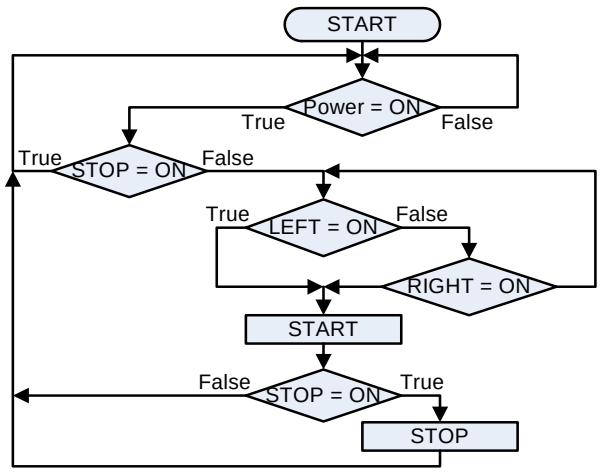

Figure 4. Algorithm operation

DAQ Assistant is a graphical interface for interactively creating, editing, and running NI-DAQmx virtual channels and tasks. A NI-DAQmx virtual channel consists of a physical channel on a DAQ device and the configuration information for this physical channel, such as input range and custom scaling. A NI-DAQmx task is a collection of virtual channels, timing and triggering information, and other properties regarding the acquisition or generation.

In this application, DAQ Assistant is configured to perform measurements of voltages, voltages that are acquired from different sensors like: voltage sensor, current sensor, angular speed and displacement sensors and temperature sensor. To acquired these signals, are used analog inputs of the data acquisition board PCI-6024. Acquired

signals are compared with their prescribed values obtained by simulation and if are exceed preset limits are generated commands necessary and warning messages are displayed.

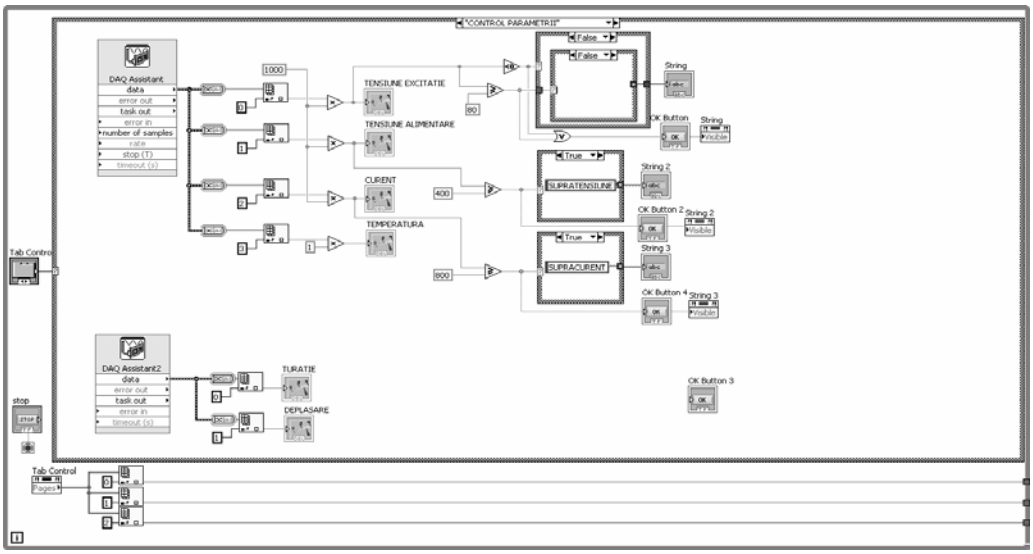

Figure 5. Block diagram of the DC motor monitoring

4. CONCLUSIONS

Using a virtual instrument as software and a data acquisition card as hardware for general or specific data acquisition or measurement system allow applications those provide dialogs and interfaces which can be used to control different processes such as DC motor operation control.

In this application of control operation for a DC motor is performed on the basis of quantities whose values can be determined, depending on operating conditions, through simulation. As hardware is used data acquisition board PCI-6024 but can be used and other hardware to ensure the correct acquisition for quantities and their values from controlled process

REFERENCES

[1]. Fransua, A., *Masini si acţionări electrice*. Ed. Tehnica, Bucuresti, 1986

[2]. Matko D., Karba R., *Simulation and Modelling of Continuous System*. Prentice Hall, New York, 1992

[3]. Pătrăşcoiu N.,*Sisteme de achizitie si prelucrare a datelor. Instrumentatie virtuala* Ed. Didactica si Pedagogica, Bucuresti, 2004

[5]. * * * *LabVIEW. User Manual*, National Instruments, April 2003 Edition Part Number 320999E-01

[6]. * * * *PCI-6023E/6024E/6025E. User Manual*. National Instruments, December 2000. Edition Part Number 322072C-01

Annals of the University of Petroşani, Electrical Engineering, 11 (2009) pages 22-31

SIMULATION SOFTWARE FOR STATIC RECTIFIERS AND STATIC SWITCH CONTROLLERS

POPESCU FLORIN GABRIEL[1], MARCU MARIUS DANIEL[2], ORBAN MARIA DANIELA[3]

ABSATRACT: *The static converters (CS) have become an important element in supply systems with electrical energy of every kind of consumers. The static converters are used in adjustable systems to the static action, in this case the assignment being an electrical engine most frequently. The simulation software for static converter function it is realized like a Windows independent application helping with Visual Basic's software package. Once the simulation software is launched one window is opened, allowing choosing the simulation type to be run, using radio buttons.*

KEYWORDS: *switch converter, static rectifier, software, simulation, bridge.*

1.INTRODUCTION

The development of industrial automation leads by default also to the improvement of electrical drives systems as more than these systems represent the most spread conversion type of the electrical energy in the mechanical energy.

The static converters (CS) have become an important element in supply systems with electrical energy of every kind of consumers. The static converters are used in adjustable systems to the static action, in this case the assignment being an electrical engine most frequently. Hereby, by an adequate command given by a controller in to a close circuit, the static converters adjust the output electrical energy parameters, to the necessity demand by electrical engine.

The rectifiers are static converters with natural switching which realize the electrical energy changeover from alternative current into continuous current and reverse due to their power semiconductor elements components.

[1] *Assistant Eng. at University of Petrosani*
[2] *PhD. Associate at University of Petrosani*
[3] *PhD. Associate at University of Petrosani*

There are single-phase rectifiers and three-phase rectifiers taking into account the phase numbers.

In dependence with the operating quadrants the rectifiers are:

- the rectifier by one quadrant- where the voltage and the current have one way (semi commanded rectifiers);
- the rectifiers with two quadrant where the output voltage can be positive or negative (the complete command rectifier);
- the four quadrant rectifiers – where the output voltage can be negative or positive and the current can get about both ways.

The two quadrant rectifiers can be with central tap (the rectifier with two pulses), the single phase bridge and rectifier with the null diode. The rectifier of one quadrant or semi commanded rectifier are realized through the bridge scheme and are made by thyristors and diodes. The rectifiers with forced switching are for two types: the unitary power factor rectifier and Pulse Width Modulation (PWM) rectifier.

The simulation software for static converter function it is realized like a Windows independent application helping with Visual Basic's software package. Once the simulation software is launched one window is opened, allowing choosing the simulation type to be run, using radio buttons. The window also contains two buttons, one for continuing the simulation (*Continua*), and the other for exit the application (*Iesire*).

Following the simulation start-up, the simulation window is opened, containing three main parts:

- a part which contains the simulation scheme. The simulation scheme is dynamically modifying its side colors which are in conduction at a certain moment.
- another part it is dedicated to the information zone. This zone is presenting the text type information as regards to function mode to the converter analyzed (semiconductor elements which are in conduction, semiconductor elements directly polarized, etc.). Inside of this zone it is also find buttons for command angle modification, for choosing the function dial, etc.
- the third part is the zone where is dynamically getting up the wave forms characteristic to the static converter analyzed.

Beside this zones, one of simulation windows also containing a pull-down menu type, for modification of some parameters or for choosing of different type of loads. The window also have two command buttons, one for starting up the simulation *(Simulare*), which then it is transforming in button for hold up the simulation *(Stop)* and a button for the exit of the window (*Iesire*).

Fig.1 Simulation the rectifiers

The main window of simulation of static rectifiers application is shown in the figure 1, from where you can choose the rectifier with two quadrant simulation, the rectifier with one quadrant simulation or the simulation of rectifier with forced changeover.

2. THE RECTIFIER WITH TWO QUADRANTS

The figure 2 presents the simulation window for two quadrants rectifier with central tap single phase (it can choose the rectifier type). During the simulation, the command angle is modified for emphases even the voltage adjusting mode and the load current. The command angle can be modifying using the up-down arrows, showing this value.

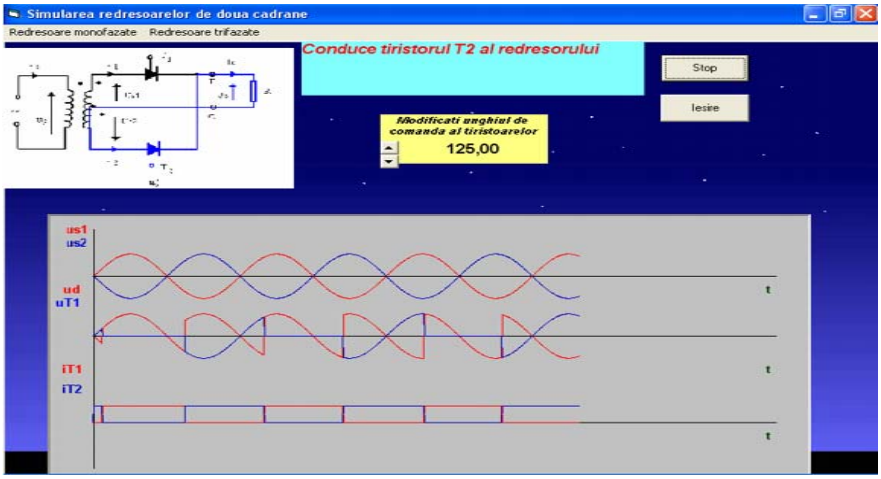

Fig.2 Single phase rectifier with central tap

The figure 3 is presenting a simulation window for a three phase's rectifier with null conductor.

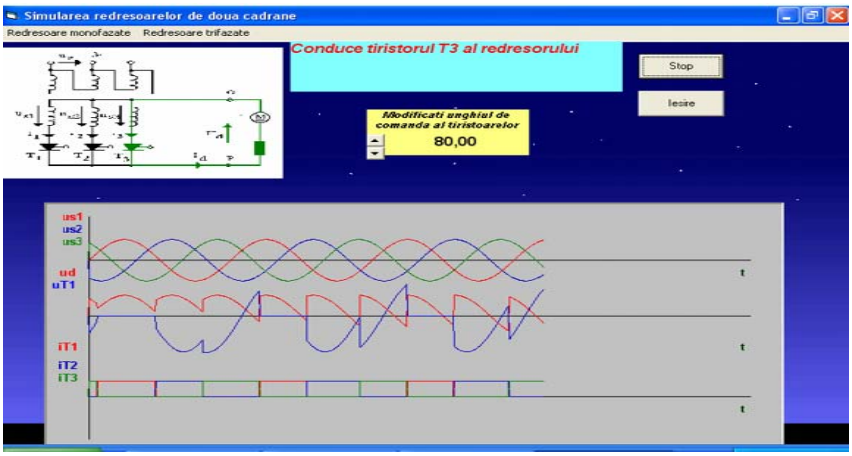

Fig.3 The three phases rectifier with null conductor

The thyristor input conduction appears when the voltage on the thyristor is positive as only the natural commutation dot.

The figure 4 is presenting a simulation window of single phase bridge rectifier. It has four thyristors and the load is connected on the continuous current diagonally, and pair of thyristors T1T4, T2 T3 is simultaneous in conduction.

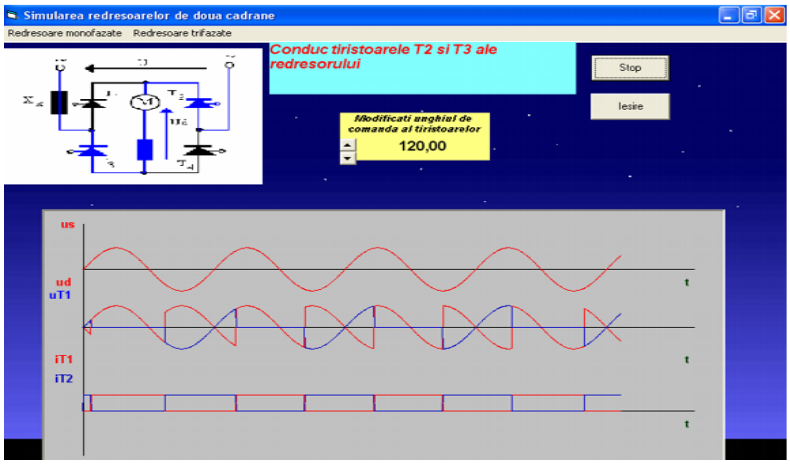

Fig.4 The single phase bridge rectifier

The figure 5 is presenting the three phase's bridge rectifier. These are the most used rectifiers. It should be taken into account divided in two rectifiers with null conductor, made the positive branch N and the negative branch N. The output straightened voltage of the three phases rectifier full commanded is given by the difference between the straightened voltages from the two branches.

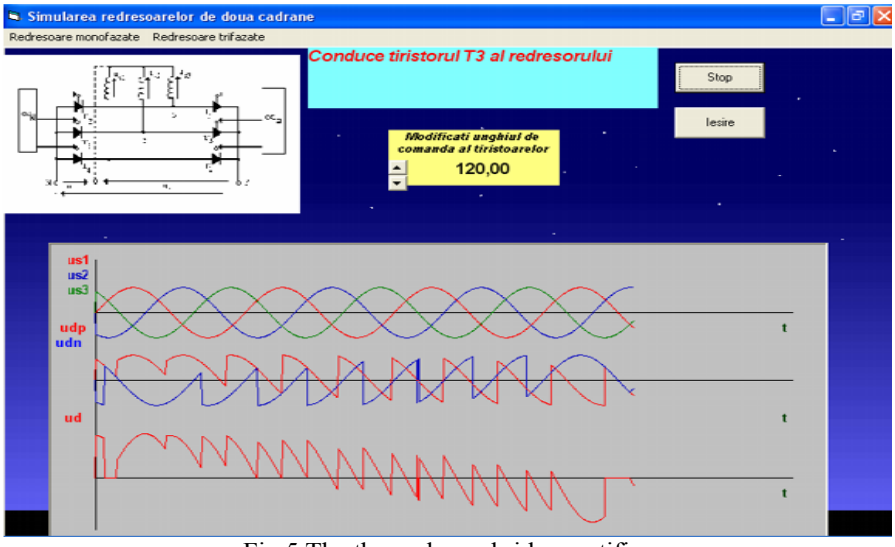

Fig.5 The three phases bridge rectifier

2.1. The rectifier with the null diode

The commanded rectifiers in phase have a lot of shortcomings as:
- the power factor is decreasing;
- the current harmonics amount even in the straightened voltage waveforms.

To improve some of these shortcomings it is necessary to put a diode in parallel with the load. The straightened voltage is polarizing the null diode in opposite way, and start the conduction when the instantaneous value of voltage begin zero. In this way the straightened voltage is only made by positive pulses.

The figure 6 is representing the simulation window for a single phase rectifier with null diode. During the simulation, it has been modified the command angle of the rectifier, in order to evidence also the way of voltage modification, respectively the load current. The command angle may be modified using up/down arrows, being shown their values.

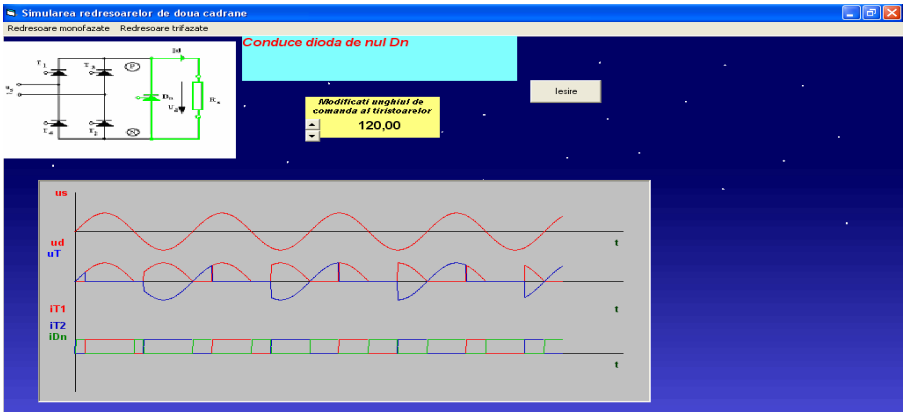

Fig.6 The single phase rectifier with null diode

It can notice that the thyristor lead the current on the π/α period of time and on the α period of time the load current is led by the null diode.

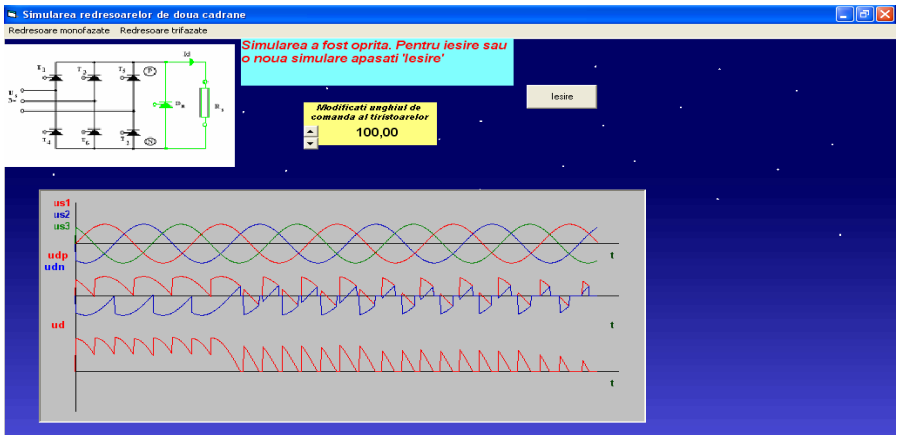

Fig.7 The three phases rectifier with null diode

In the figure 7 is represented the simulation window for a three phase rectifier with null diode. In this case the null diode start to lead only for command angle greater than $\pi/3$. Form waveforms it can notice that each thyristor switched twice into a period, and the switching period of thyristor is reducing. The null diode leads the load current on $\pi/\alpha-\pi/3$. The command angle can't overtake the value $2\pi/3$

2.2.One quadrant rectifier

The semi commanded rectifiers are only made in bridge scheme. It's made by thyristors and diodes. There are two methods of semiconductors elements placement for symmetrical or asymmetrical way for the single phase rectifier.

It can notice that the straightened voltage has only positive values and the average value of straightened voltage varies between Ua0 and zero for a command angle between 0-180 degree.

In the figure o it is shown the simulation window of single phase rectifier. One quadrant rectifier has two thyristors T1, T2 and two diodes D1, D2 and the load is connected on the bridge diagonally of continuous current. The lead way is T1, D2 respectively T2, D1.

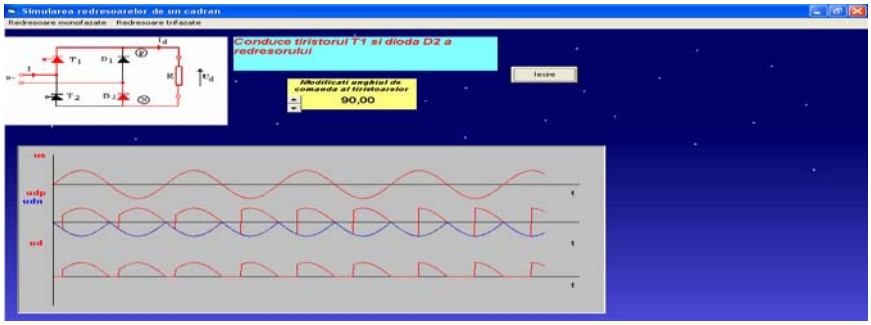

Fig.8 The single phase rectifier with one quadrant

Figure 9 represents the three phase rectifier with one quadrant. This can be considered like a semi commanded rectifier in three phase bridge made by positive branch P and negative branch N. The straightened output voltage is made by the difference between straightened voltages from the two branches.

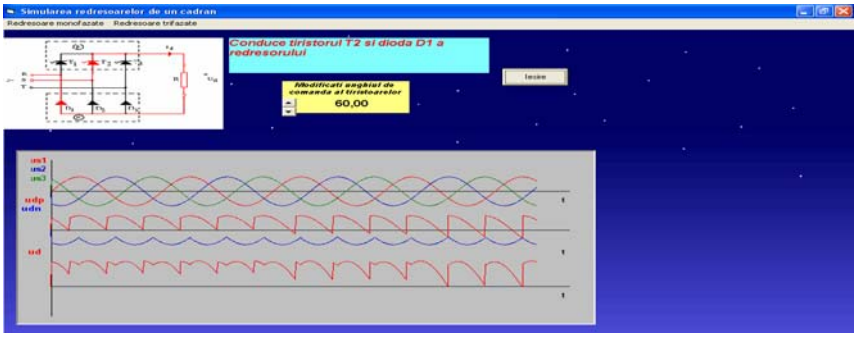

Fig.9 The three phases rectifier with one quadrant

3.STATIC SWITCH CONTROLLER SIMULATION

The static switch controllers are converters were the exit size have the same form with the entry size, after modifying the command angle α of thyristors obtaining the converter out put of voltage variation.

Figure 10 shows the application of main window of static switch controllers simulation software application, it allows selection for a. c. switch controllers, single-phase or three-phase, respectively the simulation for d.c. switch controllers.

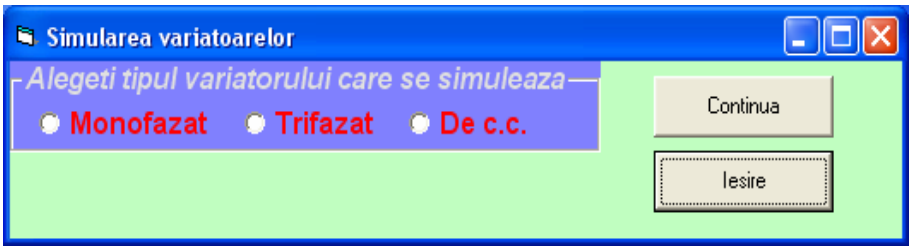

Fig.10. The application of main window of static variators simulation software application

3.1.A.c. switch controllers

Figure 11 shows the simulation window for a single-phase switch controller with resistive charge. It can be seen the main menu to choose the type of switch controller (with two thyristors, with one thyristor or with a thyristor across a diode bypass), and also the charging type. The charge may be resistive, inductive or resistive-inductive type.

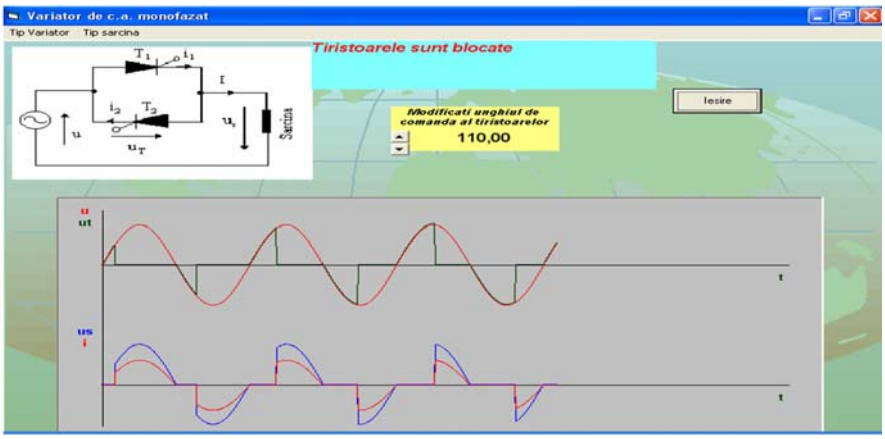

Fig.11.The simulation window for a single/phase switch controller with resistive charge

During the simulation, it has been modified the command angle of the switch controller, in order to evidence also the way of voltage modification, respectively of the current through charge. The command angle may be modified using up/down arrows, being shown their values.

Figure 12 shows the simulation windows for single-phase switch controller with resistive-inductive charge. In case of resistive-inductive charge the software request by an additional window the input of power factor value.

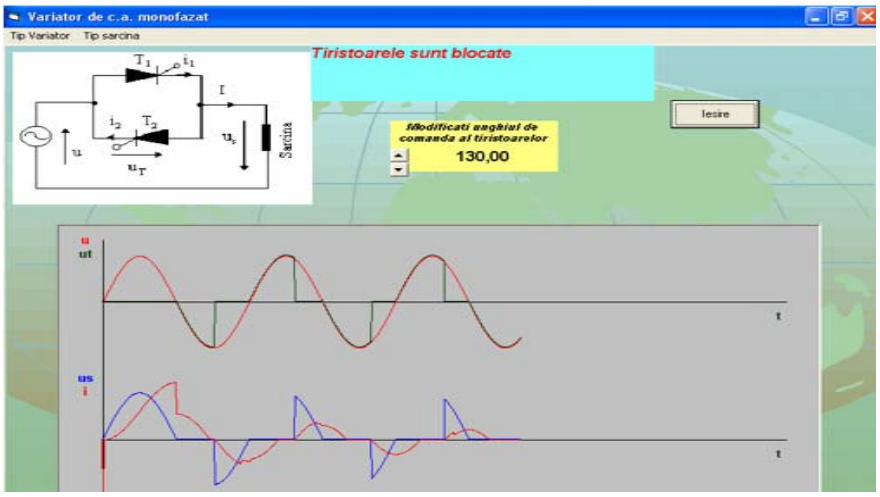

Fig. 12.The simulation windows for single/phase switch controller with resistive-inductive charge.

For the three-phase a.c. switch controller, the simulation window it is showed in figure 13 for a resistive charge. The simulation has been performed by modifying command angle.

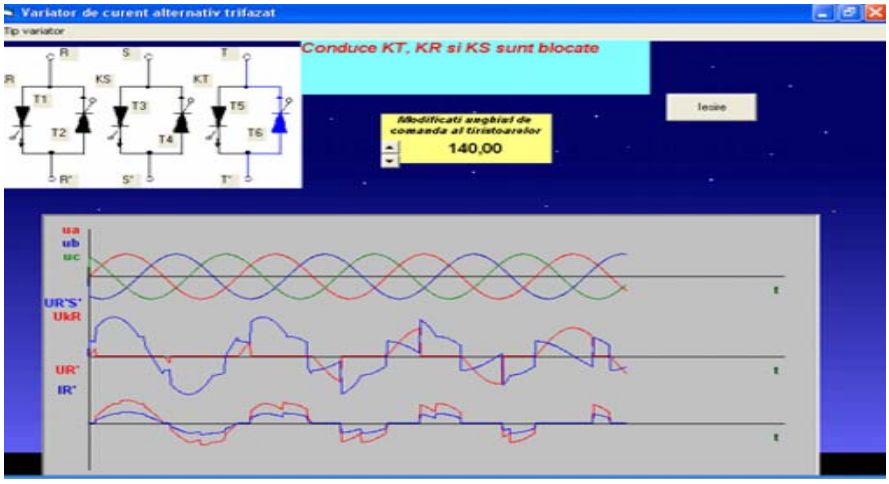

Fig.13. The simulation windows for three-phase switch controller with resistive charge.

3.2.D.c. switch controller

The d.c. switch controller, the chopper, it is the static converter who transform the entry continue voltage into a orthogonal voltage impulses. The exit voltage medium

value its may be modified between 0 and entry value of voltage, in function with the rapport between the period when the chopper is controlling and the period when this is blocked.

Figure 5 shows simulation window for function simulation of one of static variator by a quadrant realized with thyristor, being represented the wave forms characteristic to the charge, the main thyristor and the switch off circuit.

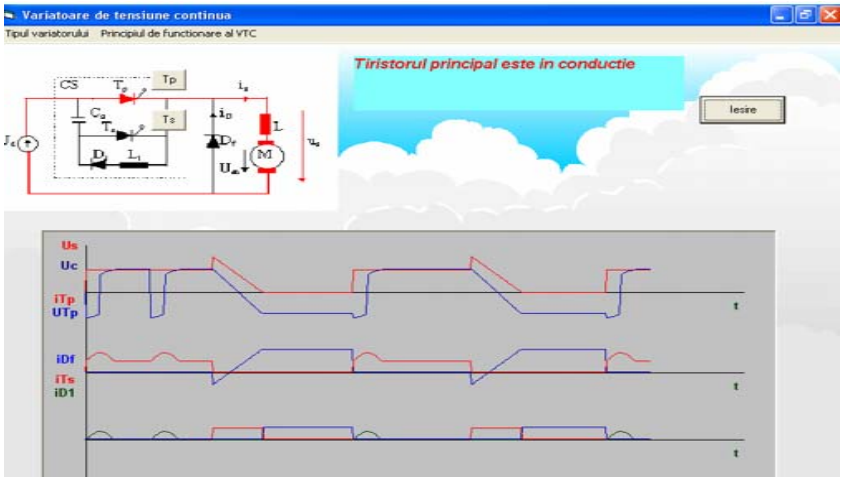

Fig. 5. Simulation window for function simulation of d.c. switch controller by a quadrant realized with thyristors.

Entering command in the main thyristor conductivity is to be done by pushing the related command button and to switch off the main thyristor, its related push button is pressed.

Figure 6 shows the simulation window related with the d.c. switch controller, in four quadrants from the same window, it is possible to be modified the operation quadrant (using the four radio buttons) and also the period for the switch controller or conductivity period.

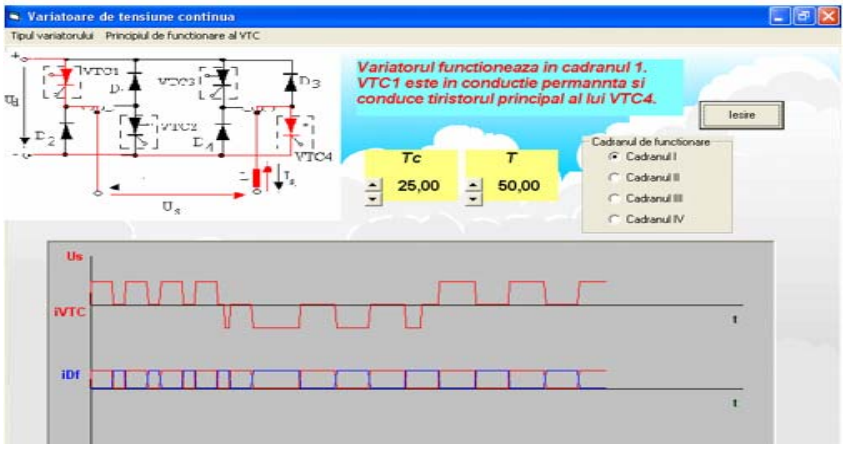

Fig.6.The simulation window related with the d.c. switch controller, in four quadrants.

4. CONCLUSIONS

This documentation describes a Windows application, useful for understanding the functioning of the static variators, converters, typing to cover all the needed aspects. This application has a teaching purpose, being useful for the students studying static converters.

REFERENCES

[1]. Marcu, M., Borca,.D. *Convertoare statice în acţionări electrice*. Editura TOPOEXIM, Bucureşti, 1999.
[2]. Tunsoiu, Ghe., *Acţionări electrice*. Editura Tehnică, Bucureşti, 1981.

Annals of the University of Petroşani, Electrical Engineering, 11 (2009) pages 32-41

VECTORIAL POSITION CONTROL SYSTEM OF THE GMF360 INDUSTRIAL ROBOT

ANGELA EGRI[1] , VALI-CHIVUTA SIRB[2] , OLIMPIU STOICUTA[3]

ABSTRACT: *The purpose of this paper is to present a new sysntesis of the estimator Gopinath extended used in vectorial control of the position of GMF360 industrial robot. The extended Gopinath observer proposed in this paper is designated to estimate the rotor flux components and the rotor resistance of the induction motor. This work presents a new strategy to assign the Gopinath matrix elements of the flux estimator in the EGO observer. The studied control system is based on the direct rotor flux orientation method (DFOC).*

KEY WORDS: *Extended Gopinath observer (EGO), Model Adaptive System (MRAS), Extended Luenberger Observer (ELO), GMF360 ROBOT*

1.INTRODUCTION

The paper presents a new flux and rotor resistance observer called Extended Gopinath observer (EGO). The design of the EGO observer is performed based on an adaptive mechanism using the notion of Popov hyperstability. Thus, this type of observer is included in the estimation methods type, based on an adaptation mechanism, along with the Extended Luenberger Observer (ELO) proposed by Kubota and the Model Adaptive System (MRAS) observer proposed by Schauder. In the second part of the paper we present the vectorial position colntoll system of the GMF360 industrial robot.

2.THE GOPINATH EXTENDED OBSERVER

The equations that define the rotor flux Gopinath observer are:

[1] *Assoc. prof. eng., phd. at the University of Petroşani;*
[2] *Lecturer eng. ,phd. at the University of Petroşani;*
[3] *Assist. eng. ,phd student at the University of Petroşani.*

$$\begin{cases} \dfrac{d}{dt}\hat{\underline{i}}_s = a_{11}^* \cdot \underline{i}_s + a_{12}^* \cdot \hat{\underline{\psi}}_r + b_{11}^* \cdot \underline{u}_s \\ \dfrac{d}{dt}\hat{\underline{\psi}}_r = a_{21}^* \cdot \underline{i}_s + a_{22}^* \cdot \hat{\underline{\psi}}_r + \underline{g} \cdot \left[\dfrac{d}{dt}\underline{i}_s - \dfrac{d}{dt}\hat{\underline{i}}_s \right] \end{cases} \quad (1)$$

where:

$$a_{11}^* = -\left(\frac{1}{T_s^* \cdot \sigma^*} + \frac{1-\sigma^*}{T_r^* \cdot \sigma^*} \right); a_{12}^* = a_{13}^* - j \cdot a_{14}^* \cdot z_p \cdot \omega_r;$$

$$a_{13}^* = \frac{L_m^*}{L_s^* \cdot L_r^* \cdot T_r^* \cdot \sigma^*}; a_{14}^* = \frac{L_m^*}{L_s^* \cdot L_r^* \cdot \sigma^*}; a_{21}^* = a_{31}^*; a_{31}^* = \frac{L_m^*}{T_r^*}$$

$$a_{22}^* = a_{33}^* + j \cdot z_p \cdot \omega_r; a_{33}^* = -\frac{1}{T_r^*}; b_{11}^* = \frac{1}{L_s^* \cdot \sigma^*}; T_s^* = \frac{L_s^*}{R_s^*}; \quad T_r^* = \frac{L_r^*}{R_r}; \quad \sigma^* = 1 - \frac{\left(L_m^*\right)^2}{L_s^* \cdot L_r^*}.$$

In the relations above, we marked with "*" the identified electrical sizes of the induction engine.The block diagram of the EGO is presented in figure 1.

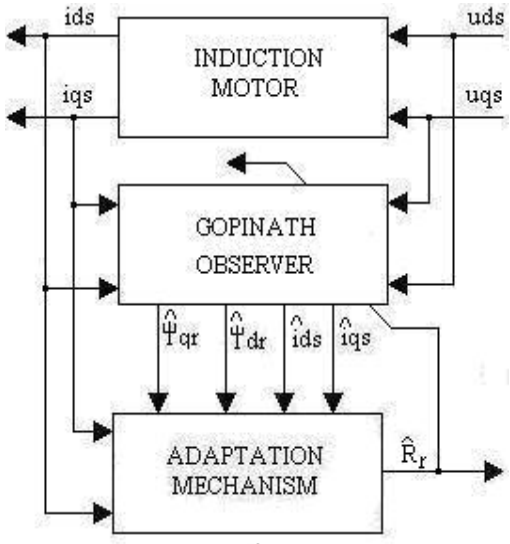

Figure 1. The Principle Schematic of the EGO Estimator

The block diagram of the system that describes the dynamic evolution of the error between the state of the reference model and the state of the adjustable model is presented in figure 2:

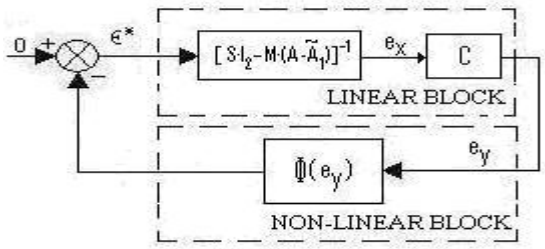

Figure 2. The block diagram of the system that describes the dynamic evolution of the error between the state of teh reference model and the state of the adjustable model

3. VECTORIAL SPEED CONTROL SYSTEM

The block diagram of the control system of the mechanical angular speed ω_r of the induction engine with a discreet orientation after the rotor flux (DFOC) is presented in fig.3.

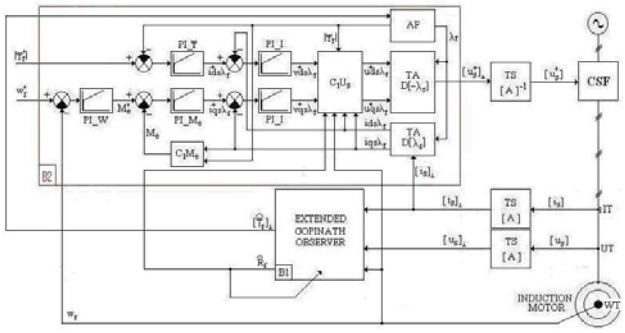

Fig.3. The block diagram of the DFCO vectorial control system which contains an EGO loop.

In fig. 3 we marked with B2 the control block of the speed control system with direct orientation after the rotor flux (DFOC) and with B1 the extended Gopinath estimator block (EGO). Some of the equations that define the vector control system are given by the elements which compose the field orientation block and consist of:
- Stator tensions decoupling block (C_1U_s):

$$\begin{cases} u^*_{ds\lambda_r} = \dfrac{1}{b^*_{11}} \cdot \left[b^*_{11} \cdot v^*_{ds\lambda_r} - a^*_{13} \cdot |\psi_r| - a^*_{31} \cdot \dfrac{i^2_{qs\lambda_r}}{|\psi_r|} - z_p \cdot \omega_r \cdot i_{qs\lambda_r} \right] \\ u^*_{qs\lambda_r} = \dfrac{1}{b^*_{11}} \cdot \left[b^*_{11} \cdot v^*_{qs\lambda_r} + a^*_{14} \cdot z_p \cdot \omega_r \cdot |\psi_r| + a^*_{31} \cdot \dfrac{i_{ds\lambda_r} \cdot i_{qs\lambda_r}}{|\psi_r|} + z_p \cdot \omega_r \cdot i_{ds\lambda_r} \right] \end{cases} \quad (2)$$

- PI flux regulator (PI_ψ) defined by the K_ψ proportionality constant and the T_ψ integration time:

$$\begin{cases} \dfrac{dx_6}{dt} = \psi_r^* - |\psi_r| \\ i_{ds\lambda_r}^* = \dfrac{K_\psi}{T_\psi} \cdot x_6 + K_\psi \cdot \left(\psi_r^* - |\psi_r|\right) \end{cases} \tag{3}$$

- Couple PI regulator (PI_M_e) defined by the K_M proportionality constant and the T_M integration time:

$$\begin{cases} \dfrac{dx_7}{dt} = M_e^* - M_e \\ i_{qs\lambda_r}^* = \dfrac{K_M}{T_M} \cdot x_7 + K_M \cdot \left(M_e^* - M_e\right) \end{cases} \tag{4}$$

- Mechanical angular speed PI regulator (PI_W) defined by the K_ω proportionality constant and the T_ω integration time:

$$\begin{cases} \dfrac{dx_8}{dt} = \omega_r^* - \omega_r \\ M_e^* = \dfrac{K_\omega}{T_\omega} \cdot x_8 + K_\omega \cdot \left(\omega_r^* - \omega_r\right) \end{cases} \tag{5}$$

- Current PI regulator (PI_I) defined by the K_i proportionality constant and the T_i integration time:

$$\begin{cases} \dfrac{dx_9}{dt} = i_{ds\lambda_r}^* - i_{ds\lambda_r} \\ v_{ds\lambda_r}^* = \dfrac{K_i}{T_i} \cdot x_9 + K_i \cdot \left(i_{ds\lambda_r}^* - i_{ds\lambda_r}\right) \end{cases}; \begin{cases} \dfrac{dx_{10}}{dt} = i_{qs\lambda_r}^* - i_{qs\lambda_r} \\ v_{qs\lambda_r}^* = \dfrac{K_i}{T_i} \cdot x_{10} + K_i \cdot \left(i_{qs\lambda_r}^* - i_{qs\lambda_r}\right) \end{cases} \tag{6}$$

- Flux analyser (AF):

$$\begin{cases} |\psi_r| = \sqrt{\psi_{dr}^2 + \psi_{qr}^2} \\ \sin\lambda_r = \dfrac{\psi_{qr}}{|\psi_r|}; \cos\lambda_r = \dfrac{\psi_{dr}}{|\psi_r|} \end{cases} \tag{7}$$

- The calculus of the couple block (C_1M_e):

$$M_e = K_a \cdot |\psi_r| \cdot i_{qs\lambda_r} \tag{8}$$

4. THE VECTORIAL CONTROL SYSTEM OF THE GMF 360 ROBOT

The vectorial control system of the GMF360 robot's position is based on the vectorial speed controll to wich a position loop is added around a PD (**P**roportional **D**iferential) regulator wich has the folowing transfer function:

.

$$G_\theta(s) = K_\theta \cdot (1 + T_\theta \cdot s) \quad (8)$$

where: K_θ is the proportionality coefficient

T_θ is the time differentiating constant of the regulator.For a precise analasys an induction based engine is chosen wich has the folowing parameters:

- Electrical parameters

$R_s = 0.371[\Omega]$; $R_r = 0.415[\Omega]$; $L_s = 0.08694[\mathrm{H}]$; $L_r = 0.08762[\mathrm{H}]$; $L_m = 0.08422[\mathrm{H}]$.

- Mechanical parameters

$$z_p = 2\,;\; J = 0.15\left[\mathrm{kg \cdot m^2}\right];\; F = 0.005\left[\frac{\mathrm{N \cdot m \cdot s}}{\mathrm{rad}}\right].$$

After tuning the regulators shown above using “poles and zeroes repartition method”, we get the folowing coefficients:

$$K_\psi = 501.3834\,;\; T_\psi = \frac{K_\psi}{2374.7}\,;\; K_i = 5.9881\,;\; T_i = \frac{K_i}{754.4176}\,;\; K_M = 10.1988\,;\; T_M = \frac{K_M}{1020}\,;$$

$$K_\omega = 10\,;\; T_\omega = \frac{K_\omega}{350}\,;\; K_R = 6\,;\; T_R = \frac{K_R}{4000}\,;\; K_\theta = 32000\,;\; T_\theta = 400\,.$$

where K_R and T_R are the proportionality constants and integration of the PI regulator of the adaptation mechanism’s component of the extended Luenberger estimator.With help of the regulators tuning coefficients of the system is completly defined.To show the role and performances of the tunig system shown above, we will present in the folowing part, the studied industrial robot. In figure 4 the GMF S360 tipe RRR robot wich has six degrees of freedom is presented.

For an in dept and clear analasys of the robot we used Matlab – Simulink to create the mathematical model in dynamic mode of the robot presented above. So, in figure 5 the Simulink block that implements this type of robot is presented, together with it’s mathematical model. The defining ecuations for the mathemathical model are:

$$T_1 = J_1 \cdot \frac{d^2\theta_1}{dt^2} + C_1 \cdot \frac{d\theta_1}{dt} + G_1 \cdot \theta_1 \quad (9)$$

$$T_2 = J_2 \cdot \frac{d^2\theta_2}{dt^2} + C_2 \cdot \frac{d\theta_2}{dt} + G_2 \cdot \theta_2 \quad (10)$$

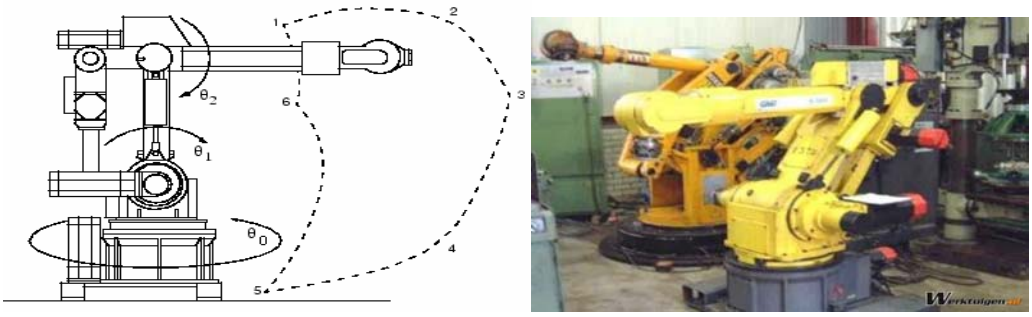

Figure 4. Industrial robot GMF S360

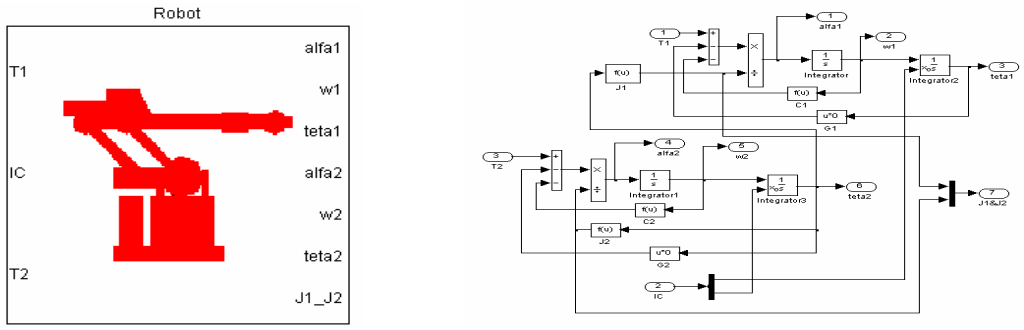

Figure 5. Mathematical model in Matlab – Simulink of the GMF S360 robot

where: J_1 and J_2 are the inertia moments of the joints one and two; C_1 and C_2 are the Coriolis coefficients of joints one and two, G_1 and G_2 are the gravitational coefficients of the two joints. In the mathematical model we considered joint 0 stationary so that $\theta_0 = 0[grade]$. Alfa$_1$ and alfa$_2$ are the accelerations of the two joints; w_1 and w_2 are the speeds of the two joints and teta$_1$, teta$_2$ the two joint's angles wich are shown in figure 4.In the robots model the folowing value were considered for the variables presented:

$$J_1 = 174.272 \cdot \theta_2^2 + 79.578 \cdot \theta_2 + 170\left[kg \cdot m^2\right];\ J_2 = 50\left[kg \cdot m^2\right]$$

$$C_1 = 84.5[N];\ C_2 = 50[N]$$

And the gravitational coefficients were considered to be 0.In the folowind we present the Simulink schemathic for the position's regulation system's analisis of the GMF S360 industrial robot.

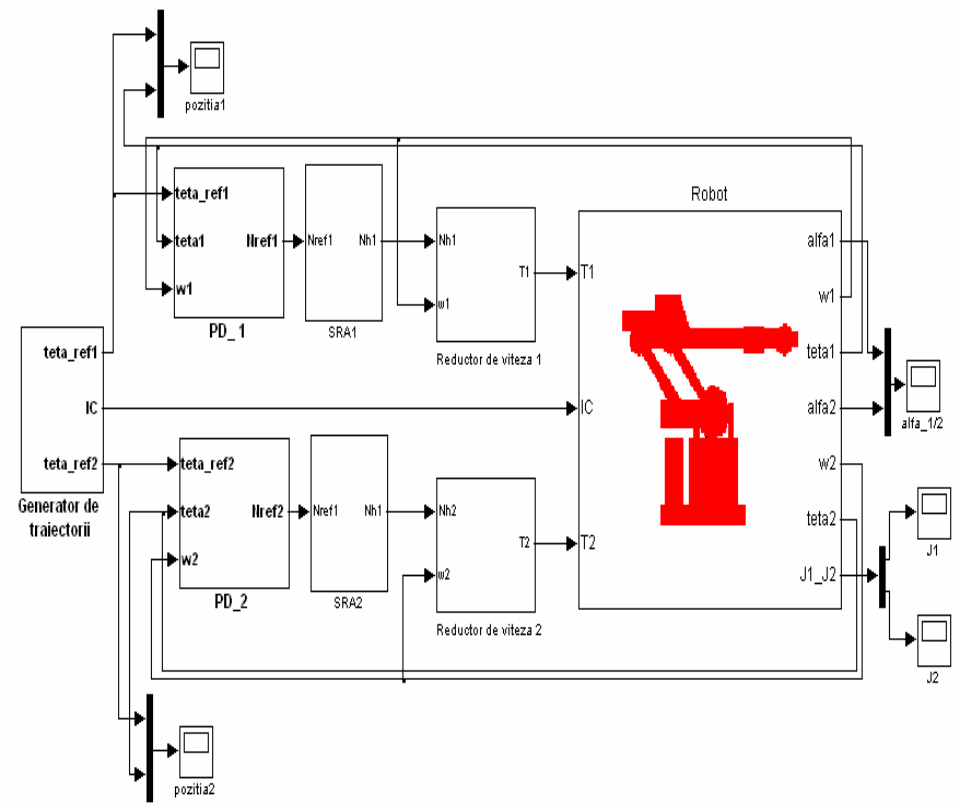

Figure 6. Matlab – Simulink simulation schematic of the GMF S360 robot

From the sismulation schemathic we notice that two systems of position regulation are used designed around the vectorial speed controll systems, refered to as SRA1 si SRA2. The automated regulator type PD of the position presented in the simulation schematic in the previous figure was implemented outside of the block schematic of SRA1 and of SRA2.

In the simulation, we took into consideration the mechanical speed reduction used by joints one and two of the GMF S360 robot . The reduction coefficient for both of the joints is 1/130.In the simulation we created a trajectory generating block, where we imposed a variation of the angle θ_1 between $\left(-\frac{\pi}{6} \quad \frac{\pi}{6}\right)$ and of the angle θ_2 between $\left(-\frac{\pi}{4} \quad \frac{\pi}{4}\right)$. After simulating we get the folowing results, presented in graphical form in the folowing figures:

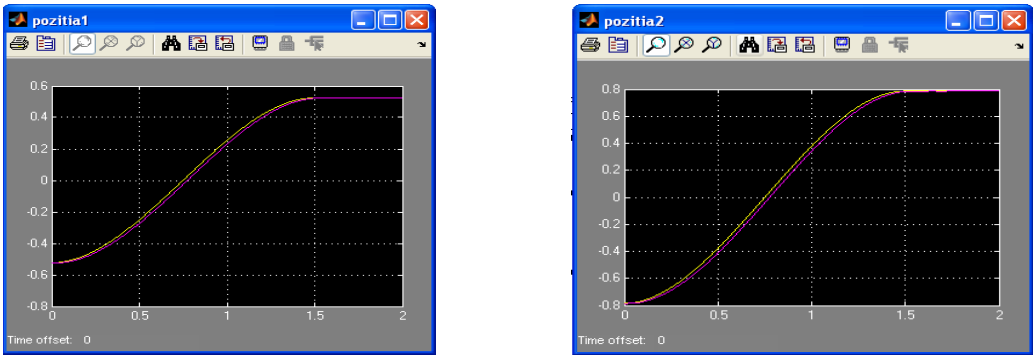

Figure 7. Teta1 and teta2 of the GMF S360 robot imposed (yellow) and mesured (purple)

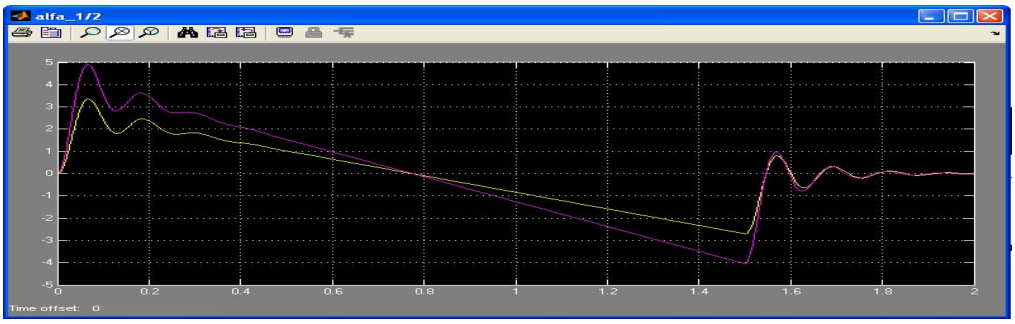

Figure 8. Accelerations of joints one (yellow) and two (purple) of the GMF S360 robot.

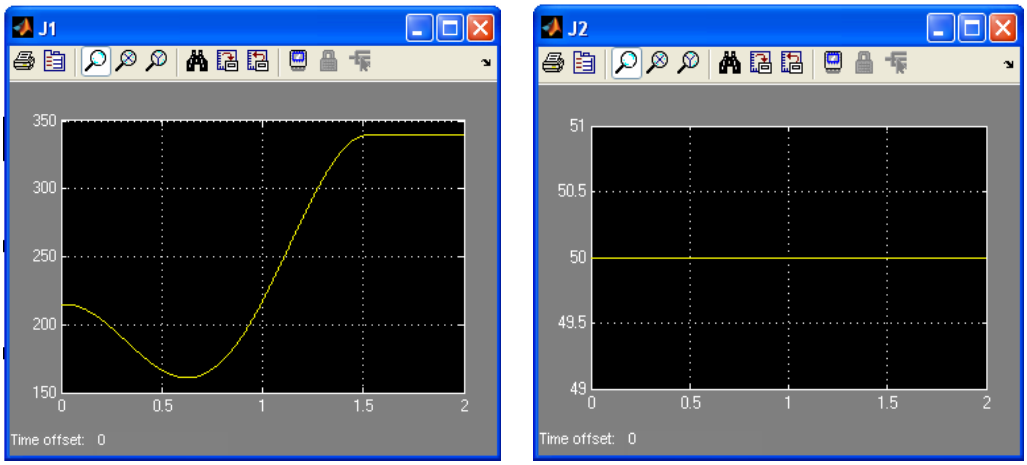

Figure 9. Variation in time of the inertia moments J_1 si J_2 GMF S360 robot.

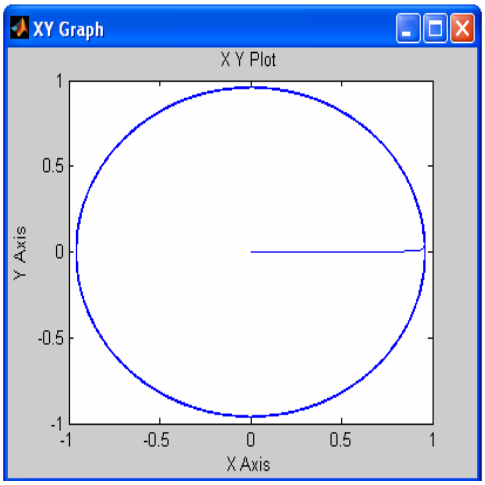

Figure10. Diagram of the estimated rotoric Flux of the induction motor

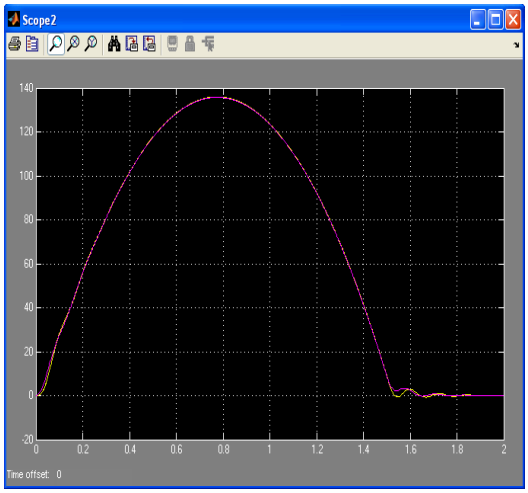

Figure 11. Variation in time of the imposed speed (purple) and the estimated (yellow) of the induction motor wich controlles joint one.

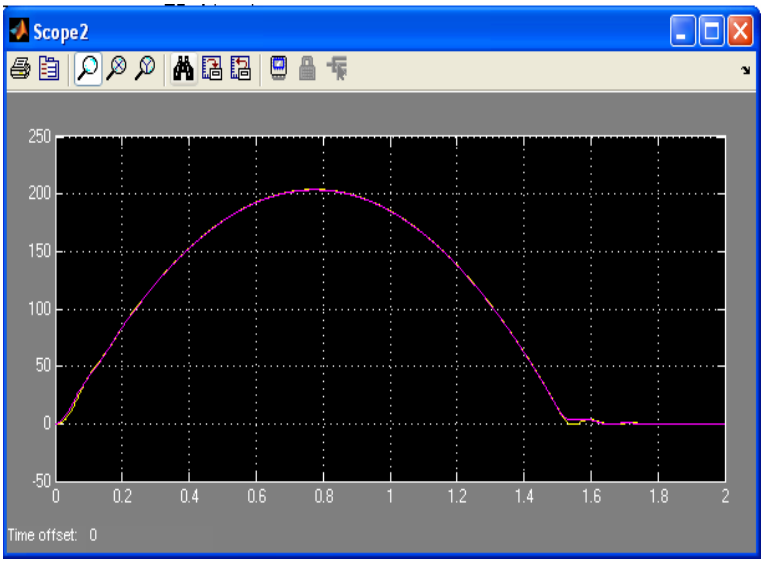

Figure. 12. Variation in time of the imposed speed (purple) and the estimated (yellow) of the induction motor wich controlles joint two.

From what we shown above we conclude that the regulation system presented in figure 6 has very good dynamic performances, so that it can be used successfully in practical aplications that need to modify the position of industrial robots.

5. CONCLUSIONS

This paper presents a new type of flux estimator and rotoric resistence of an induction motor called the extended Gopinath estiamtor.

The Gopinath flux estimator, whose gate matrix is calculated with the relations (3), ensures the adjustment system very good dynamic performances that gives us the possibility to assert, that such an estimator could be successfully used in industrial applications.

The paper imposes using induction servodrives versus countinous current servodrives in industrial robots.

This fact has a great impact on industrial robotics because of the advantages of induction servodrives comapared to the ones using continous current.

The only disadvantage of a system like this is the current relative high cost.

Because of the fact that the speed control system is made around an extended Gopinath estimator that estiamtes of course rotoric resistance, we can say that the vectorial control system of position is stabil at slow speeds when rotoric resistence increases with the increase of temperature.

REFERENCES

[1]. Schauder C., *Adaptive Speed Identification for Vector Control of Induction Motors without Rotational Transducers,* IEEE Trans. Ind.Applicat., vol.28, no.5, pages 1054- 1061, Sept- Oct., 1992.

[2]. Vas P., *Vector Control of AC Machines,* Clarondon press, Oxford, 1990.

[3]. Popov M., *Hyperstability of Control Systems,* Springer Verlag, New York, 1973.

.

Annals of the University of Petroşani, Electrical Engineering, 11 (2009) pages 42-49

THE EXPLOITATION OF HIGH ELECTRICAL POWER TRANSFORMERS AND AUTOTRANSFORMERS

ANDREI ROMANESCU[1], DRAGOS PASCULESCU[2]

ABSTRACT: *In the present work there is about the exploitation of transformers and autotransformers of high power of the national energy system, transformers that are found in all plants for the production of electricity authorized ANRE, as stations of transmission and distribution of electricity. The primary operation of these equipments includes the following:*

- *handling operations: the removal or placing under tension;*
- *operations command: batteries fans, switch contacts;*
- *operations to monitor the main nominal sizes that characterize the operation of power transformers: primary and secondary voltage, active and reactive power, frequency, loss;*
- *mode of action in some events;*
- *possible faults and their remedy in operation.*

KEY WORDS: *transformer, autotransformer, interface, switch box, control panel.*

1.GENERAL CONSIDERATIONS

In the power stations from Romania, according to the settlements issued by ANRE, the voltage produced in the electrical generators is 6-24kV. The economic transport of the produced power requires high voltages.

In place of use, however, the electricity must have a low voltage to be used by consumers. So, it is required the processing power of a certain voltage of electricity in different power. This problem is resolved simply and economically only in the case of the alternately current through transformers and power autotransformers.

Operation of transformers and high power autotransformers is based on ensuring uninterrupted operation of electrical installations, which have special importance, both because that follow disturbances in operation or exploitation of

[1] *Eng., Ph.D. student, Transelectrica, transport branch Sibiu, Alba Iulia Station, Romania*
[2] *Lecturer Eng., Ph.D., University of Petrosani, Romania*

maneuvers can be serious, but also because the electrical installations are more exposed upset than other types of installations. The gravity consequences comes primarily from the presence of the electrical installations, in general, in a complex energy system and is electrically interconnected with one another, a flaw appeared in a place, puts out of order the normal functioning of the entire system, secondly, the gravity faults in electrical installations is due to very high energies involved in carrying out their destructive effects leading to extremely high.

2.OPERATION OF TRANSFORMERS AND AUTOTRANSFORMERS

In the National Energy System disconnecting transformers (autotransformers) is usually on the load and then on the supply. Logging operation is done in reverse order. Maneuvers to impose tension in the empty AT-sites will be reduced to the minimum possible to avoid the demands and electrodynamics shock current magnetisation.

A particular attention should be paid for switching maneuvers contacts:

- avoid the automatic on extreme contacts;
- if the temperature of oil in autotransformers is below -10 ° C the operation of the contacts switch is prohibited;
- the switch contacts will act only after approval has been requested from the dispatcher with the authority of its decision and approval, and the commutation is going to be confirmed.

Figure 1. Power autotransformer S=200MVA

It is always necessary to look at the voltmeters when the contacts commutation and the increase/decrease tension were correctly done. When the transformers are put into function this operation is repeated in all stages.

If the autotransformer is back (not under tension) and should be put into service, even if the oil temperature in the autotransformer is less than -10 ° C, it will proceed as follows:

- according to the dispatch center's approval having authority of decision, the autotransformer will be put under tension by connecting it to the high-voltage switch (400 kV);
- when the oil from the autotransformer comes warm the switch will be operated;
- the switch of low voltage will be connected (220 kV).

In an overload operation, a continuous surveillance of the measuring equipment will be made:

- primary and secondary current;
- primary and secondary voltage;
- the oil temperature.

In the absence of the indicated factory building, the transformers cooled by natural circulation of oil and blowing air (NS) it is given a long operation to 60% of nominal power in its absence. Concerning the transformers with forced oil circulation and cooling blow air or water (FS or FA) , the operation of the transformer is allowed when the pumps or fans are stopped for a period of up to 10 minutes at full load or one hour at idle.

Chart 1

Overload [%]	30	60	75	100	140
Time[minutes]	120	30	15	7,5	3,5

Forced ventilation is turned on reaching a temperature of 55 ˚ C oil in the upper strata, and to overcome whatever the nominal current regardless the oil temperature. The cooling water installation in the transformers with forced cooling water will always be kept in operation regardless of the load size that is charged the transformer. At the service installation, the oil pump starts first and then that of the water and to the removal from service, it stops the water pump first and then the oil (to remove the possibility of entering the water in oil).

Figure 2.Trafo Guard Interface

Monitoring temperature, oil level control and automatic cooling installation of the transformer cooling / autotransformers of CNTEE Translelectrica is provided by the Trafó Guard (AKM). Trafo Guard calculates the autotransformer's wrappings temperature according to the oil temperature at a

higher level and the amount of current through wrappings, and the touch of the adjusted to thresholds it is recommended the operating run of cooling batteries or transformer / autotransformer release.

Trafo Guard oversees, and displays the screen through the following:

- higher oil temperature;
- current temperature on wrappings, date and time;
- the temperature of the core transformer (R, S, T phases);
- the oil level in the compartment related to the autotransformer and the oil level from the consrvatory compartment related to the switch contact;
- Start / stop automatic two-tier cooling batteries : Tr 1 at 75 ° C and Tr 2 to 85°C;
- the transformer release when the oil temperature reaches 90 C or if the windings temperature reach 100 ° C.

The cooling autotransformer consists of four fundamental cooling batteries and a back-up cooling battery. Each cooling battery consists of an oil electro pump and three fans, having three ways of operation:

- automatically when connect the switch;
- function depending automatically of temperature;
- manual.

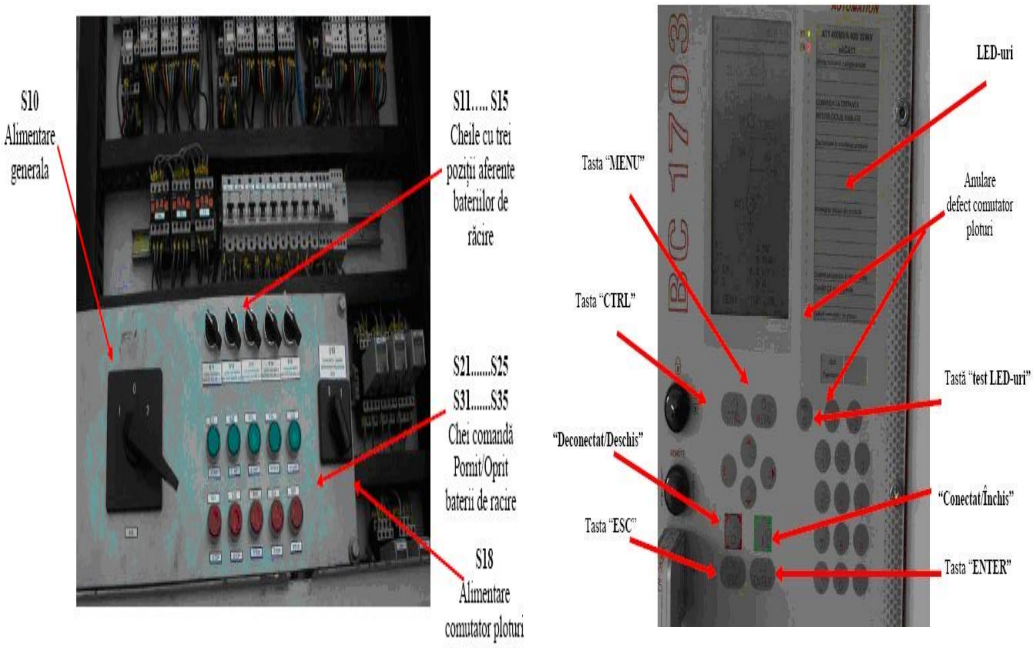

Figure 3. Local box and the transformer control panel from the relay cabin

The order of startup / shutdown cooling batteries run manually using the switch with four positions. The cooling installation is supervised with information about each cooling battery to the working point of the camera control (fig. 4).

In the normal scheme, all switches in the AT electric switch box and from the operation device of the switch contacts are in position "REMOTE" position, executing

commands from the control room, the working point . During operation the neutral will be rigidly connected to the ground.

There are visual controlled twice on a shift the following :

- the tank (if there is loss of oil);
- the conservative level of oil;
- the insulators;
- the air filters;
- the earth connections (2 links to the AT vat and another one to the AT null);
- the noise during the autotransformers operation ;
- the primary links to the terminals of the AT (heating etc);
- the restrictions and inscriptions;
- the cells and the equipment from the cell.

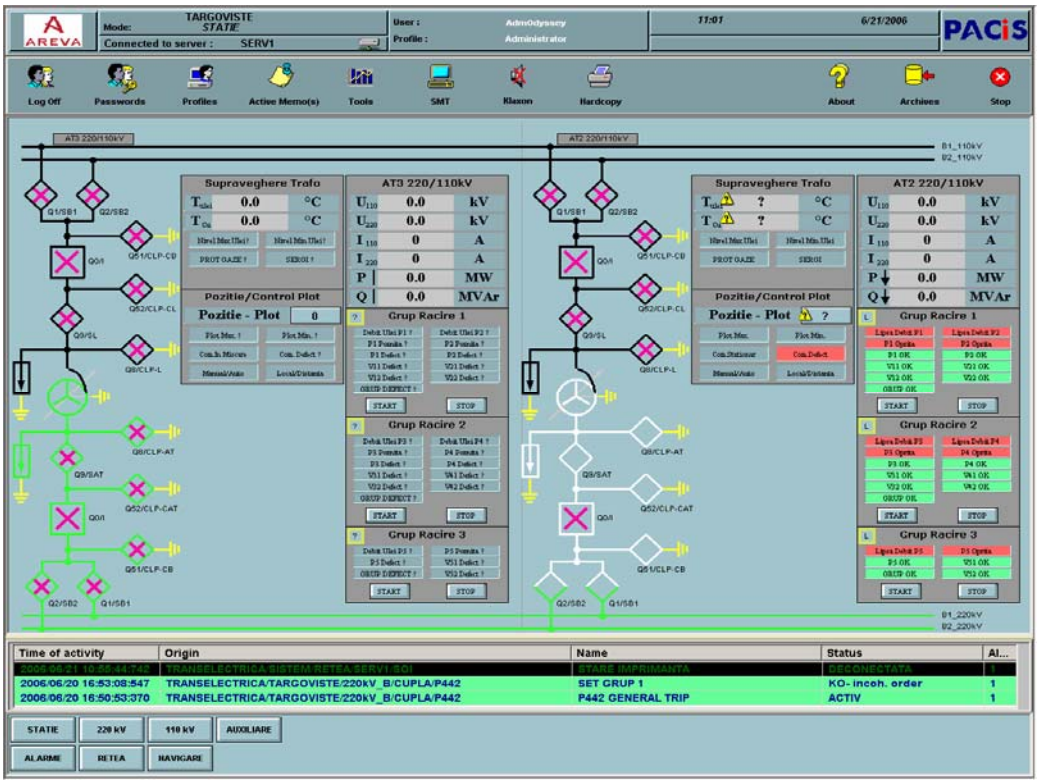

Figure 4. The interface of a system command and data acquisition of a transformer

Figure 5.Electric switch box transformer

In case of an event such as the signal of gas or the AT release through the protection of gas check, there are verified the chemical content of gases collected in the relay. If the gas is colorless and fireproof, the relay operation was due to the air from the transformer vat (autotransformer). If the gases are flammable, the power is caused by the faults in the autotransformer. The damage is immediately liquidated by the removal under the tension and it is brought the primary equipment into a separate visible state.

In case of overload it is announced the dispatch center, which takes the appropriate measures, and the operational personnel must continuously monitor the indicator devices.

In case of an event such as the signal of gas or the AT release through the protection of gas check, there are verified the chemical content of gases collected in the relay. If the gas is colorless and fireproof, the relay operation was due to the air from the transformer vat (autotransformer). If the gases are flammable, the power is caused by the faults in the autotransformer. The damage is immediately liquidated by the removal under the tension and it is brought the primary equipment into a separate visible state.

In case of overload it is announced the dispatch center, which takes the appropriate measures, and the operational personnel must continuously monitor the indicator devices.

The operation of the cooling installations will be checked at short intervals of time.

Any abnormal operating transformer found in the operation of the transformer/ autotransformer (oil leaks, over heating limits, abnormal noises, etc.), must be immediately communicated to the dispatch center with authority and decision management center operation, is recorded in the operative register and in the nonconformities (damages).

If the oil temperature increases: the operational staff will try to trace the causes of increase temperature, and then take remedial measures. It will be verified as loading transformers / autotransformers and the temperature corresponding to this load, the operation of the cooling installation (number of cooling batteries). It will follow the operation of oil pumps and fans for the battery. [4.5]

If the autotransformer / transformer are released:

- there are checked the alerts protections that have worked;
- there are investigated possible external causes that could produce the release (short-circuit network, overloading, damages to the installation protection);
- it is checked if the transformer / autotransformer, have no visible signs of damage.

If the release is due to external causes to the autotransformer, these can be in tension with the approval of the technical manager of the branch and of the center dispatcher authoritative decision.

If you can not find the cause release, in according with the technical manager of the branch, the transformer / autotransformer can be put into operation, if there are simultaneously satisfied the following conditions:

-the gas collected from gas relay do not smell and are not flammable;

-the release was ordered only by one of the basic protections of the autotransformer;

-samples and measurements had best results;

-in the absence of a primary event (back-up protections didn't start). [5.6]

3.CONCLUSIONS

The most important objectives for any company be it generation, transmission or distribution, in the settlement of the electricity market is to cut costs and increase safety in operation.

Because of this, the correct operation and maintenance of power transformers of SEN, it becomes more important because they are among the most expensive equipments, and their failure leads to the reduction of transport capacity and hence the industry efficiency.

Romanian Power System (SEN) is operating a number of 135 principal units and totalize 34525 MVA, as follows:

- 2 x 750/400 kV;
- 44 x 400/220 kV;
- 89 x 220/110 kV.

Economically and functionally, it is very important the management efficiency operation of these transformers, aimed at maximum use of existing transformers, taking the most efficient and remedy measures of the major faults.

REFERENCES

[1]. C. Saal, *Acţionări electrice şi automatizări*, Ed. Didactică şi Pedagogică, Bucureşti, 1980.
[2]. I. Boldea, *Transformatoare şi maşini electrice*, Ed. Politehnică, Timişoara, 2006
[3]. I. Dumitrache, *Optimizări în automatizări industriale*, Ed. Tehnică, Bucureşti, 1979.
[4].Al. Fransua, *Masini electrice uzuale, exploatare şi regimuri de funcţionare*, Ed. Tehnică, Bucureşti, 1973
[5]. *Regulament de exploatare tehnică a echipamentului din distribuţia primară, Icemenerg*, Bucureşti, 1987
[6]. *Documentaţii tehnice transformatoare şi autotransformatoare de mare putere*

Annals of the University of Petroşani, Electrical Engineering, 11 (2009) pages 50-59

COMPARATIVE STUDY FROM THE KALMAN FILTER'S STABILITY POINT OF VIEW AND THE LUENBERGER ESTIMATOR WITHIN A VECTORIAL CONTROL SYSTEM IN WHICH THE LUENBERGER ESTIMATOR IS PROJECTED ON SELF VALUE ROTARY BASED METHOD

CORNELIU MANDRESCU[1],OLIMPIU STOICUȚA[2]
NADIA STOICUȚA[3]

ABSTRACT: *In this paper it is considered that the vectorial electric acting system is a speed regulating system with a rotor flux orientation and the estimation of the rotor flux position is done through a Luenberger type estimator and respectively a Kalman type estimator. The purpose of this paper is the comparative study of the estimator's stability and of regulating systems that have included in their loop both the Luenberger and respectively the Kalman estimators.*

KEYWORDS: *Kalman estimator, Luenberger estimator, system stability, vectorial control.*

1.INTRODUCTION

The study is accomplished considering the following start data:

- The considered motor is an induction motor with a short-circuit rotor;
- The stability study is done by considering various variations of the motor speed and of the sampling time, in both, presence and absence of the measurement and process noises. In addition, in this study the digitization degree of the models used is to be considered;
- The regulators' tuning parameters within the vectorial regulation scheme are calculated for a regulation scheme with direct flux measurement as armature gap and with rotor flux orientation case. These parameters will be the same for both, the vectorial regulating scheme in which a Luenberger type estimator is used as well as in the case when a Kalman type estimator is used;

[1]*Assoc. prof. eng. phd at the University of Petroşani*
[2]*Assist. eng. phd student at the University of Petroşani*
[3] *Assist. phd student at the University of Petroşani;*

- The estimators' stability study is done considering the regulating loops.

For a better understanding of the studied issue we will make a short introduction of the Luenberger and Kalman type estimator.

2.THE KALMAN ESTIMATOR

In this paper the equations defining the Kalman estimator were written based on the stochastic type model of the induction motor, mathematical model given by the state canonical equations:

$$\begin{cases} x(k+1) = F_k \cdot x(k) + H_k \cdot u(k) + w(k) \\ y(k) = C \cdot x(k) + v(k) \end{cases} \tag{1}$$

in which the noise vector of the process $w(k)$ and the measurement noise $v(k)$ are considered to be Gaussian type with the following properties:

$$\begin{aligned} &E\left[w(k)\right] = E\left[v(k)\right] = 0; \\ &E\left[w(i) \cdot w^T(j)\right] = Q_k \cdot \delta_{ij}; \\ &E\left[v(i) \cdot v^T(j)\right] = R_k \cdot \delta_{ij} \end{aligned} \tag{2}$$

where E is the statistical mediae and δ_{ij} the Kronecker operator.

The F_k and H_k are obtained from the A_k and B matrixes of the induction motor's model in time domain through digitization. In practice, two such models have imposed themselves: one obtained through complete digitization that makes the Kalman estimator to be more precise but needs a performing processor in which to be implemented in:

$$\begin{aligned} F_k &= I + A_k \cdot T + A_k^2 \cdot T^2/2; \\ H_k &= B \cdot T + A_k \cdot B \cdot T^2/2 \end{aligned} \tag{3}$$

and another one obtained through simplified digitization that makes the Kalman estimator to be less precise but doesn't need a performing processor:

$$\begin{aligned} F_k &= I + A_k \cdot T; \\ H_k &= B \cdot T \end{aligned} \tag{4}$$

In the relations (3) and (4) the T variable is sampling time and the A_k, B and C matrixes have the following structure:

.

$$A_k=\begin{bmatrix} a_{11} & 0 & a_{13} & a_{14}\cdot\omega_k \\ 0 & a_{11} & a_{14}\cdot\omega_k & a_{13} \\ a_{31} & 0 & a_{33} & -\omega_k \\ 0 & a_{31} & \omega_k & a_{33} \end{bmatrix};\ B=\begin{bmatrix} b_{11} & 0 & 0 & 0 \\ 0 & b_{11} & 0 & 0 \end{bmatrix}^T;\ C=\begin{bmatrix} 1 & 0 & 0 & 0 \\ 0 & 1 & 0 & 0 \end{bmatrix} \tag{5}$$

where:

$$a_{11}=-\left(\frac{1}{T_s\cdot\sigma}+\frac{1-\sigma}{T_r\cdot\sigma}\right);\ a_{13}=\frac{L_m}{L_s\cdot L_r\cdot T_r\cdot\sigma};\ a_{14}=\frac{L_m}{L_s\cdot L_r\cdot\sigma};$$

$$a_{31}=\frac{L_m}{T_r};\ a_{33}=-\frac{1}{T_r};\ b_{11}=\frac{1}{L_s\cdot\sigma};\ T_s=\frac{L_s}{R_s};\ T_r=\frac{L_r}{R_r};\ \sigma=1-\frac{L_m^2}{L_s\cdot L_r}$$

and L_s, L_r, L_m the stator, rotor and mutual inductances; R_s, R_r the stator and rotor resistances and σ the dispersion mutual coefficient.

In these conditions, considering the measures of the entry vector the stator tensions reported to the dq oriented axis system:

$$u(k)=\left[u_{ds}(k)\quad u_{dq}(k)\right]^T \tag{6}$$

the measures of the state vector the stator currents and the rotor fluxes in the *dq* oriented axis system:

$$\hat{x}(k)=\left[i_{ds}(k)\quad i_{qs}(k)\quad \psi_{dr}(k)\quad \psi_{qr}(k)\right]^T \tag{7}$$

and the measures of the exit vector the stator currents in the *dq* oriented axis system:

$$y(k)=\left[i_{ds}(k)\quad i_{dq}(k)\right]^T \tag{8}$$

the algorithm of the Kalman estimator is:

$$\begin{aligned} &\Gamma(k/k-1)=F_{k-1}\cdot P(k-1/k-1)\cdot F_{k-1}^T+Q_{k-1} \\ &K(k)=\Gamma(k/k-1)\cdot C^T\cdot\left[C\cdot\Gamma(k/k-1)\cdot C^T+R_k\right]^{-1} \\ &\hat{x}(k/k-1)=F_{k-1}\cdot\hat{x}(k-1/k-1)+H_{k-1}\cdot u(k-1) \\ &\hat{x}(k/k)=\hat{x}(k/k-1)+K(k)\cdot\left[y(k)-C\cdot\hat{x}(k/k-1)\right] \\ &P(k/k)=\left[I_4-K(k)\cdot C\right]\cdot\Gamma(k/k-1) \end{aligned} \tag{9}$$

where $K(k)$ is the Kalman matrix, $\hat{x}(k/k)$ the estimated states vector at the $k\cdot T$ moment, $\Gamma(k/k-1)$ the co-variation matrix prior to the $\hat{x}(k/k-1)$ extrapolated state and $P(k/k)$ the co-variation matrix following the $\hat{x}(k/k)$ estimated state.

The estimation error of the Kalman estimator is $\tilde{x}(k/k)=x(k)-\hat{x}(k/k)$ and the initial conditions are $P(0/0)=P_0$ and $\hat{x}(0/0)=\hat{x}_0$ where $\hat{x}_0$ is considered a null vector

and P_0 is determined as a solution of the Ricatti estimator. The Q and R co-variation matrixes are constant and are tuned based on the following formulae [3]:

$$R=\begin{bmatrix}\sigma_u^2 & 0\\ 0 & \sigma_u^2\end{bmatrix};\ Q=\begin{bmatrix}\sigma_i^2 & 0 & \rho\cdot\sigma_\psi\cdot\sigma_i & 0\\ 0 & \sigma_i^2 & 0 & \rho\cdot\sigma_\psi\cdot\sigma_i\\ \rho\cdot\sigma_\psi\cdot\sigma_i & 0 & \sigma_\psi^2 & 0\\ 0 & \rho\cdot\sigma_\psi\cdot\sigma_i & 0 & \sigma_\psi^2\end{bmatrix} \tag{10}$$

where σ_u is the variant introduced by the u_s entry; σ_i and σ_ψ the variants introduced by the (i_s and ψ_r) state vector.

3.THE LUENBERGER ESTIMATOR

As it is the case with the Kalman estimator, the equations defining the Luenberger estimator were written based on the mathematical model of the induction motor, model given by the state canonical equations (1) in which the process noise vector $w(k)$ and measurement noise $v(k)$ are considered null. Based on the preceding the Luenberger estimator equation is:

$$\hat{x}(k+1)=F_k\cdot\hat{x}(k)+H_k\cdot u(k)+L_k\cdot\left(y(k)-C\cdot\hat{x}(k)\right) \tag{11}$$

where F_k and H_k matrixes are obtained from the A and B matrixes of the induction motor model in time domain through digitization using one of the methods given by the relations (3) and (4).

In on-line computing of the Luenberger matrix is used the method of rotating its self-values. These formulae composing the Luenberger matrix are to be deduced from the continuous case, obtaining the L matrix, from which, through digitization, the L_k matrix is deduced.

Through assuring the proportionality of the rotated self-values, it results the stability of the estimator no matter what the ω_k speed is. Obviously, the proportionality of the rotated self-values $\lambda_{estimator}=k\cdot e^{j\cdot\theta}\cdot\lambda_{motor}$ will not be maintained following the digitization, but the stability will. The mathematical expression of the L matrix is:

$$L=\begin{bmatrix}k_{11} & -k_{12}\\ k_{12} & k_{11}\\ k_{21} & -k_{22}\\ k_{22} & k_{21}\end{bmatrix} \tag{11}$$

where:

$$k_{11}=(a_1+a_2)\cdot(1-k_r)+\omega\cdot k_i;k_{12}=\omega_k\cdot(1-k_r)-k_i\cdot(a_1+a_2);$$

.

$$k_{21} = (a_3 + \gamma \cdot a_1) \cdot (1 - k_r^2 + k_i^2) - \gamma \cdot k_{11}; k_{22} = -2 \cdot k_r \cdot k_i \cdot (a_3 + \gamma \cdot a_1) - \gamma \cdot k_{12};$$
$$a_1 = a_{11}; a_2 = a_{33}; a_3 = a_{31}; \gamma = 1/a_{14}; k_r = k \cdot \cos(\theta); k_i = k \cdot \sin(\theta).$$

From (11) through digitization we obtain:

$$L_k = L \cdot T + A_k \cdot L \cdot T^2/2 \tag{12}$$

the Luenberger matrix obtained through complete digitization, respectively:

$$L_k = L \cdot T \tag{13}$$

the Luenberger matrix obtained through simplified digitization.

The estimating error of the Luenberger estimator is:

$$\tilde{x}(k) = x(k) - \hat{x}(k). \tag{14}$$

4.THE STUDY OF THE REGULATING SYSTEMS' STABILITY

The algorithm by which the study of the regulating systems' stability containing in their regulating loop both Kalman and Luenberger type estimators is the one determined in this paper [4]. The stability study is done by determining the self-values of an enlarged matrix. The matrix that is the basis of the stability study is:

$$F_\Delta = \begin{bmatrix} F_{k-1} - H_{k-1} \cdot M_a(k-1) & H_{k-1} \cdot M_a(k-1) \\ 0 & (I - K_a(k) \cdot C) \cdot F_{k-1} \end{bmatrix} \tag{15}$$

where M_a is the command matrix that links the entry vector with the state vector and K_a equals the $K(k)$ Kalman matrix in the case of studying the regulating system's stability containing in his loop a Kalman estimator, respectively the L_k Luenberger matrix in case the regulating system contains in his loop a Luenberger estimator.

The relation that the M_a command matrix has to verify is:

$$u(k) = -M_a(k) \cdot \hat{x}(k) \tag{16}$$

The M_a matrix that verifies the (16) relation has the following structure:

$$M_a(k) = \begin{bmatrix} 0 & 0 & -\dfrac{u_{ds}(k)}{|\psi_r(k)|} & \dfrac{u_{qs}(k)}{|\psi_r(k)|} \\ 0 & 0 & \dfrac{u_{qs}(k)}{|\psi_r(k)|} & -\dfrac{u_{ds}(k)}{|\psi_r(k)|} \end{bmatrix} \tag{16}$$

5.APPLICATION

In order to exemplify the preceding an induction motor with a short-circuited motor having the following values of the parameters was considered:

$$P_N = 500\,[W];\ U_N = 127\,[V];\ I_N = 2.9\,[A];\ n_N = 1400\,[rot/\min];$$
$$z_p = 2;\ M_N = 3.41\,[Nm];\ R_s = 4.495\,[\Omega];\ R_r = 5.365\,[\Omega];$$
$$L_s = 165\,[mH];\ L_r = 162\,[mH];\ L_m = 149\,[mH];\ J = 0.00095\,[Kgm^2].$$

The study of the stability was realized through real-time simulation in Matlab-Simulink using S_function type blocks. First of all, we have to mention that for different tachograms of the reference speed as well as for different tuning parameters of the regulators the self-values of the regulating system that contains in his loop one of the two estimators will be different during transitory time. Because of this, the tuning parameters of the regulators used within the regulating system will be identical in both cases, when using a Kalman estimator or a Luenberger estimator.

The tuning parameters of the *PI* regulator were calculated for a direct flux measurement as armature gap and with rotor flux orientation scheme. These values are:

- For the speed regulator, the proportional component $k_\omega = 10$ and the time component is $T_\omega = 9000$ [sec];
- For the couple regulator the proportional component $k_M = 10.1988$ and the time component $T_M = 1020$ [sec];
- For the current regulators the proportional component $k_I = 5.9881$ and the time component $T_I = 754.4176$ [sec];
- For the flux regulator, the proportional component $k_\psi = 501.3834$ and the time component $T_\psi = 2374.7$ [sec].

Similar to the case of the regulators' tuning parameters, the reference tachogram of the regulating system will be identical in all the cases of the stability study from the time of speed increase to the reference level point of view. In all the studied cases, the increase time is one second, no matter what the imposed reference speed is.

From these considerations, the first case studied is when the Luenberger and Kalman estimators are implemented using the complete digitization method. The study of the stability in this case is done at very high speeds and a very low sampling time with no measurement noises. Following the simulation were obtained the following graphs of the self-values variations in case of using the Luenberger estimator (fig.1.a) and the Kalman estimator (fig.1.b), when the reference number of rotations is 30000 [rot/min] and in the case of the Luenberger estimator the value of the *k* coefficient is 1.3 and $\theta = 5\,[\text{deg}]$. In the graphs the self-values of the estimator in open system will be emphasized with black color; the self-values of the motor with blue color and with red the self-values of the regulating system that contains in his loop one of the two estimators.

.

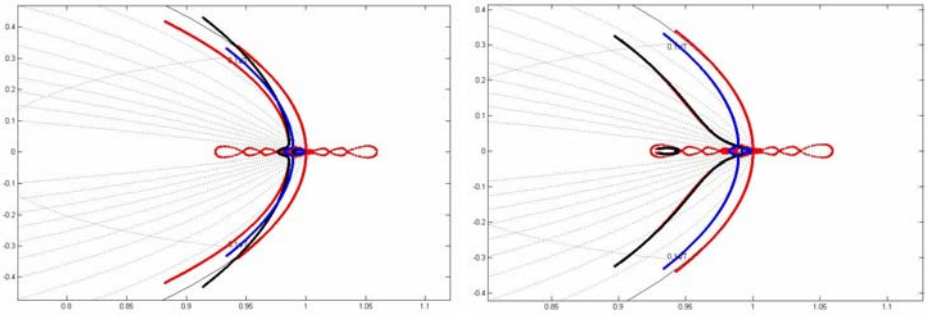

Figure 1. The graphs of the self-values: Luenberger (a) and the Kalman (b)

The sampling time used is $T = 53.3\,[\mu\text{sec}]$ specific for TMS320F2812 processor, when a commutation speed of 18.75 [kHz] is wanted for the IGBT's. Comparing the two graphs, one may notice that the Luenberger estimator in open loop is closing to the edge of stability even becoming unstable starting with a rotation speed of 22800 [rot/min] while the Kalman estimator in open loop behaves very well even at the imposed reference speed. On the other hand, both, the regulating system that contains in his loop the Luenberger estimator and the regulating system that contains in his loop the Kalman estimator is internally stable. One may notice that in the moment when the engine is started the regulating system is unstable and, as the speed of the motor tends towards the reference speed it becomes internally stable. From the dynamic performance point of view it is interesting to notice the fact that when the self-values of the motor are on the right side of the self-values of the estimator, the dynamic performances of the regulating system are very good. Comparing the two graphs from this point of view, we may say that the Luenberger estimator behaves very well from both, from stability point of view as well as the dynamic performances point of view to the speed of 12000 [rot/min] while the Kalman estimator behaves very well for the entire variation range. At speeds exceeding 40000 [rot/min] both, the Kalman estimator and the regulating system containing the Kalman or Luenberger estimators becomes unstable.

The second case studied is when the complete digitization method is used to implement the Kalman and Luenberger estimators, but the sampling time is higher. In this case, too, the process and measurement noises are null. Following the simulation with a sampling time of $T = 426.7\,[\mu\text{sec}]$ corresponding the processor mentioned above, for an IGBT commutation speed of 2.34 [kHz] one may obtain the following two graphs corresponding to the Luenberger (fig.2.a) and respectively the Kalman estimator (fig.2.b).

The imposed reference speed in this case is 10000 [rot/min]. One may notice that the instability of the Luenberger estimator as well as that of the regulating system that contains in his loop a Luenberger estimator occurs at a speed much smaller than in case of using a sampling time smaller than in this case. As in the preceding case a staying behind phenomenon occurs for the self-values of the estimator compared to the self values of the motor, phenomenon that leads to a decrease in dynamic performance. This thing happens when exceeding the speed of 5500 [rot/min] in the

case of the Luenberger estimator and 9000 [rot/min] in that of the Kalman estimator. As for the preceding case, when starting the motor the regulating system is unstable tending to be internally stable as the motor speed tends to the reference speed. The regulating systems become unstable at speeds near the reference speed soon after the dynamic performances of the estimators are lost.

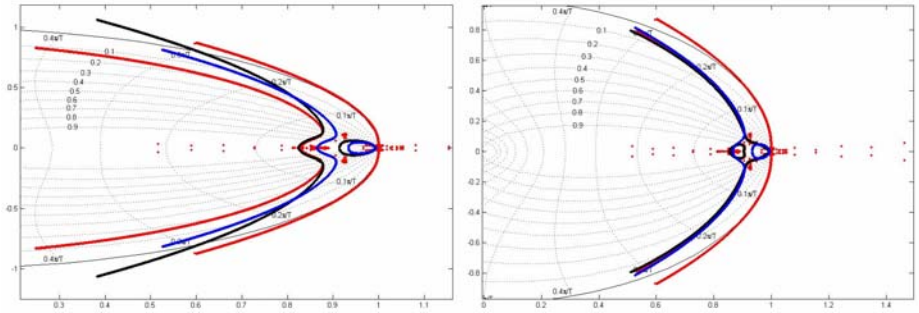

Figure 2. The graphs of the self-values: Luenberger (a) and the Kalman (b)

The third case analyzed is when the simplified digitization method is used to implement the Luenberger respectively the Kalman estimator. In this study the sampling time used is identical to the one in the first case. The study of the stability is done in this situation too without considering the process and measurement noises at a speed of 10000 [rot/min]. Following the real-time simulation one may obtain the following graphs corresponding to the Luenberger (fig.3.a) and respectively the Kalman estimator (fig.3.b). Comparing the two graphs one may notice that the effect of simplified digitization is very much like using a higher sampling time. The speed at which the estimator instability occurs higher speed than the preceding case. In this case the regulating system becomes unstable at medium speeds so that this method cannot be used within high speed regulating systems. In all the prior cases presented the analysis of the Luenberger estimator was done for $k = 1.3$ and $\theta = 5[\text{deg}]$.

In final we present the self-values of the estimator and of the regulating system that contains in his loop the Luenberger estimator, was done for $k = 20$ and $\theta = 5[\text{deg}]$. The result of the real-time simulation for the priory presented case is exposed in the following graph (fig.3.c).

The study of the stability in this case was realized for a complete digitization using the same sampling time as in the first case. In this case too the study was conducted lacking the process and measurement noises, for a reference speed of 10000 [rot/min]. One may notice that the estimator and the regulating system becomes unstable right after the speed of 5129 [rot/min] is exceeded. In another words, the higher k is the lower the speed at which instability occurs.

In case the study of the stability is done with the presence with process and measurement noises, the graphs of the self-values are approximately identical with the difference that the speed limit where dynamic performances are good decreases. This occurs more emphasized in case of the estimator and regulating system that uses in its loop a Luenberger estimator.

.

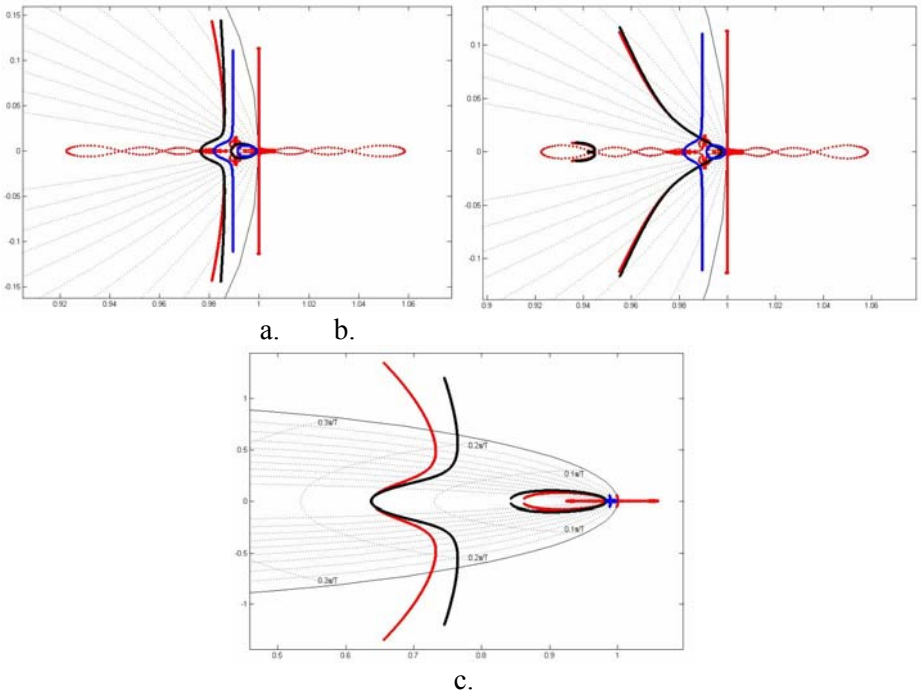

a. b.

c.

Figure 3. The graphs of the self-values

5.CONCLUSIONS

This paper presents an algorithm for studying the stability that can be used during vectorial control system's operation with an induction motor. Consequently, such algorithm can be implemented in parallel to the regulating system within a performing processor.

In the case of the estimator and that of the control system that has included in its loop a Luenberger estimator, one may notice that the estimator becomes unstable at high speeds and in the case of using simplified digitization the instability occurs quicker due to the amplification factor k. This thing remains valid for the regulating system too, becoming unstable as soon as the dynamic performances of the estimator get worse, in another words when the self-values of the estimator remain behind the self-values of the motor.

In the case of the Kalman estimator, the conclusions are identical with the difference that the speed values at which the instability occurs are much greater than the case of Luenberger. We may notice that in the case of using a high sampling time, the self-values of the motor, estimator and some of the self-values of the regulating system are almost identical, with the difference occurring at high speed where the dynamic performances of the estimator decrease.

Comparing the two estimators and the regulating systems we may say without any doubt that the estimator and regulating system that has in its loop a Kalman estimator are superior to the estimator and regulating system that has in its loop a

Luenberger estimator. The only practical disadvantage is the high computing effort as well as tuning the co-variation matrixes Q and R.

Based on the presented algorithm one may realize a real-time simulation with hardware included in the loop that will allow the obtaining of the self-values of the estimator, motor and regulating system for various working regimes of the motor.

REFERENCES

[1]. Mandrescu C., Stoicuta O., *Stability Analisys of the Direct Field Oriented Control System of the Induction Motor*, Control Systems and Computer Science CSCS-15, Bucuresti, Romania, 2007

[2]. Stoicuta O., Campen H., Pana T., *Comparative Study of the Stability Vector Control Systems with Luenberger and Kalman type Estimation***,** International Conference AQTR, Cluj-Napoca, Romania, pp. 35-41, 2006

[3]. Stoicuta O., Pana T., *Asymptotic Stability Study of induction motor vector control systems, with Luenberger observer***,** International Conference AQTR, pp. 242-247, 2008

[4]. Stoicuta O., Pana T., *Asymptotic Stability of a Speed Vector Control System for an Induction Motor that Contain in it's Loop a Gopinat Observer*, In Proceeding of the National Conference on Electrical Drives, 14th Edition, Timisoara, Romania, pp. 253-258, 2008

[5]. Stoicuta O., Pana T., Mandrescu, C., Egri, A., Sirb, V., Stoicuta, N. *Asymptotic Stability Study of an Induction Motor Speed Control System with Extended Gopinat Observer,* Control Systems and Computer Science CSCS-17, Bucuresti, Romania, pp. 87-94, 2009

[6]. Stoicuta O., Pana T., *Stability Study of an Induction Motor Vector - Controlled System using Extended Gopinath Estimator*, 8th International Conference on Advanced Electromechanical Motion Systems ELECTROMOTION Lille, France, (2009).

[7]. Pana T., Stoicuta O., *Stability Study of Kalman Filter in IM Vector-Controlled Systems*, National Conference CNAE, Cluj-Napoca, Romania, pp. 191-196, (2006).

[8]. Pana T., Stoicuta O., *Small speed asymptotic stability study of induction motor sensorless vector control systems with extended Luenberger estimator*, AQTR 2008, Cluj – Napoca, Romania, Pages: 248 – 253, (2008).

[9]. Pana T., Stoicuta O., *Small speed asymptotic stability study of an induction motor sensorless speed control system with extended Luenberger estimator*, In proceedings of the International Conference on Optimization of Electrical and Electronic Equipment – OPTIM 2008, 11th EDITION; Brasov, Romania, Pages: 175 – 180, (2008).

[10]. Pana T., Stoicuta O., *Small speed asymptotic stability study of an induction motor sensorless speed control system with extended Gopinath observer*, In proceedings of the European Conference on Modelling and Simulation – ECMS 2009, Madrid, Spain, Pages: 175 – 180, (2009).

.

Annals of the University of Petroşani, Electrical Engineering, 11 (2009) pages 60-65

POSSIBILITIES TO MODERNIZE THE DISPATCH SYSTEMS, COMMAND AND CONTROL OF THE NEUTRALIZATION INSTALLATIONS OF INDUSTRIAL WATERS

CONSTANTIN STEFAN[1], DRAGOS PASCULESCU[2]

ABSTRACT: *The object of this work is to improve the dispatching systems, the command and the control of the neutralization installations of the waters from the industrial processes.*

This work aims to solve the problem of the sewage from the industry (in the installation of metal roofing of chroming and phosphating as well as the power and thermoelectric stations) through the development of modern treatments (neutralization) of sewage.

We can also talk about the partial or total reuse of treated sewage in the technological processes from the station, and of those derived from metal roofing (phosphating, chroming) through its discharge to the sewer in accordance with the worldwide.

KEY WORDS: *dispatch systems, industrial waters, monitoring system, enivromental technologies, higher dispatch*

1.GENERAL CONSIDERATIONS

Considering the major environmental changes that have an impact on the water resources of the planet, the water problem should be seen in a global context.

As we know, the demographic development of the planet recorded and it is possible to record in the future a constant rhythm which brings for discussion a possible water crisis, maybe not at the level of requirement but especially at the level of administration.

In this global context the International Committee of Standardization ISO/TC 224 has been established in 2001, to develop standard that provides guidelines for drinking water and sewerage, standards intended to help the authorities department and

[1] *Eng., Ph.D. student, S.C.Pirelli & ECO. Technology*
[2] *Lecturer Eng., Ph.D., University of Petrosani, Romania*

their operators to achieve the quality level that can best meet consumer expectations and the principles of a sustainable development [6].

For all these requirements, it was defined the concept of "**environmental technology**".

The "environmental technologies" are those technologies through the application of which to obtain a lower impact on the environment than that generated by the existing relevant alternative technologies. The definition should be understood in a broader sense, the environmental technologies, including methods and procedures, materials and services, utilities and administrative and organizational systems. The environmental technologies include, in general, the "clean" technologies, as: the technologies for the pollution control (the control of water pollution, of the air and the waste management), the application of new technologies-less polluting, products and services less consuming of energy and natural resources, practices of a more efficient use of natural resources (e.g. efficient systems for water treatment, efficient technologies concerning the energy). The advantages of the application of environmental technologies are, in general, in a large potential to reduce operating costs and increase the productivity, thereby contributing to an increased competitiveness as a result of reducing the consumption of raw materials and energy, the level of emissions pollutants and by preventing the waste engendering.

In the context defined above, the environmental technologies are applied in almost all the sectors of activity, their use generating long term advantages that outrun the initial costs of investment and create the premises for reducing the environmental externalities generated by economic activities.

The water authorities control additional unannounced, at irregular periods of time, taking place at a random check to see if the self-monitoring results are reliable.

The current authorizations for water include the following essential components as core content:

- heavy metals, if they are relevant as a result of their use;
- the concentration values and the quantities for copper, nickel, and chromium from the metal coating lines, reductions in sewage around 90% after the neutralization;
- the requirements for the improvement of the sewage conditions (further measures);
- the monitoring settlement:
  - -self-control (proper monitoring)
  - monitoring by the authority

The most important requirements to be really fulfilled are that the limiting adequate values to be frequently monitored. As a result, comprehensive obligations of self- monitoring are imposed to the enterprises.

2. OBJECTIVES

To find an easy way to use these requirements, it is trying to develop a system of an effective dispatching (management) that should simultaneously assure the leadership of the technology process to enable the information exchange with a

superior network and should be uniform as the technical development, operation and maintenance.

The main purpose in the management of a technological facility lies in optimizing its operation in compliance with the requirements for total cost and environmental protection, ensuring in the same time the maximum availability and the safety operation.

Therefore, the system of management should ensure:

- the increased safety in the installations' operation, avoiding damages to the effects on personnel or equipments and increasing the availability of manufacturing capacity;
- the economics operation achieving reduced consumptions of certain high yields and thus obtaining lower production costs;
- the improvement of working conditions and reduces the volume of operations that require physical effort and increase the skills of the operating personnel.
- reduce the need for routines activities, thus providing the possibility to minimize the labor involved in the operating activities, maintenance and administration;
- a flexible concept of communication that allows access to all data process necessary to manage the operational process, a system of management with programmable equipments, also allowing the integration of different automation systems from different generations;
- conveying the information to a superior network (internal dispatching);
- to allow further developments it is necessary an open system [2].

3.SOLUTIONS

The solution that is going to carry out is to provide information to the next higher level that can be found in figure 2 to that of the local monitoring represented in figure 1 as follows:

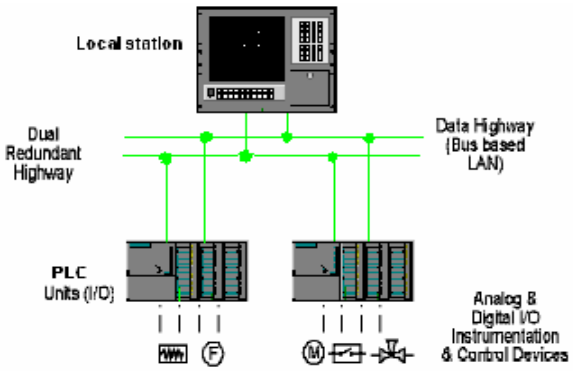
Local station
Dual Redundant Highway
Data Highway (Bus based LAN)
PLC Units (I/O)
Analog & Digital I/O Instrumentation & Control Devices

Figure 1. Local monitoring system

- to represent in the form of a synoptic scheme the whole technological process represented in figure 2. These schemes allow the visual modeling representation in the form of a picture which are placed on items such as values collected from the process equipment and measurement field, elements related to other schemes , representations of diagrams, etc…

- maintaining and permanently updating a database that contains either momentary values neither average account, database evolution etc….

- the chronological records of events (overshoot/recurrences in size of the analogue limits, binary changing states);
- the publication of reports at the time, day and month;
- printing the reports and the evolution if data graphs;
- visual alarm in fault operating conditions;
- displaying the current and the historical process of size. The current graphs should allow a quick view of the graph's size to see its evolution. Historical charts allow the grouping of several sizes on the same diagram in order to review the data;
- orientation to communications based on the protocol TCP/IP (Transmission Control Protocol/Internet Protocol), which allows access to the specialized users in data acquisition process of the neutralization installations;
- accessing the data or the operation of various functions LAN (Local Area Network) network, through several computer stations active simultaneously;
- the possibility of distance communication with a higher level (dispatcher) to its request, for transmitting data from remote process parameters followed in the process by an Ethernet interface communication and a suitable communication system described in figure 2 [3,4];
- to implement the programs and the service units with an extended program.

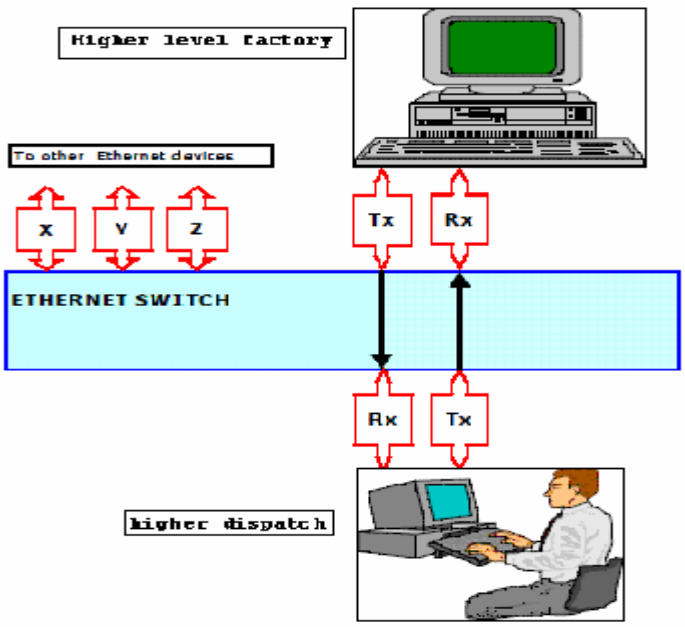

Figure 2. Higher level dispatching using a PC intermediated by the Internet.

IT System SCADA (System Control and Data Acquisition) is a software designed to allow the dispatching and the flow monitoring technology through a supervisor system PC, which receives the data transmitted by remote communication networks Profibus or Ethernet from the programmable logic controller from the process, data can be: electrical and process parameters of the state machines, alarms

and commands from the remote programmed and measured recipes. This information, incorporated into a database, will enable their storage, to display and transmit the request through the Internet.

The system will be designed on several levels of access:

- Total access, or
- partial access, where only a part of the authorized persons can view the operation of the Internet without being able to order equipment in the flow. The synoptic scheme related to the technological flow will be achieved on a display LCD with high resolution.

The dispatcher will be equipped with a server that will store information and coupled to the Internet for data transmission to a higher level.

Contributions that are expected to be brought to the development of scientific knowledge:

- Reducing energy consumptions by 10% - - -15%;
- reducing stationary time due to the reliability and the action of the automation components;
- reducing costs in the maintenance-repair using appropriate and reliable equipment;
- generating factor for the training of the staff operator maintenance;
- factor for reducing the cost price on the final product;
- an efficient control over the chemical nature of water discharged to the sewage.

4.EQUIPMENTS FOR EXPERIMENTS

To enforce these solutions it is necessary to use the following components:

- subsystem for data acquisition and their primary processing: level transducers, pH-meter, redox-meter, the agitators starting, the command of the electro valves and the pumps, PLC (Programmable Logic Controller), block operator HMI (Human Machine Interface);
- subsystem of communication: Profibus, Ethernet, wireless modem, antennas and communication servers;
- factory dispatcher subsystem (PC, printer and software required to view and control the equipment);
- automatic acquisition of technological process parameters through transducers that generate unified signals (4….20mA; 0/2….10 mV).

5.CONCLUSIONS

A modern system of automation, equipment based on logic programmable area, ensure increased quality of business management in all phases of the operation normal-start-stop (deliberate or damage). The management system based on equipment with programmable logic is used for office automation, an area of performance.

The innovation of this project is mainly the possibility of introducing the

modular decentralized structures distributed on the process and performed by the PLC (Programmable Logic Controller), with all the facilities provided by them, as well as the possibility to interface several interactive systems as HMI with PC by the agency of SCADA.

REFERENCES

[1]. Adriana Alexandru, *Tratat de inginerie electrica. Senzori si traductoare*, Editura Matrix Rom, Bucuresti 2004.
[2]. Cristian Mateescu si Luminita Mateescu, *Sisteme de comanda si control. Analiza, proiectare, aplicatii.* Editura Matrix Rom, Bucuresti 2005.
[3]. Daniel Popescu, *Automate programabile. Constructie, functionare, programari si aplicatii*, Editura Matrix Rom, Bucuresti 2006.
[4]. David Bailey, *Practical SCADA for Industry*. Linare House, Jordan Hill Edwin Wright Oxford IDC Tehnologies 2003.
[5]. **Dusa V., VaidaV**., *Comanda si controlul functionarii retelelor electrice*, Editura Tehnica Bucuresti 2001.
[6]. Carmen Teodosiu - *Tehnologia apei potabile si industriale I si II,* Editura Economic, Bucuresti, 1998.

Annals of the University of Petroşani, Electrical Engineering, 11 (2009) pages 66-71

CIM CONTROL WITH EXTENDED KANBANS SYSTEM

VALI-CHIVUTA[1], SIRB ANGELA EGRI[2] ,OLIMPIU STOICUTA[3]

ABSTRACT: *The purpose of this paper is to present the extended KANBANS system that are utilized in the modeling and simulation of CIM systems.*

KEYWORDS: *Extended KANBAN control system, generalized stochastic Petri Nets, flexible manufacturing systems*

1.INTRODUCTION

The paper presents a KANBAN systems allow dealing with different kinds of those strategies, trying to smooth and balance material flows by using several appropriately controlled intermediate inventories. In essence KANBANS are cards that circulate between a machine (or a sequence of machines) and a downstream buffer. When a withdrawal operation liberates a position of an intermediate buffer, a card is re-circulated in order to allow the production of a new part to compensate "the previous loss" in the inventory site.

The number of KANBANS around a machine(s)-buffer subsystem determines the buffer size. In a KANBAN controlled system, production of parts is triggered in response to "intermediate demands". The primary goal of many manufacturing systems can be expressed in terms of the maximization of the production rate, the minimization of the work-in-process (WIP) inventory, and minimization of the delivering delay (difference between the date of a demand and the date of serving it). For example, minimizing WIP usually leads to higher delivering delays, what may even represent losing some selling opportunities (impatient clients). Among the many imaginable strategies for the management of production systems, push control is based on the idea of "advancing" tasks relative to production as much as possible. Thus the behavior of the production plant is externally constrained by the raw materials available, and by the capacity of buffers for storing finished products. Under this strategy, raw materials

[1] *Lecturer eng. ,phd. at the University of Petroşani;*
[2] *Assoc. prof. eng., phd. at the University of Petroşani;*
[3] *Assist. eng. ,phd student at the University of Petroşani.*

"push the production", and delivering delays are minimized at the expense of, eventually, important WIP costs. In many cases push-type behaviors use demand forecasts to generate the production plans. On the contrary, under the basic pull control strategy, the customer's demands trigger the production,"pull the production".

Thus the WIP cost is reduced to a minimum, at the expense of more important delays for delivering, i.e., at the expense of decreasing the quality of customer service. In the manufacturing area, it is well known that just in time (JIT) approaches that lead to low WIP costs. In order to conciliate the above mentioned contradictory performances, many hybrid push/pull control algorithms have been proposed in the literature. The number of KANBANS around a machine(s)-buffer subsystem determines the buffer size. In a KANBAN controlled system, production of parts is triggered in response to "intermediate demands". As was already mentioned in the cell manufacturing , the parts in any intermediate buffer try to "protect" the operation of downstream machines from possible interruptions of upstream machines. If the repairing time of the machine that is under failure is "not too big", the buffer will not empty and the failure will not affect the downstream machine.

Therefore intermediate buffers "can be perceived" as condensers in electrical circuits or resorts in mechanical systems, allowing relatively uncoupled behaviors on production lines subsystems. The point here is that at a general level, Petri nets –with some timed interpretation, for example, Generalized Stochastic Petri Nets can be used to model different designs and control strategies. By using appropriate performance evaluation models, the optimization of the strategy used to control the material flow (i.e., making the more appropriate decisions), even the tuning of its parameters, can be formally studied.

2.TYPE OF KANBAN CONTROL SYSTEM

A basic pull control system (base stock control system, BSCS) is presented in figure 1. It consists of two production stages (with k1 and k2 parts finished in stage 1 and stage 2, respectively), feeding an assembly stage initially with k3 finished parts). When a customer's demand appears, places dr1 and dr2 receive a (new) token, in order to produce another part for each stage. Customers demand allows serving finished parts, represented by tokens in place f3, initially marked with k3 tokens. A main problem in this basic schema is that the limitation of the WIP is not assured in any of the three simultaneous KANBAN control system (SKCS) and independent KANBAN control system (IKCS) are modeled in figures 2 and 3 As happened before, in both cases two production stages are followed by an assembly stage.

The difference among SKCS and IKCS is that the first one feeds simultaneously the assembly stage and the new production order for the (two) previous stages. In the second case, separate KANBANS feed stages 1 and 2, while feeding the assembly stage is automatic, when appropriate parts exists (in b1 and b2).

.

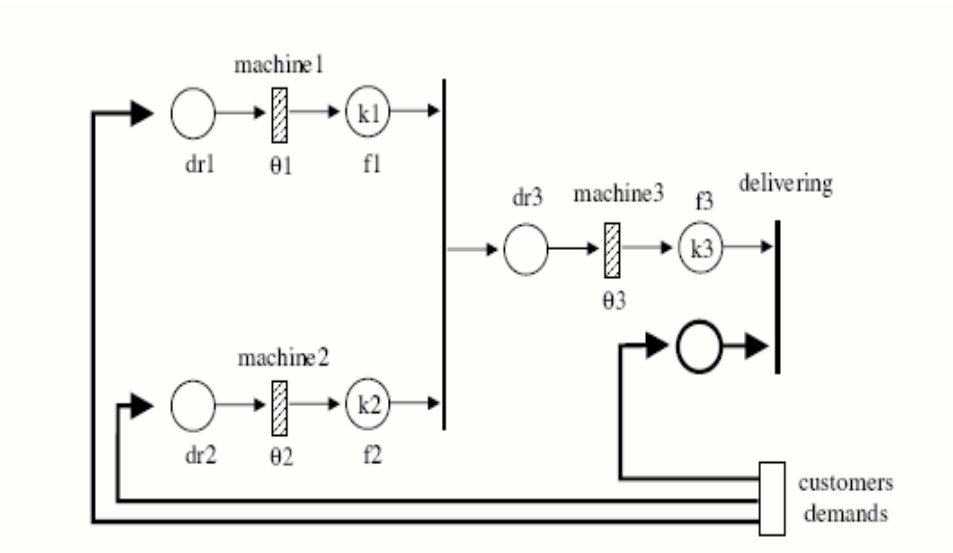

Figure1. Production of parts A and B (stages 1 and 2) and final assembly (stage 3), with a basic stock (pull) control system (BSCS) and assuming single server semantics

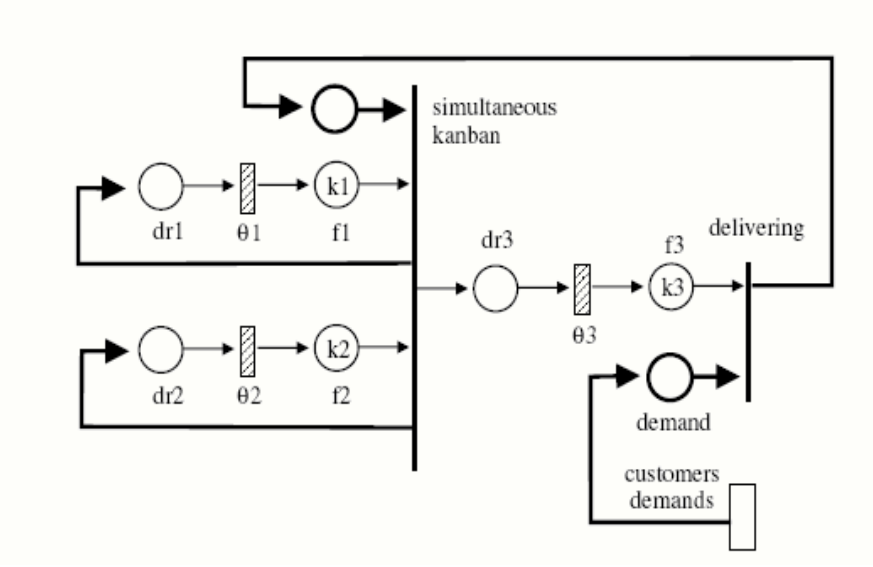

Figure 2. Simultaneous KANBAN control system (SKCS).

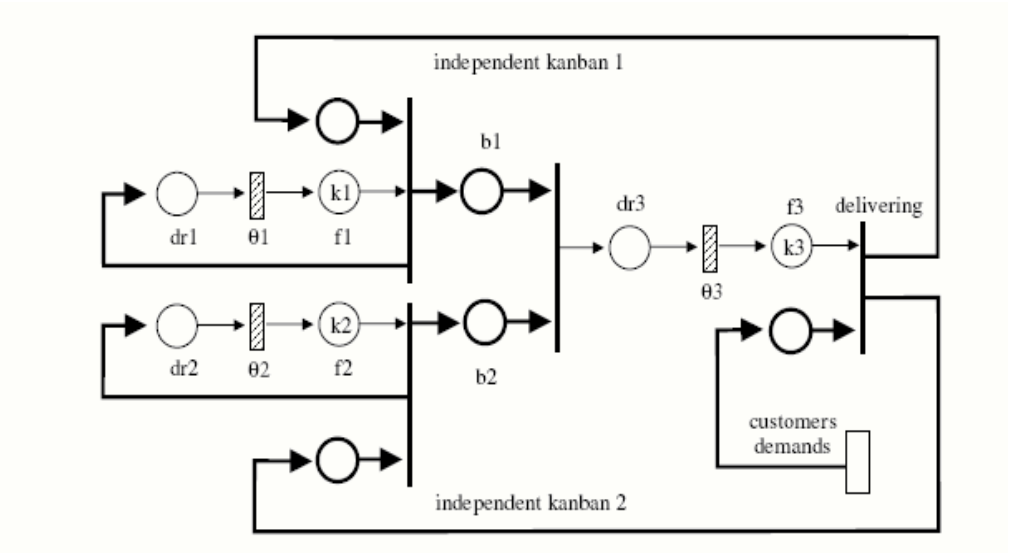

Figure 3. Independent KANBAN control system (IKCS): KANBANS are independently generated for machine 1 and machine 2

Obviously, in transient behaviors, the independent case can be better than the simultaneous one. A more elaborated KANBAN system is presented in Figure 1.7. It is the so called independent extended KANBAN control system (IEKCS). Under saturation of customers demands it behaves exactly like the above schemes (SKCS and IKCS). Nevertheless, in this case different KANBANS send simultaneously requests for the production of primary parts (in stage 1 and stage 2), for an assembly to be done, and for the delivery of a finished part. This may lead to some interesting behaviors, potentially reducing the WIP, while keeping a good reactivity to demands.

3. EXTENDED KANBAN CONTROL SYSTEM

These (fig 4.) control policies have been simulated assuming in all cases that 1 = 1, 2 = 3 = 2, k1 = 2, k2 = 3, k3 = 2, and for IEKCS, s1 = s2 = s3 = 1. A burst of 5 simultaneous demands is simulated at 30 T.U. The results for the different control systems in Figures 2.7-2.10 are represented in Figure 2.11, where (a) shows the marking of place demand (unsatisfied demand), (b) shows the marking of place f3 (complete products in stock), and (c) shows the throughput of the assembly station. Because the “delivering” transition is immediate, the unsatisfied demand at 30 T.U. is equal to 5 minus the products in stock: 1 for BSCS, 3 for SKCS and IKC S, and 4 for IEKCS. It can be seen that SKCS and IKCS are in this case equivalent. BSCS is the first to “satisfy the demand” (the marking of the place demand returns to zero), while IEKCS is the last one. However, the stock of complete products in absence of demand is much larger under BSC S (4), than under IEKCS (1). With respect to the throughput, SCKS, IKCS and IEKCS, work on demand, so the throughput is zero before the demand. Under BSCS, a first outburst of the production appears, since the intermediate stocks f1 and f2 are used to produce the final assembly. In other words, the system tries

.

to complete as much products as it can, instead of keeping stocks of intermediate elements. That is the reason why although the stock under BSCS is 4 and under IEKCS is only 1, it does not take four more times to satisfy the demand in the latter case, but only about twice. Many other schemes of this type can be imagined. The important point at this level is that modeling with PNs is frequently quite straightforward (if control strategies do not depend too much on particular data),and analysis can provide useful information about the behavior of the intended control strategy

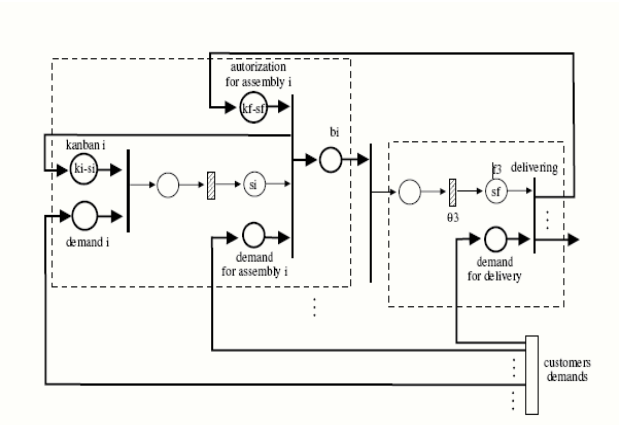

Figure 4. Independent extended KANBAN control system (IEKCS).

4.SIMULATION OF CONTROL SYSTEM

We consider the assembling CIM (fig.5) composed by 3 deposits D1, D2, D3, to tool machines, to conveyors C1, C2, an assembling station and a robot R. Technological flow is composed on the next operations: C1 conveyors transports type 1 crude pieces D1 deposit on M1 tool machine, M1 (M2) processes the type 1 crude piece resulting type 1 intermediary product, when both M1 M2 processes are finish, robot R transport type 1 intermediary products from M1 to A, and then type 2 intermediary products from M2 to A and robots R transport the finite product from A to D3 deposit. The simulation results is presented in figure 6.

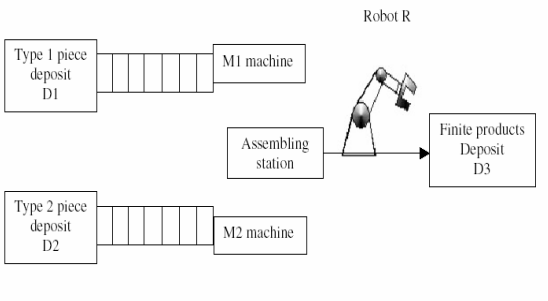

Figure 5. The structure of CIM

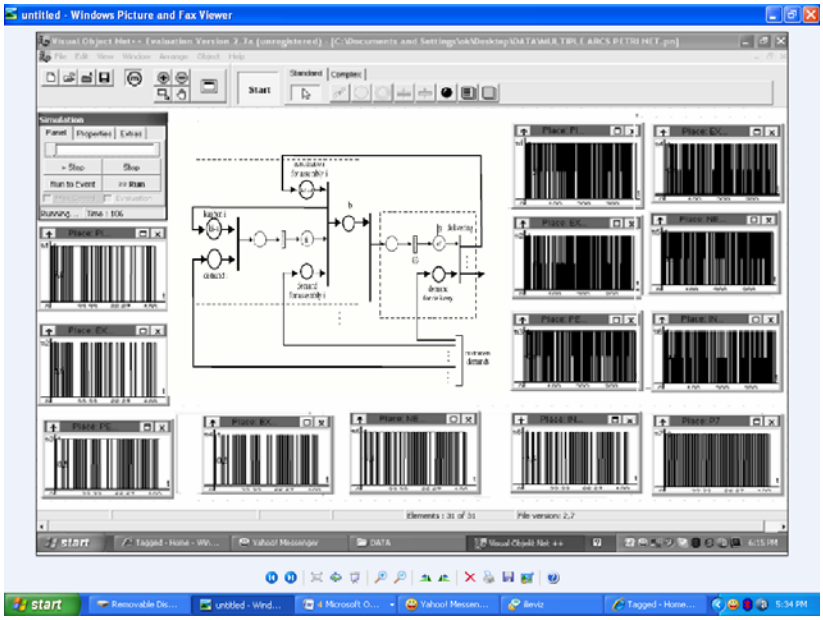

Figure 6. Simulation

5.CONCLUSIONS

The modeling, simulation and control of assemblig CIM used the extended KANBANS system is a verry good solutions and offers high performance.

REFERENCES

[1]. Sirb,V., Pop, E., *Contributii privind modelarea si simularea liniilor flexibile de fabricatie,* Simpozionul International SIMPRO Petrosani, 2005.

[2]. Sirb,V., *Modelarea si simularea unui CIM de productie,* Raport de cercetare stiintifica, Petrosani, 2007.

.

Annals of the University of Petroşani, Electrical Engineering, 11 (2009) pages 72-77

MONITORING QUALITY OF ELECTRICITY FROM A LINE LIGNITE EXTRACTION TECHNOLOGICAL

ILIE UTU[1]

ABSTRACT: *The paper undertakes a study of the quality of the electric energy in an open pit. Some measurements have been made within electronic devices. We also used a personal computer for data acquisition and for interpreted the results o the measurements. Using analytic formula we calculated the influence of the voltage and current harmonics for the quality parameters of the electric energy.*

KEYWORDS: *voltage harmonic, current harmonic, electric energy quality, data acquisition, PWM converter.*

1.INTRODUCTION

The current systems of shareholders, regardless of method used for adjusting the speed, power induction motor generally tends to be made from static frequency converters, which can make changes both amplitude and frequency of supply voltage.

The power structure used consists of a rectifier and an inverter wrong with pulse width modulation, called the PWM inverter. For vector control inverter can be viewed either as a source of tension is, in most cases, the power source.

Extensive use of rectifier diodes wrong with the power inverter has the major negative growth "harmonic pollution. Power system can operate properly in the presence of a "quantity" limited by harmonics.

Until recently injecting harmonics into the system can be considered negligible. Currently, however, increasing dependence of large consumers of equipment with linear features makes this phenomenon can no longer be neglected. The introduction of harmonics in power supply system is one problem, the very functioning of electrical equipment may be affected.

[1] *Associate Professor Eng., Ph.D. at the University of Petrosani*

2. VOLTAGE AND CURRENT HARMONICS EFFECTS ON QUALITY OF ELECTRICITY

The presence of harmonics in power supply system can generate a broad range of undesired effects. For example, harmonics may cause interference signals, over voltage, loss of data transmission lines of information. Harmonics can also generate overheating, inadequate operation or malfunction of equipment in general.

Harmonics can cause excessive heating in transformers and capacitors, resulting in reduced lifetime of these devices or their failure. Another effect is heating of the electric motors and produces a pulsating torque. The harmonics in the supply system lead to loss of overall power, reducing the efficiency of AC motors, increased maintenance cost.

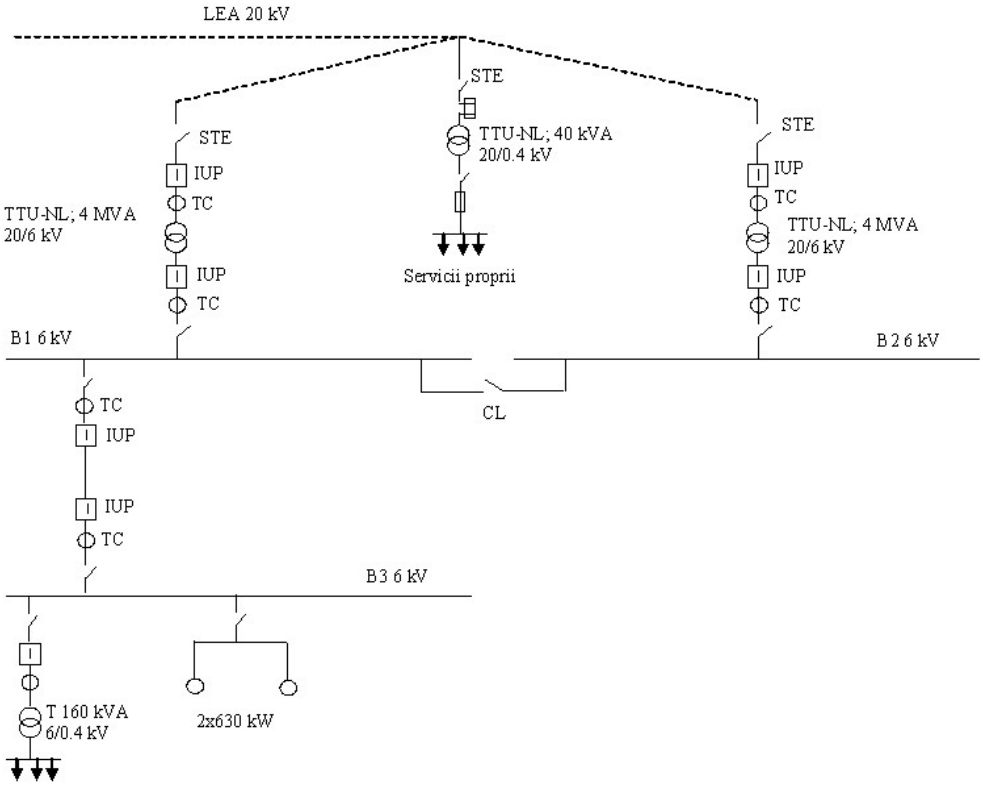

Figure 1. Schedule Station no. 3 of 20 / 6 kV to EM Rosia

The magnitude and order of harmonic components present in the system depends on several factors: the source of harmonics: the power system, system operation under normal or resonance. Even harmonics produced by a single plant may vary depending on the system of work. For example, an electric arc furnace can produce harmonic voltages ranging between 8% and 25% of basic. The power supply of computer systems, harmonic currents were recorded with values between 5.5% and 140% amplitude of basic.

Nonlinear loads can also produce harmonics multiple of three. They need special attention as leading to a current in the neutral conductor, which sometimes exceed the amplitude of phase current. Such tasks are arc furnaces, which in normal operation produce harmonic currents of order three with amplitude of 20% of fundamental.

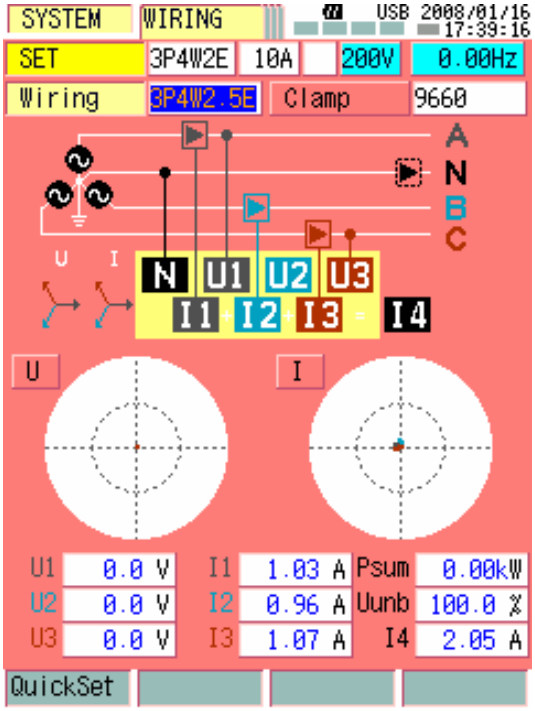

Figure2. Wiring diagram of the device

After raising the number of power electronic equipment, together with the whole range of undesirable ancillary effects of the above, various national and international bodies have issued recommendations for limiting the harmonic currents injected into the network, the network to maintain acceptable quality of food.

The reduction of harmonics and their amplitude requires the use of passive or active filters. In the particular case of electrical drives can be adopted and controlled rectifier solution. These can be controlled so that the power factor of equipment to be quasi-uniform and harmonic content is minimized. It requires even acceptable maximum distortion factor (THD) of current wireless network absorbed less than 5%.

In this work we present measurements of measurements to study the system as distorting and electricity systems introduced by existing shareholders at a technological line of E.M. Roşia. Measurements were made with an apparatus for analyzing power quality type Hioki 3197, connected to the processing station serving line equipment technology. Current and voltage probes were installed in cells measuring the processing station. Schedule Station no. 3 in which measurements were made is given in Figure 1.

How to connect the measuring device is given in Figure 2.

3. MEASUREMENTS MADE TO CONVEYOR BELTS OF EXCAVATORS

It goes on to present the results of measurements of electrical drives supply line of conveyor belts T500 T501 and MAM-1. Measurements were made in different operating regimes of shareholders on the supply line.

Measurement results are presented in the following figures, given how the variation of voltages and currents, values of active power, reactive power factor variation and variation of deformation factor.

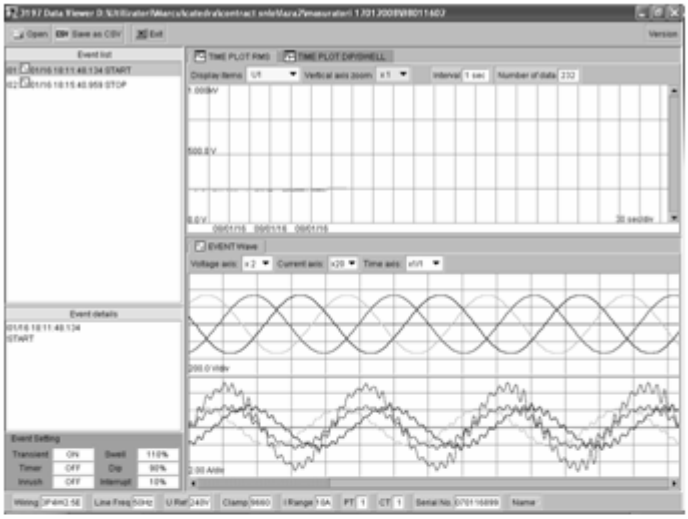

Figure 3. Effective voltage variation

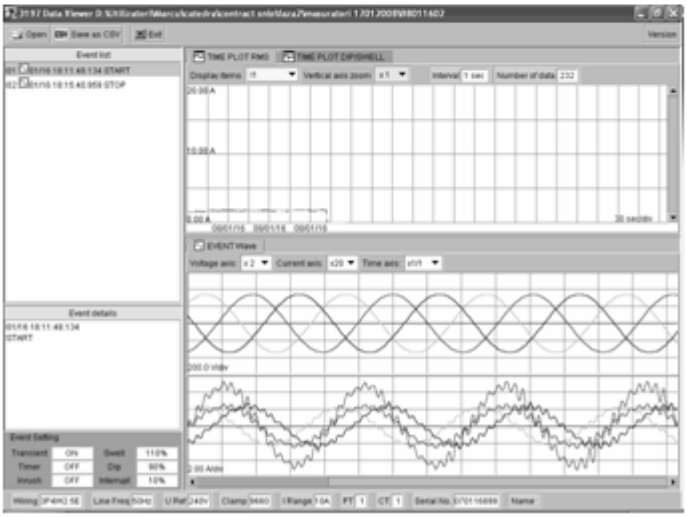

Figure 4. Effective current variation

Measurement results are presented in the following figures, given how the variation of voltages and currents, values of active power, reactive power factor variation and variation of deformation factor.

The analysis of these graphs it may be concluded that there is strong disturbance in voltage and current changes. Changes in power factor are poor, which is below 0.5 and even lower in elevated pregnancy.

Regarding the factor of distortion, it is low in these charts can not draw lessons clear. For this reason it has further catches made using power quality analyzer, the data are measured values, harmonic analysis and temporal variation in flow and pressure at different times.

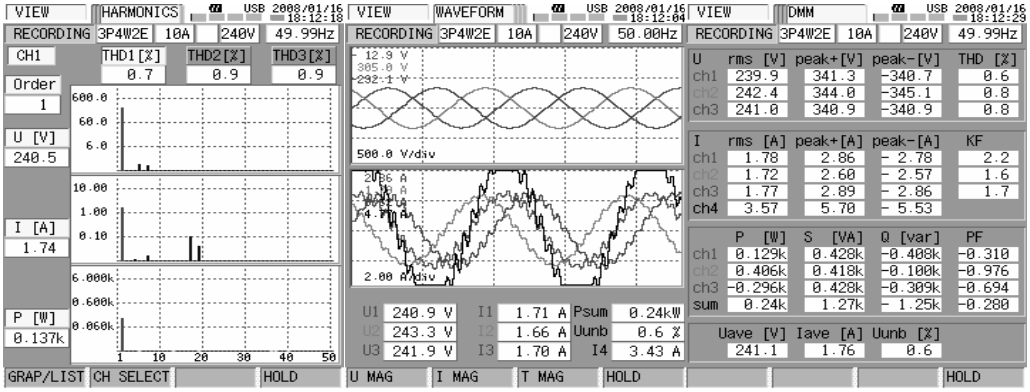

Fig.5. Capture voltage and current

On the basis of such catches were calculated current and voltage harmonic amplitudes and coefficients distorting features of the regime. The results of calculations for voltage and current amplitudes are shown in Tables no. 1 and 2, and the coefficient values of the regime characteristics are given in Table 3 format.

Table 1. The values of harmonic voltage

Harmonic Order	Voltage Harmonic/Set of measurement				
	1	2	4	5	6
1	6052,5	6012,5	6015	6002,5	6002,5
5	20,17	30,06	20,04	30	20
7	10,08	20,04	20,04	40	10
17	10,08	0	0	0	10
19	5,04	0	0	0	5

Table 2. The values of harmonic currents

Harmonic Order	Current Harmonic/Set of measurement				
	1	2	4	5	6
1	158	174	3	176	175
3	1,58	0,43	0,30	0,44	4,37
5	3,16	1,74	3,66	1,76	3,50
7	2,37	8,70	2,44	0,44	0,43
17	9,48	5,22	0,30	3,52	10,50
19	6,32	0	6,10	1,76	7
23	4,74	0	4,27	3,52	0
25	3,95	0	0,30	0,44	0

Table no. 3.

Nr.	Actual value Voltage (V) Current (A)		Distortion coefficient TDH (%)	Weighted Distortion coefficient Dw	Harmonic factor FA
1	U	6052,5441	0,38	0,038	0,0016
	I	158,5874	8,59	1,57	0,021
2	U	6012,6085	0,6	0,034	0,0025
	I	174,3047	5,91	1,023	0,0144
3	U	6015,0667	0,47	0,028	0,0019
	I	9,1685	94,4	0,2876	0,28
4	U	6002,7082	0,83	0,0529	0,0033
	I	176,4345	7	1,191	0,021
5	U	6002,552	0,41	0,038	0,0016
	I	175,544	7,8	1,28	0,021

REFERENCES

[1]. **Chiuță, I.** *Compensarea regimului energetic deformant.* Editura Tehnică, Bucureşti, 1989.
[2]. **Puşcaşu, S., Marcovici, J.** *Mărimi şi regimuri electrice nesinusoidale.* Editura Scrisul Românesc, Craiova, 1974.
[3]. **Uțu, I.** *Reducerea consumului de energie electrică în acționările electrice de mare putere din industria minieră*. Teză de doctorat, Petroşani 1998.

Annals of the University of Petroşani, Electrical Engineering, 11 (2009) pages 78-87

A VOICE COMMANDED WPF DATABASE MANAGEMENT APPLICATION

BADEA IONUT FLORIN[1]

ABSTRACT: *This article presents the design and implementation of a voice commanded WPF database management application. The application was written to manage the database for a timetable application. The application is written in WPF with C# using Visual Studio 2008 and the .NET Framework 3.5 with SP1. The application is prototype that presents a possible implementation for database management applications. The application can easily be changed to manage other databases*

KEYWORDS: *WPF, database management, speech recognition, layout and control design, entity framework*

1.INTRODUCTION TO WPF

Windows Presentation Foundation is a graphical subsystem for rendering user interfaces in Windows based applications. WPF, previously known as "Avalon", was initially released as part of .NET Framework 3.0.

Designed to remove dependencies on the aging GDI subsystem, WPF is built on DirectX, which provides hardware acceleration and enables modern UI features like transparency, gradients and transforms, 3D graphics and rich media content. WPF provides a consistent programming model for building applications and provides a clear separation between the user interface and the business logic.

2.BUILDING A UNIVERSITY TIMETABLE

In most of the Romanian universities the timetables are built by specialization. What this means is that each specialization has its own timetable. Specializations can be automatics, computer science, electrical engineering, transports and others.

[1] *Ph.D Student at University of Petrosani*

Each specialization is composed of a number of groups (usually 4), one for each year of study. As an example we will have for groups (C11, C21, C31 and C41) for the computer science specialization. Group C11 will hold students in the first year; C21 will hold students in the second year and so on.

The timetable grid for a specialization will also take into account the days of the week (Monday to Friday) and also the time periods in each day (Period1 to Period7). A period is a time interval that spans 1 hour and 30 minutes with a break of 15 minutes. Considering this we will have the first period starting at 8:00 and ending at 9:30, followed by a 15 minutes of break then followed by another period (period 2) starting at 9:45 and ending at 11:15.

To understand this better you can look at an empty timetable for the computer science specialization which can be seen in the image below.

		COMPUTER SCIENCE			
		C11	C21	C31	C41
MONDAY	P1				
	P2				
	P3				
	P4				
...	...				
FRIDAY	P1				
	P2				
	P3				
	P4				

Figure 1. Empty timetable

In order to construct the timetable each cell in this table will be filled with timetable entries as I call them. These entries are subjects assigned to a group at a particular hour in a particular day.

In the Romanian system a student attending at a university doesn't have the possibility to choose which subjects to take. The subjects are provided for a particular specialization and year. The student will search each specialization and will choose to enroll in the specialization that has the subjects that mach most of his desired subjects. This is why every entry in the timetable is centered on a subject. As I understand, in other countries, students have the possibility to pick their subjects.

Some subjects can be held for one hour per week while others can be held for 2, 3 or 4 hours per week. Since this hour per week format doesn't mach with the period format (one period has 1.5 hours) often appear situations where a subject spans half a period or a period and a half. To see how we represent this please look at the image below.

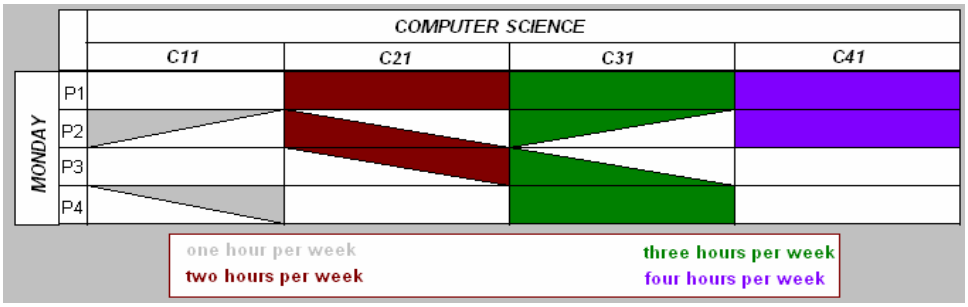

Figure 2. Timetable entry shape variations

Another thing that I should mention is the semi-group. When a group has more than 15 students that group is split up into 2 or more semi-groups. These semi-groups are represented in the timetable by a vertical line. The image below shows the semi-group representation.

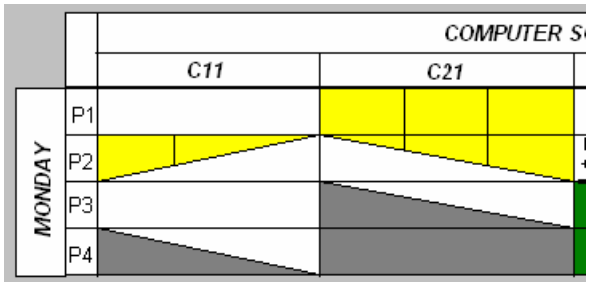

Figure 3. Semi-group representation

3.THE DATABASE DESIGN

Now, that you have a basic understanding about the way to build a timetable, its time to talk about the database design.

The above figure below shows the database tables and the relationship between them for the timetable application. This database will be used to hold the necessary data in order to generate the timetable parts. These parts will be the courses that will be held at a university. The courses will have additional information attached but the main part of a timetable entry will be represented by a course.

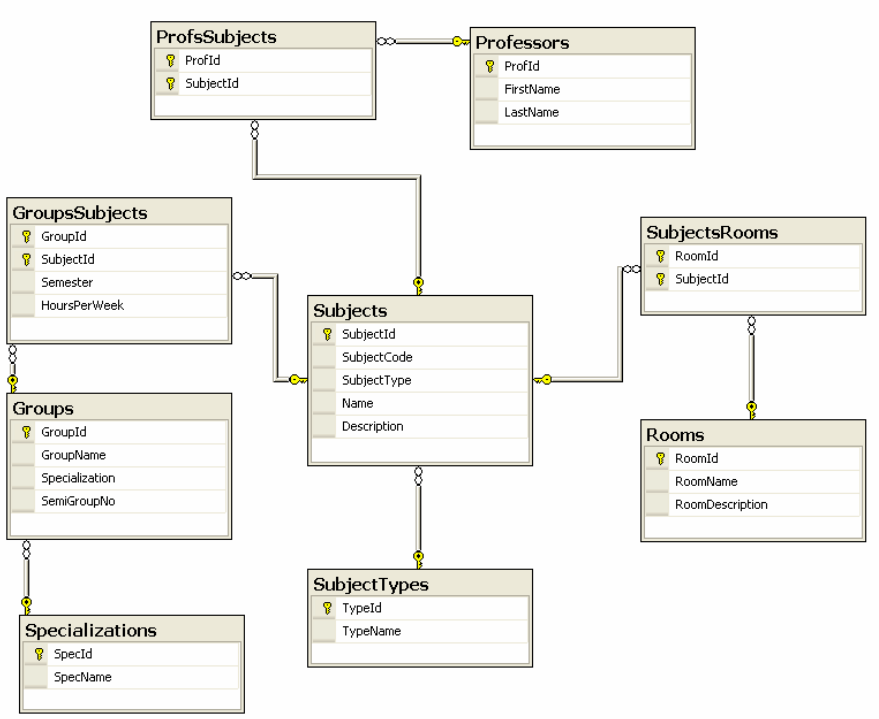

Figure 4. The timetable database

The Specializations table will be used to hold information about the different specializations that exist at a university.

The Groups table will be used to hold a group's information. The group represents students that are in a certain year of study at a certain specialization.

The Professors table is used to hold the data about the professors that will be teaching during a particular semester.

The Subjects table is used to hold all the subjects that will the taught at the university.

The SubjectTypes table is used to hold the subject types. The type data refers to whether the subject is a course, a lab or a seminary.

The ProfsSubjects table is used to link the professors and the subjects table. The GroupsSubjects table is used to link the groups and subjects table. The RoomsSubjects table is used to hold room preferences for a particular subject.

The Rooms table is used to hold all the rooms that can hold classes.

4.THE ENTITY MODEL

The timetable management application is a WPF application that uses the entity framework as the database access technology. This layer is created by using the Visual Studio IDE. The image below shows the final, fully configured entity model.

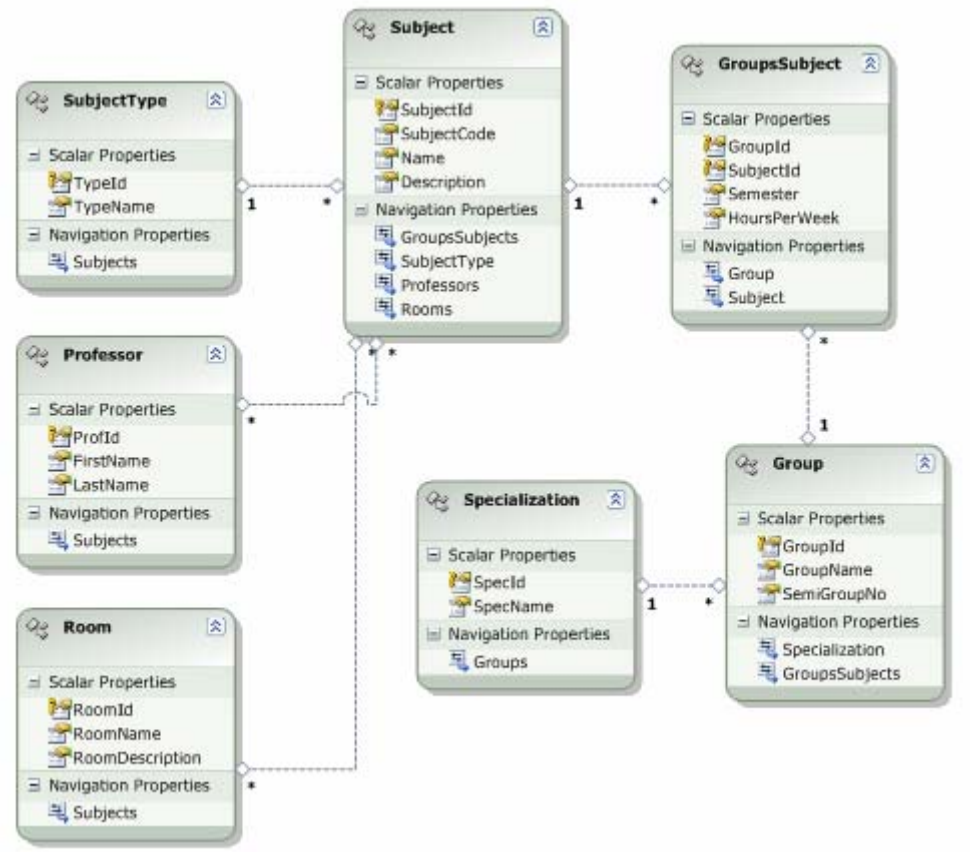

Figure 5. The entity model

As you can see from the figure above the entity model closely resembles the database structure. The entity model is a collection of xml and source code files. The c# source code files are generated on the xml files.

The model contains 3 xml files. The firs file represents the conceptual schema. This file tells the code generation tool how to construct the classes that will be used to build the application. The second file represents the store schema. This file shows the database structure. The last file is the mapping file. This file holds all the data that links the store representation with the conceptual representation.

5.THE APPLICATION DESCRIPTION

The main screen of the application can be seen in the image below.

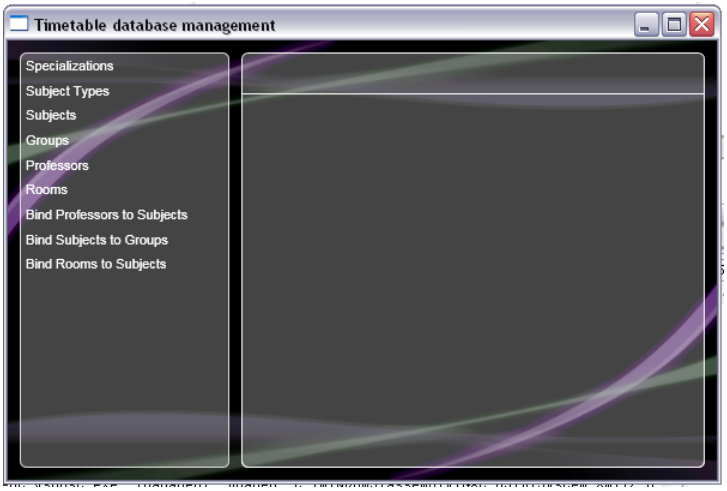

Figure 6. The main application window

As you can see the application gives the user the possibility to manage all the tables of the database. The user can choose which table to edit by selecting an item from the list on the left. When this happens, the right part of the main window will offer the UI to edit the respective table. An example of this can be seen in the image below.

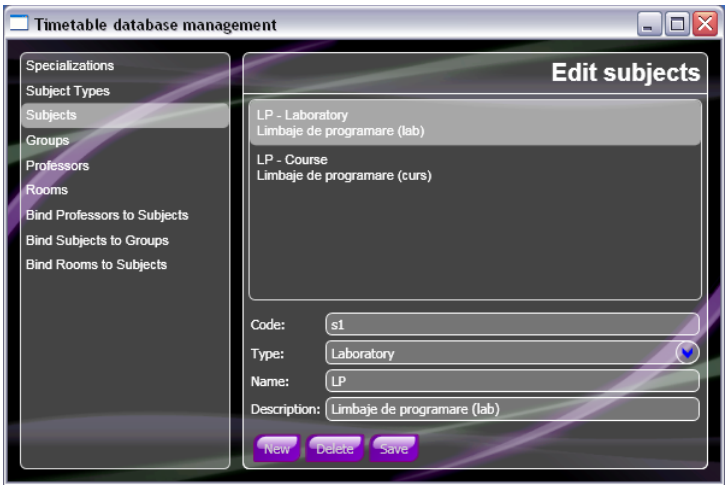

Figure 7. The subjects' user control

As you can see the control above (like all the controls in the application) offers possibilities to add entries, edit entries, delete entries and save changes.

The main window of the application doesn't have much code. The code that is contained in this window is used to load the user controls that are used to edit the tables. This code is run when the user selects an entry from the list on the left. The window also contains the code that integrates the speech recognition engine used for the voice commands.

All of the user controls that the application is using are implemented in the same way with little variations. This is why the paper will describe only one user control.

6.THE SPECIALIZATION CONTROL

The specialization user control is used to edit the Specialization table. This user control has a very simple UI. The control can be seen in the image below.

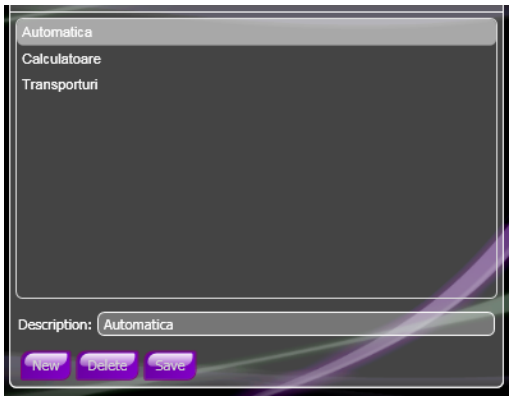

Figure 8. The specialization user control

The top section shows a list with all the specializations in the table. The section at the bottom shows the details for the selected specialization. The user can add a specialization, delete a specialization and save changes by using the 3 buttons at the bottom.

The xaml for the list can be seen below.

```
<ListBox Name="lstSpecializations" Margin="4"
ItemsSource="{Binding}"
                IsSynchronizedWithCurrentItem="True"></ListBox>
```

As you can see the ItemsSource property is bound to the entire data context. The data context will be set in code.

The text box is bound to the SpecName property of the currently selected specialization. The xaml for the text box can be seen below.

```
<TextBox Grid.Column="1" Margin="2"  Name="txtDescription"
      ToolTip="{Binding RelativeSource={RelativeSource Self},
            Path=(Validation.Errors)[0].ErrorContent}">
      <TextBox.Text>
           <Binding Path="SpecName"
            UpdateSourceTrigger="PropertyChanged">
                  <Binding.ValidationRules>
<vr:EmptyStringValidation></vr:EmptyStringValidation>
                  </Binding.ValidationRules>
```

```
            </Binding>
        </TextBox.Text>
</TextBox>
```

As you can see, I'm also setting the tool tip to show the validation errors. The list of specializations is retrieved in a separate thread in order to not block the UI. For this I'm using a BackgroundWorker.

The DoWork handler code can be seen below.

```
private void worker_DoWork(object sender, DoWorkEventArgs e)
{
             specializations = new
ObservableCollection<Specialization>(context.SpecializationSet.T
oList());
}
```

After getting the specializations list on a background thread I'm binding the UI. This has to be done in the same thread as the UI. The RunWorkerCompleted handler runs on the same thread as the UI, so this will be the perfect place to bind the list of specializations to the UI list.

The code can be seen below.

```
private void worker_RunWorkerCompleted(object sender,
RunWorkerCompletedEventArgs e)
{
      view =
(CollectionView)CollectionViewSource.GetDefaultView(specializati
ons);
      DataContext = view;
      EnableButtons(true);
}
```

In order to add a new specialization I'm using the new button. This button uses the new command. The new command handler can be seen in the code below.

```
private void new_Executed(object sender, ExecutedRoutedEventArgs
e)
{
      Specialization spec = new Specialization();
      context.AddToSpecializationSet(spec);
      specializations.Add(spec);
      view.MoveCurrentTo(spec);
      txtDescription.Text = "";
}
```

As you can see I'm creating a new specialization and I'm adding it to both the context and the specializations list (which is an observable collection).

To delete a specialization I'm using the delete button and the delete command. The code for the delete handler can be seen below.

```
if (lstSpecializations.SelectedItem != null)
{
     Specialization type =
(Specialization)lstSpecializations.SelectedItem;
     context.DeleteObject(type);
     specializations.Remove(type);
     lstSpecializations.Focus();
}
```

To save changes I'm using the save button. The code for the save command handler can be seen below.

```
btnSave.IsEnabled = false;
context.SaveChanges();
MessageWindow.Show("Changes saved");
```

7.VOICE COMMANDS

Speech recognition is a feature that translates user-spoken audio into text. As with speech synthesis, speech recognition is a feature of the Windows operating system. Speech recognition is built into Windows Vista but not Windows XP. Instead, it's available to Windows XP users through Office XP or later, the Windows XP Plus! Pack, or the free Microsoft Speech Software Development Kit.

Speech recognition is also a Windows accessibility feature. For example, it allows users with disabilities to interact with common controls by voice. Speech recognition also allows hands-free computer use, which is useful in certain environments.

The most straightforward way to use speech recognition is to create an instance of the SpeechRecognizer class from the System.Speech.Recognition namespace. You can then attach an event handler to the SpeechRecognized event, which is fired whenever spoken words are successfully converted to text:

```
SpeechRecognizer recognizer = new SpeechRecognizer();
recognizer.SpeechRecognized += recognizer_SpeechReconized;
```

You can then retrieve the text in the event handler from the SpeechRecognizedEventArgs.Result property:

```
private void recognizer_SpeechReconized(object sender,
SpeechRecognizedEventArgs e)
{
     MessageBox.Show("You said:" + e.Result.Text);
}
```

Another way to use speech recognition is to use a custom grammar. This is the approach I chose.

The grammar I'm using might not be the best but it works well with the application. I'm building the grammar with the function below.

```
private Grammar GetAppGramar()
{
     GrammarBuilder builder = new GrammarBuilder();
     builder.Append(new Choices(" ","computer"));
     builder.Append(new Choices(" ","select","details"));
     builder.Append(new Choices(" ", "save", "new", "delete",
"add", "remove","remaining", "main"));
     builder.Append(new Choices(" ","rooms", "groups",
"subjects", "professors","subject types",
"room","professor","subject","semester","number of hours","semi
group",
"specializations","specialization","bind subjects","bind
professors","bind rooms"));
     builder.Append(new Choices(" ", "name", "description",
"first name", "last name", "type", "code", "list"));
     builder.Append(new Choices(" ", "next",
"previous","first","last","open list","close list","exit
application"));
     return new Grammar(builder);
}
```

This grammar is then applied to the SpeechRecognizer by using the LoadGrammar() or LoadGrammarAsync() functions. This can be seen in the code below.

```
speech = new SpeechRecognizer();
speech.LoadGrammarAsync(GetAppGramar());
```

The rest of the interesting code is in the SpeechRecognized handler. The handler analyzes the recognized commands and depending on the command it executes a task. The SpeechRecognized handler checks for the following commands: main list selection (the top part of most controls), adding entries, deleting entries, editing entries, saving changes, selecting text boxes and other elements in the controls, open and close combo box pop-ups, list navigation commands (first, next, previous and last) and application exit.

REFERENCES

[1]. Julia Lerman, *Programming Entity Framework, 1st edition*, O'Reilly Media, Inc, 2009
[2]. Matthew MacDonald, *Pro WPF in C# 2008, 2nd edition*, Apress, 2008

Annals of the University of Petroşani, Electrical Engineering, 11 (2009) pages 88-92

FUZZY CONTROL OF DC DRIVE

TEODOR TĂBĂCARU[1]

ABSTRACT: *An industrial DC drive (22 kW) with fuzzy controller is simulated. Two models (linear and nonlinear) and two controllers (PID and fuzzy) are investigated. Using fuzzy controller for DC drive operation was successful. Two mathematical models of a DC drive are used. The first model is build as linear transfer function of converter and DC motor. The second model is build using advanced blocks from Power System Blockset (PSB) library. The library is an extension of Matlab/Simulink environment from The MathWorks. Inc. Using fuzzy logic and PSB library model seems to be new and promising approach to control of an electric drive.*

KEYWORDS: fuzzy control, DC drive, simulation

1. LINEAR MODEL OF DC DRIVE

A linear and nonlinear model of DC drive will be used. The linear model consists of two parts: converter/rectifier and DC motor. A linear model of DC motor (Fig. 1) was build using Simulink blocks.

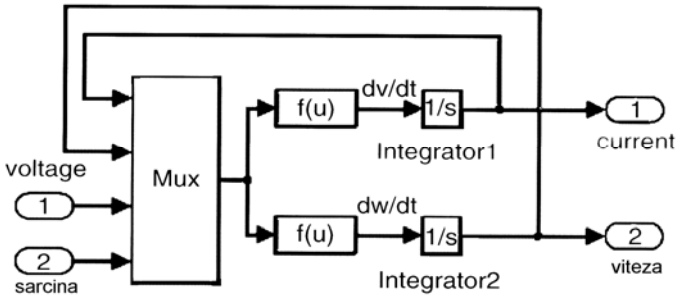

Figure 1. A linear model of DC motor

There are two inputs (voltage and load) and two outputs (angular motor

[1] *Associate Professor PhD. at University of Petrosani*

velocity and current). Its parameters are computed automatically from nominal catalogue data: motor power, voltage, current, speed, etc.). It is very convenient to use nominal motor data as rotor inductance and resistance. DC motor constant and other internal motor parameters are difficult to find. Converter/rectifier is described as first-order inertia:

$$G_{conv} = \frac{k_s(s)}{T_{mip}s + 1} \tag{1}$$

where k_p is gain of converter/rectifier and T_{mip} is mean dead time of converter/rectifier.

The dead time T_{imp} may vary from zero to one-half the period of an AC source (0.01 s for 50 Hz). It is assumed that six-phase thyristor bridge with mean dead time T_{imp} = 1.67ms is used in the converter. A classic DC drive with two PID controllers is presented on Fig. 2. It was assumed to neglect a derivative signal and to use PI operation of a current controller only. Parameters of the current controller were derived from the model parameters using rules of module and symmetry. Then Nonlinear Control Design Blockset (NCD) was used for automatic tuning of the controller parameters to minimize the transient overshot.

Simple transfer function model of motor current versus voltage was used:

$$G_{mot} = \frac{k_{ia}}{T_a s + 1} \tag{2}$$

where k_{ia} is gain of DC motor and T_a, the armature circuit time constant.

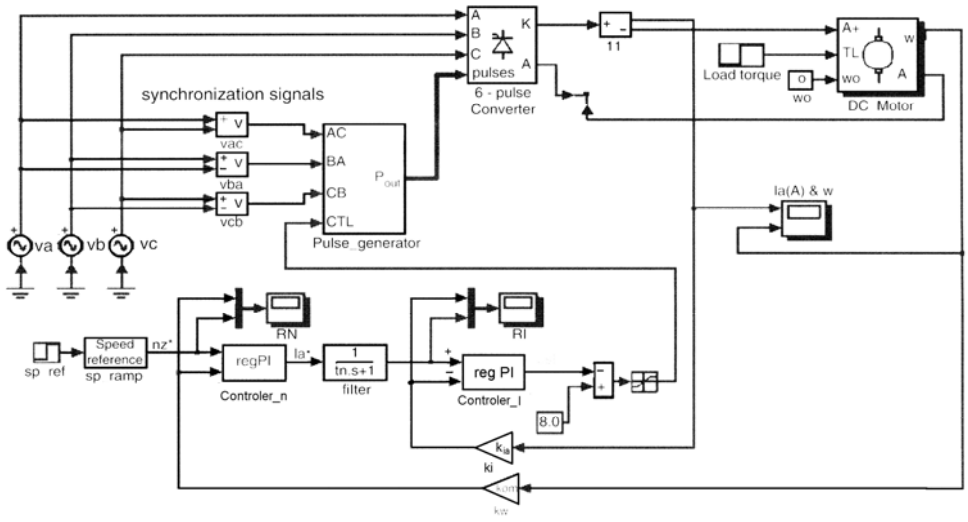

Figure 2. A classic DC drive with two PID controllers

Similar procedure was used to find parameters of velocity controller. The

simulation results (DC motor current and angular velocity vs. time) are presented on Fig. 3. This is raw simulation as linear model has very low granularity: AC component of current and switching of currents in thyristor bridge are neglected. Only envelope of transients can be seen on simulation output.

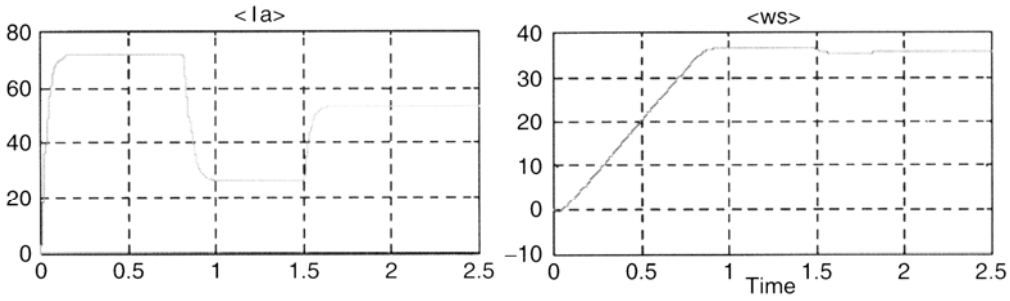

Figure 3. Simulation results (DC motor current and angular velocity vs. time)

2. USING PSB TO MODEL THE DC DRIVE

An advanced set of linear and nonlinear blocks can he found in PSB. Three AC sources. three-phase six-pulse converter, pulse generator, and DC motor are taken from the library. They are used to prepare high-quality model of three-phase DC drive (see Fig. 2). The three-phase bridge converter is the most frequently used motor control system. Two of six thyristors conduct at any time instant. Gating of each thyristor initiates a pulse of load current; therefore this is a six-pulse controlled rectifier. The three-phase six-pulse rectifier is also capable of inverter operation in the fourth quadrant. Electrical phenomena of thyristor bridge and DC motor are modeled very exactly. Simulation results (Fig. 4) are *almost exact* with real *measurement data on industrial object,* but computation is slow comparing to linear model.

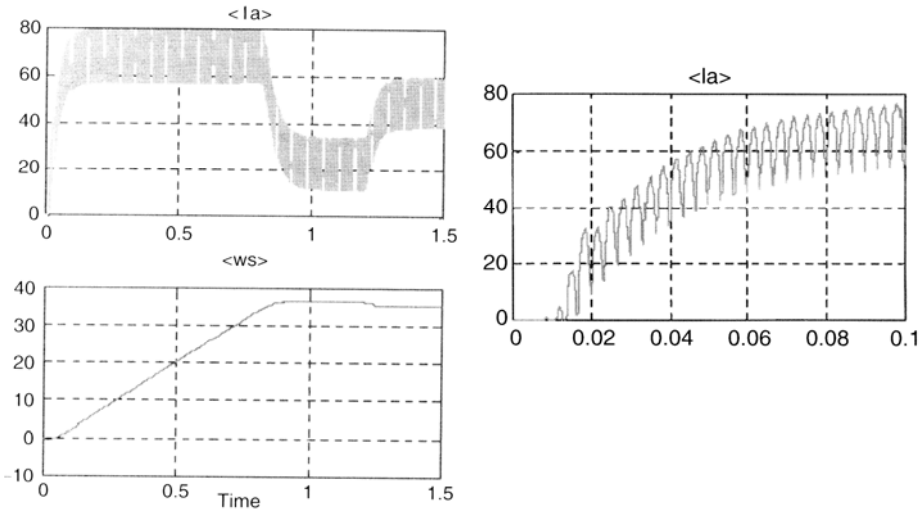

Figure 4. Simulation results for electrical phenomena

3. FUZZY CONTROLLER OF DC DRIVE

The fuzzy controller is presented on Fig. 6. Advanced model using PSB is used, but transfer function model can also be useful for preliminary tuning of controller parameters.

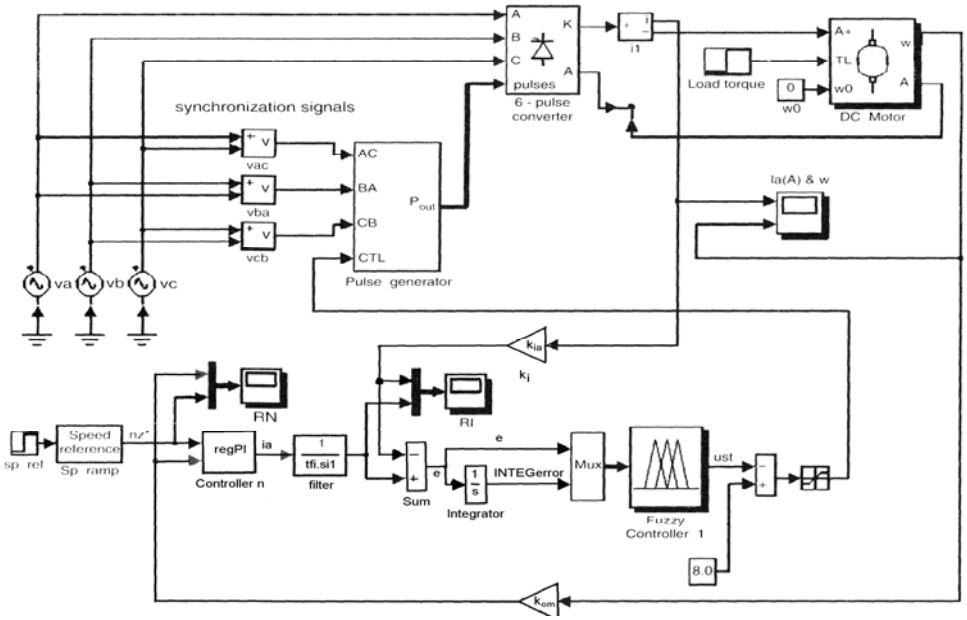

Figure 6. Fuzzy controller

4. LINGUISTIC VARIABLES AND RULES

There are two variables (error and INTEG error) and seven linguistic variables (from *big negative* to *big positive*). The fuzzy controller attributes are:

```
type: 'mamdani'
 andMethod: 'prod'
 orMethod: 'max'
defuzzMethod: 'centroid'
impMethod: 'prod'
aggMethod: 'max'
input: [1x2 struct]
output: [1x1 struct]
rule: [1x25 struct]
```

The membership functions (pimf and gausmf are used) and rules are design tools that give opportunity to model a control surface and controller properties. It is obvious that using this attributes one can more precisely fulfill a quality criterion in full operational range. The control surface (Fig. 7) is defined with 25 rules.

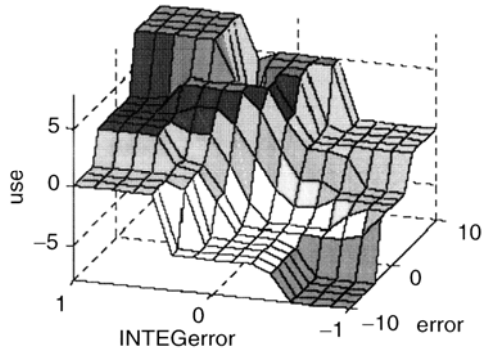

Figure 7 Control surface

5. RESULTS

Simulation output for fuzzy controller is similar to PI controller output presented unless one considers how controller reacts for external disturbation. The investigation showed that even simple fuzzy controller used to control DC drive operation (fig.6) is more precise and faster than of PI controller (Fig. 8).

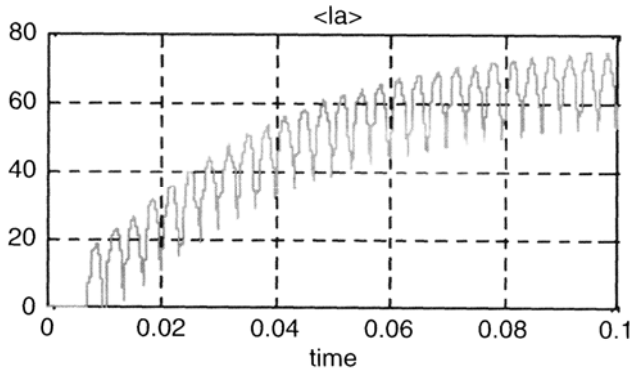

Figure 8. Simulation output for fuzzy controller

REFERENCES

[1]. Driankov D., and all., *An introduction to fuzzy control*. Springer, Berlin Heidelberg New York

[2]. Ross T.J, *Fuzzy logic with engineering application*. McGraw-Hill, New York

[3]. Sivanandam S.N., and all., *Introduction to Fuzzy Logic using MATLAB*, Springer Berlin

[4]. *http//www.mathworks.com*

Annals of the University of Petroşani, Electrical Engineering, 11 (2009) pages 93-101

INFLUENCE OF THE LOAD DISTRIBUTION ALONG LINE ON THE LOCATION OF SERIES CAPACITOR IN MEDIUM VOLTAGE NETWORKS

ANDREI ROMANESCU[1], DRAGOS PASCULESCU[2]

ABSTRACT: *In this paper is analyzed the influence of the load distribution along line on the capacitor location and its reactance value. The determination matter of the capacitor location is treated as a matter of optimization whose object function is sum of square deviations of the voltage in the consumption buses. It determines the series capacitor location and its reactance value for lines with distributed uniform loads and on lines with distributed linear loads.*

KEY WORDS: *series compensation, capacitor location, distribution networks, distributed loads.*

1. INTRODUCTION

Series compensation represents an effective method by adjustable voltage control in distribution networks. A series capacitor installed to an electrical line causes a boost
in voltage at the capacitor location that is proportional to current magnitude and the sine of power factor angle. Thus, it reduces the voltage drop on line and the voltage profile at the loads downstream from capacitor is improved. However, this boost in voltage is both instantaneous and continuous depending on rapid load changes. It is safe to say that the series capacitor is an automatic regulator with an insignificant response time, which contributes to the improving of voltage quality through the reducing of voltage fluctuations [1], [2] and [3]. Accordingly, the series capacitor can dispose of some matters relative to flicker and voltage fluctuations, which appear in the network at the starting of large motors, as well as on the electrical line which supplies arc furnaces, welders, sawmills, mine equipments (rolling mills, crusher motors) etc

[1] *Eng., Ph.D. student, Transelectrica, transport branch Sibiu, Alba Iulia Station, Romania*
[2] *Lecturer Eng., Ph.D., University of Petrosani, Romania*

The series compensation contributes to the improvement of distribution network performances through the decreasing of voltage drops, power losses and improvement of the power factor of networks, also. The efficiency of the series capacitive compensation of medium voltage lines depend on both the load, the load power factor, the line parameters and the capacitor location and reactance value.

The voltage profile along line, that is installed the series capacitor, is influenced both the capacitor location and its reactance value [4]. For improving of the voltage profile on MV lines is important the finding of optimal capacitor location and its reactance value. Based on this idea, the paper develop an optimization method to determine the series capacitor location and the optimal and reactance value on lines with distributed uniform loads and on lines with distributed linear loads. The object function consists of minimizing the sum of square deviations of the voltage in the consumption nodes under several constraints.

2. THE ESTABLISHING OF THE SERIES CAPACITOR LOCATION

The voltage profile on a line depends on the circuit parameters, the power factor of the load and the load magnitude. This voltage profile varies in time as the steady-state load changes. Usually, the peak load is the one of greatest interest, because it causes the maximum voltage drop and the voltage to consumer terminals is decreased. Taken in account these, the object function can be defined that sum of square deviations of the voltage in the consumption buses to be minimum, to peak load:

$$\phi_l = \sum_{i=1}^{n} \left(\frac{U_i - U_n}{U_n} \right)^2 = \min \tag{1}$$

Also, at the establishing of the capacitor location and of the optimal reactance value must take into consideration to constraints as:

• in any section of the line the voltage is within the admissible range [5] both in the normal and in a shortcircuit regime.

• the overvoltage to capacitor terminals in the short-circuit regime is less than the admissible value or equal it.

• the overload of the capacitor in the short-circuit regime is less than the admissible value or equal it.

These constraints are given in relations (2):

$$\begin{cases} U_{\min adm} \le U_i \le U_{\max adm} \\ \Delta U_{C\max} \le 1{,}1 \cdot \Delta U_{C adm} \\ I_{C\max} \le 1{,}3 \cdot I_{C adm} \end{cases} \tag{2}$$

where:

U_i is the voltage in a section of line *i*;

$\Delta U_{C\max}, \Delta U_{C\,adm}$ - the maximum and admissible voltage at capacitor terminals;

$I_{C\max}, I_{C\,adm}$ - the maximum and admissible current via capacitor.

By using a proper protection of the capacitor, the over voltage at capacitor terminals and overload during shortcircuits that occur behind the capacitor can be eliminated. So, the only constraint that has to be fulfilled is the one regarding the voltage profile along the line.

2.1. The line with distributed uniform loads

Consider an electrical network with balanced and distributed uniform loads (Fig.1). At moment *t* (peak load) we know electrical load *I* from the line beginning.

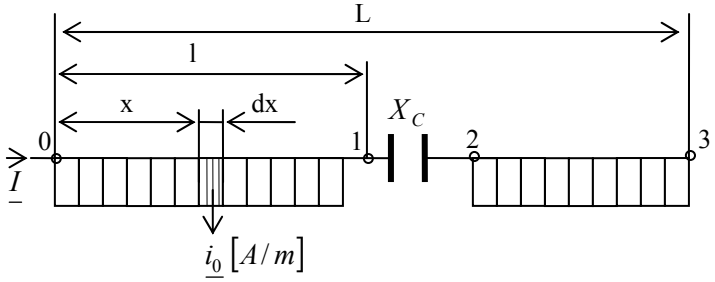

Figure1. Line with distributed uniform loads

Considering the electrical line with parameters per unit length distributed ($\underline{z_0} = r_0 + j \cdot x_0$, impedance per unit length) and the constant load density $\underline{i_0} = const.$ ($\underline{i_0} = i_{0a} - j \cdot i_{0r}$, in $[A/m]$), the voltage drop for the line without compensation is (3):

$$\Delta \underline{U} = \Delta U + j \cdot \delta U = \sqrt{3} \cdot \int_0^L \underline{z_0} \cdot \underline{i_0} \cdot x dx = \sqrt{3} \cdot \underline{z_0} \cdot \underline{i_0} \cdot \frac{L^2}{2} \tag{3}$$

where:

$\Delta U = \sqrt{3} \cdot \left(i_{0a} \cdot r_0 + i_{0r} \cdot x_0\right) \cdot \frac{L^2}{2}$ - is the longitudinal component of voltage drop;

L – length of line;

$\delta U = \sqrt{3} \cdot \left(i_{0a} \cdot x_0 - i_{0r} \cdot r_0\right) \cdot \frac{L^2}{2}$ - the cross component of voltage drop.

In the case in which the electrical line is provided with series capacitive compensation and we omit the cross component of the voltage drop, the determination relation a voltage before from the capacitor, in point 1 is:

$$U_l = U_0 - \Delta U \cdot \int_0^l \left(L - x\right) dx = U_0 - \frac{\Delta U}{2} \cdot l \cdot \left(2L - l\right) \tag{4}$$

where:
U_0 is the voltage at the line beginning;
$r0$, $x0$ – specific resistance and reactance, related per unit length;
l – distance from beginning of line up capacitor;
$\Delta U = \sqrt{3} \cdot (r_0 \cdot i_{0a} + x_0 \cdot i_{0r})$ - voltage drop per unit length $[V/m^2]$;
i_{0a}, i_{0r} – active and reactive component of the current per unit length $[A/m]$.

The voltage in point 2, after capacitor is:

$$U_2 = U_0 - \frac{\Delta U}{2} \cdot l \cdot (2L - l) + \sqrt{3} \cdot X_C \cdot i_{0r} \cdot (L - l) \tag{5}$$

The voltage at the end line is:

$$U_3 = U_2 - \Delta U \cdot \int_l^L (L - x)dx = U_2 - \frac{\Delta U}{2} \cdot (L - l)^2 =$$

$$= U_0 - \frac{\Delta U}{2} \cdot L^2 + \sqrt{3} \cdot X_C \cdot i_{0r} \cdot (L - l) \tag{6}$$

From the condition (1) after derivation ($\partial\varphi_l/\partial X_C$, $\partial\varphi_l/\partial l$) and the achievement of calculations the series capacitor location and reactance value result:

$$l = L - \sqrt{\frac{2}{3} \cdot \left(L^2 - 2 \cdot \frac{(U_0 - U_n)}{\Delta U} \right)} \tag{7}$$

$$X_C = \frac{\Delta U}{3 \cdot \sqrt{2} \cdot i_{0r}} \cdot \sqrt{L^2 - \frac{2 \cdot (U_0 - U_n)}{\Delta U}} \tag{8}$$

Analyzing expression (7) and (8) it notes that the capacitor location and its reactance value depend on the length line, on the voltage magnitude U_0 at the line beginning, parameters per unit length of the line and the flowed load on line. According as the voltage U_0 increases the capacitor location draws away by the line beginning and the reactance value of series capacitor decreases. It observes that the capacitor is placed near to the line beginning and the reactance value is greater for lines with less section conductors or for more loaded lines.

2.2. Line with distributed uniform loads wherefore two capacitor banks achieve the compensation

In the case long lines and loaded if one series capacitor is not sufficient for the improvement of the voltage profile on line, two and more series capacitors can be used. Thus, it avoids the possibility that the voltage downstream from capacitor pass over

admissible upper limit. Forwards we consider an electrical line with distributed uniform loads and its reactance compensation it carry out with two capacitors (Fig. 2).

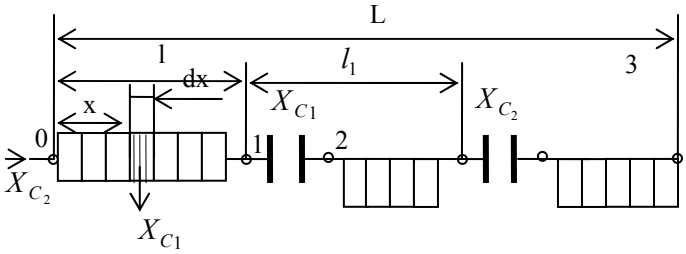

Figure 2. Line with distributed uniform loads and two series compensation installation

As in the previous case, for the determination of the two capacitor locations and optimal reactance values, the same procedure is used. Thus, voltages in the interest points are given by relations (9 ÷ 13):

$$U_1 = U_0 - \Delta U \int_0^l (L-x)dx = U_0 - \frac{\Delta U}{2} \cdot l \cdot (2L-l) \tag{9}$$

$$U_2 = U_0 - \frac{\Delta U}{2} \cdot l \cdot (2L-l) + \sqrt{3} \cdot X_{C_1} \cdot i_{0r} \cdot (L-l) \tag{10}$$

$$U_3 = U_2 - \frac{\Delta U}{2} \cdot l_1 \cdot \frac{2(L-l)-l_1}{2} + X_{C_1} \cdot i_{0r} \cdot (L-l) \tag{11}$$

$$U_4 = U_3 + \sqrt{3} \cdot X_{C_2} \cdot i_{0r} \cdot (L-l-l_1) \tag{12}$$

$$U_5 = U_0 - \frac{\Delta U}{2} \cdot \frac{L^2}{2} + \sqrt{3} \cdot X_{C_1} \cdot i_{0r} \cdot (L-l) + \sqrt{3} \cdot X_{C_2} \cdot i_{0r} \cdot (L-l-l_1) \tag{13}$$

After the achievement of calculations result reactance values X_{C_1}, X_{C_2}, on the side the two capacitor locations *l* şi l_1:

$$X_{C_1} = \frac{\sqrt{15}}{30} \cdot \frac{\Delta U}{i_{0r}} \cdot \sqrt{L^2 - \frac{2 \cdot (U_0 - U_n)}{\Delta U}} \tag{14}$$

$$X_{C_2} = \frac{\sqrt{30}}{30} \cdot \frac{\Delta U}{i_{0r}} \cdot \sqrt{L^2 - \frac{2 \cdot (U_0 - U_n)}{\Delta U}} \tag{15}$$

$$l = L - \frac{2}{\sqrt{5}} \cdot \sqrt{L^2 - \frac{2 \cdot (U_0 - U_n)}{\Delta U}} \tag{16}$$

$$l_1 = \frac{2-\sqrt{2}}{\sqrt{5}} \cdot \sqrt{L^2 - 2 \cdot \frac{(U_0 - U_n)}{\Delta U}} \tag{17}$$

From the analysis of relations (16) and (17) it can note that the (C_1) capacitor location draws away of the line beginning if the voltage on the MV bus of the substation increases, while the distance l_1 between the two capacitors decreases. From (14) and (15) it observes that between the two capacitors there is the relation $X_{C_2} = \sqrt{2} \cdot X_{C_1}$. If the voltage at the line beginning increases and decreases the power factor, the reactance values of capacitors lower, namely the reactive component of the current on line increases. It notes that for same load distributed on a line with less section conductors, reactance values of the two capacitors increase (ΔU greater), the capacitor location (C_1) draw to the line beginning and the distance between the two capacitors increase, also.

2.3. The line with distributed linear loads

Consider a homogenous electrical line, with distributed uniform specific parameters, and the load is linear distributed as in Fig 3.

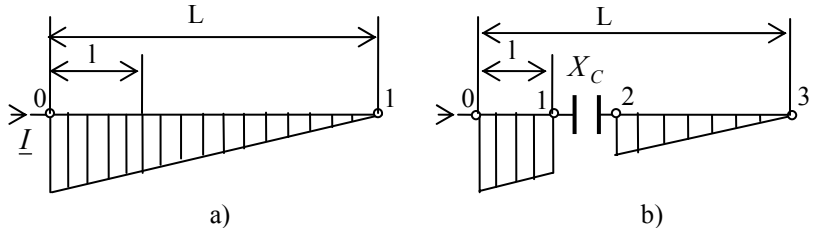

Figure 3. Line with distributed linear loads

At distance *l* the load current through line is:

$$\underline{I_l} = \underline{I} \cdot \frac{(L-l)^2}{L^2} \tag{18}$$

The voltage drop on the whole line is given of expression:

$$\Delta \underline{U} = \sqrt{3} \cdot \int_0^L \underline{z_0} \cdot \underline{I_l} dl = \sqrt{3} \cdot \underline{z_0} \cdot \underline{I} \cdot \frac{L}{3} \tag{19}$$

where:

$\underline{z_0} = r_0 + j \cdot x_0$ - is the line impedance per unit length;

$\underline{I} = I_a - j \cdot I_r$ - the all load current, at the line beginning.

From the relation (19) results that in the case the linear variation of load, the voltage drop on line is equal with the voltage drop produced of concentrated load $\underline{I}$, placed in the centre of triangle (Fig. 3).

If it neglects cross component of the voltage drop, then the voltage loss on the line without compensation is:

$$\Delta U = \sqrt{3} \cdot \left(r_0 \cdot i_{0a} + x_0 \cdot i_{0r}\right) \cdot \frac{L^2}{3} \tag{20}$$

Leaving from the voltage drop expression given by the relation (20), it establishes calculus relations of voltage in the interest points, (Fig.3), thus.

The voltage before capacitor is given by relation:

$$\begin{aligned} U_l &= U_0 - \frac{\Delta U}{L^2} \cdot \int_0^l (L-x)^2 \, dx = \\ &= U_0 - \frac{\Delta U}{3 \cdot L^2} \cdot l \cdot \left[3L \cdot (L-l) + l^2\right] \end{aligned} \tag{21}$$

where:

U_0 is voltage at the line beginning;

$\Delta U = \sqrt{3} \cdot \left(r_0 \cdot I_a + x_0 \cdot I_r\right)$ - voltage drop per unit length;

r_0, x_0 - specific resistance and reactance, related per unit length;

I_a, I_r - active and reactive component of the load current at the line beginning.

The voltage after capacitor is:

$$U_2 = U_0 - \frac{\Delta U}{3 \cdot L^2} \cdot l \cdot \left[3L \cdot (L-l) + l^2\right] + \sqrt{3} \cdot X_C \cdot I_r \cdot \frac{(L-l)^2}{L^2} \tag{22}$$

The voltage at the line end is:

$$U_3 = U_2 - \frac{\Delta U}{L^2} \cdot \int_l^L (L-x)^2 \, dx = U_0 - \Delta U \cdot \frac{L}{3} + \sqrt{3} \cdot X_C \cdot I_r \cdot \frac{(L-l)^2}{L^2} \tag{23}$$

Substitution of relations (21), (22) and (23) into relation (1), after the achievement of calculations result the capacitor location and its reactance value:

$$l = L - \frac{\sqrt[3]{18}}{6} \cdot \left(l - i \cdot \sqrt{3}\right) \cdot \sqrt[3]{L^2 \cdot \frac{3 \cdot (U_0 - U_n)}{\Delta U} - L^3} \tag{24}$$

$$X_C = \frac{2 \cdot \sqrt[3]{18} \cdot \sqrt{3}}{27 \cdot I_r \cdot \left(l + i \cdot \sqrt{3}\right)} \cdot \sqrt[3]{L^2 \cdot \frac{3 \cdot (U_0 - U_n)}{\Delta U} - L^3} \tag{25}$$

3. NUMERICAL APPLICATION

To make out the influence of the electrical load distribution along line on the capacitor location and the reactance value, as the compensation efficiency of line reactance we consider an overhead line of $20\,kV$, having conductors of the section

$95\,mm^2$ and length $40\,km$, with the distributed uniform load. The apparent power at line beginning is $S = 3{,}5 \cdot \exp(j\varphi)\,MVA$ and the voltage on MV bus of substation is $U_0 = 20{,}4\,kV$.

In the Table 1 are given obtained results for the series compensated line with distributed uniform load and for line with distributed linear load, respectively for line with the distributed uniform load without compensation.

From the table 1 it observes that the capacitor location depend on both the power factor and the load distribution along line. For the line with distributed uniform load and one series capacitor, the location capacitor will be at more distance of the line beginning. The capacitor reactance has the least value for the line with distributed linear loads to $\cos\varphi = 0{,}8$. In point of the relative deviations of voltages, in relation to the rated voltage, from the interest buses it is noted that the least values result for the line with distributed linear loads and $\cos\varphi = 0{,}9$, and values result for the line with distributed linear loads, and the most values result for lines with uniform distribution load and $\cos\varphi = 0{,}8$. If it compares the relative deviations of voltages at the line end provided with compensation and at the line without compensation it observes that, the relative deviation of voltage in relation to the rated voltage is about thrice greater in the case of line without compensation.

Table 1. **The series capacitive compensation – comparison between the uniform and linear distribution of load**

	cos φ	l [km]	l1 [km]	XC1 [Ω]	XC2 [Ω]	εU1 [%]	εU2 [%]	εU3 [%]	εU4 [%]	εU5 [%]	Σ εUi [%]	Linia fara compensare
Uniform distribution with one capacitor	0,8	11,67		11,12		-2,03	2,03	-2,03			12,326	-6,08
	0,9	11,95		14,3		-1,88	1,88	-1,88			10,552	-5,625
Uniform distribution with two capacitors	0,8	8,96	9,09	6,09	8,61	-1,22	1,22	-1,22	0,405	-2,03	8,71	-6,08
	0,9	9,27	9	7,83	11,08	-1,13	1,13	-1,13	0,375	-1,88	7,457	-5,625
Linear distribution	0,8	10,06		7,83		-1,13	1,13	-1,13			3,825	-3,385
	0,9	10,4		10,6		-1,03	1,03	-1,03			3,171	-3,085

4. CONCLUSIONS

The paper here presents importance because gives general valid information concerning the capacitor location and its reactance value in medium voltage distribution networks. Namely,

• the capacitor location and its reactance value depend on the load distribution on line, in proportion as the load is concentrated at the line beginning the capacitor location is more closed of the line beginning and the reactance value is littler.

• the capacitor location and its reactance value depend on the line length. If the line length increases the capacitor location closes in of the line beginning and the reactance value increases.

• the capacitor location and its reactance value depend on the power factor, in proportion as the load is greater the distance between the line beginning and the capacitor location increases, and the reactance value increases also.

• the capacitor location and its reactance value depend on the flowed load on line, in proportion as the line is more loaded the distance between the line beginning and the capacitor location decreases, and the reactance value increases.

REFERENCES

[1]. Buta, A., Pană, A., Milea, L., *Calitatea energiei electrice*, Editura AGIR, Bucureşti, 2001;
[2]. Grzybowski S., Kordus A., Krolikowski C. Seidel Şt., Zeydler-Zborowski J., *Condensatoare în electroenergetică (Capacitors in power systems),* Editura Tehnică, Bucureşti, 1966.
[3]. Satoru I., Walter J. Ros: *Distribution Series Capacitors for Improved Power Quality, GE Transmission, Distribution & Industrial Systems*, 1999
[4]. Buta A., Bucatariu Ilona, Pană A.: *Utilizarea indicatorilor integrali de calitate ai tensiunii la stabilirea valorilor reactanţelor compensatoarelor serie şi paralel în reţelele electrice de distribuţie,* Revista "Producerea, transportul şi distribuţia energiei electrice şi termice", Bucureşti, 2002, pp.17-22.
[5]. ***SR EN 50160, *Caracteristicile tensiunii furnizate de reţelele publice de distribuţie (Characteristics of provided voltage by distribution utility networks),* November, 1998.
[6]. Poeată, A. Arie A., Crişan O., Eremia M., Alexandrescu V., Buta A., *Transportul şi distribuţia energiei electrice (Electric Energy Transport and Distribution),* Editura Didactică şi Pedagogică, Bucureşti,1981.

INDEX OF AUTHORS

B
BADEA, F., 78

E
EGRI, A., 32,66

G
GAIȚĂ – LUKACS, I., 5, 16

M
MANDRESCU, C., 50
MARCU, M., 22

O
ORBAN, D., 22

P
PĂSCULESCU, D., 42, 60, 93
PĂTRĂŞCOIU, N., 5, 16
POANTA, A., 10
POPESCU, F., 22

R
ROMANESCU, A., 42, 93

S
SOCHIRCA, B., 10
SIRB, V., 32,66
STOICUȚA, N., 50
STOICUȚA, O., 32, 50, 66

Ş
ŞTEFAN, C., 60

T
TĂBĂCARU, T., 88
TOMUŞ, A., 5, 16

U
UȚU, I., 72